Title

Topography and physiology of single neurons within the isofrequency domain of cat primary auditory cortex

Permalink

https://escholarship.org/uc/item/8n18d3d7

Author

Sutter, Mitchell Lawrence

Publication Date

1991

Peer reviewed|Thesis/dissertation

Topography and Physiology of Single Neurons Within the Isofrequency Domain of Cat Primary Auditory Cortex   by

Mitchell Lawrence Sutter

DISSERTATION

Submitted in partial satisfaction of the requirements for the degree of

DOCTOR OF PHILOSOPHY

in

Bioengineering

in the

GRADUATE DIVISION

of the

UNIVERSITY OF CALIFORNIA

San Francisco

Date . . . . University Librarian

Degree Conferred: . . . 3/25/91 . . . .

Copyright Page

Copyright 1991

by

Mitchell Lawrence Sutter

DEDICATION

I dedicate this dissertation to my father, Allan Sutter. By choosing a research career, I feel as if I may be achieving one of his unfulfilled dreams. This career choice would not have been possible if my father had not sacrificed to allow me the freedom to pursue educational and intellectual opportunities; opportunities which he himself did not have because of the depression, and World War II.

ACKNOWLEDGEMENTS

ABSTRACT

Physiology and Topography of Single Neuron Responses Within the Cat Primary Auditory Cortex.

By Mitchell Lawrence Sutter

This dissertation looked at the spatial distribution single neuron response properties relative to Schreiner and Colleagues' (1988, 1990) multiple unit maps. The results strongly indicate that dorsal and ventral AI are functionally different. In dorsal AI, neurons can be found which respond to multiple bands of frequencies, while not responding to frequencies between the bands. The frequency response ranges of these "multi-peaked" neurons were usually separated by less than an octave and often approximated second and third harmonics of a fundamental series. Multi-peaked neurons have longer latencies than single-peaked neurons. The response latency to tones in the high frequency response range was usually longer than the response to tones in the low frequency response range. Within the frequency tuning curve, inhibition was often prominent between the two response ranges, and two-tone enhancement could often be observed. Multi-peaked neurons, which were present in AI dorsal to the sharply tuned multiple unit area, were not found in ventral AI.

While multi-peaked neurons tended to be broadly tuned 40 dB above the neurons threshold (Broad BW40), single

peaked neurons in dorsal AI could also have broad BW40 values; in fact in dorsal AI, the single neuron spatial distribution roughly approximated the multiple unit topography. Contrasting this, in ventral AI all single units were sharply tuned, even in areas with broad multiple unit responses. This ventral difference between multiple and single neurons could be accounted for by scatter in the characteristic frequencies of the neurons.

Single neurons throughout AI tended to be more sharply tuned to amplitude than multiple unit recordings. In ventral AI the topographical trends between single and multiple neurons were similar, but offset in magnitude. In the two non-monotonic areas threshold scatter of single neurons was low, indicating that coherence in the intensity response area is responsible for multiple unit sharp amplitude tuning. On the basis of the dissertation work, it is concluded that dorsal and ventral AI are physiologically distinct.
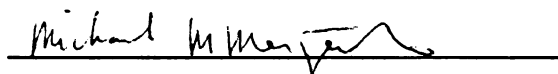
_____

Chair of Committee

TABLE OF CONTENTS

LIST OF TABLES

LIST OF FIGURES

Introduction

How can a cat distinguish a dog's bark from a cat's meow? How do humans distinguish the sound of a bell from a horn or the vowel \e\ from the vowel \a\? How do mammals localize an acoustic source in space? In order to answer these questions, one needs to understand how animal auditory systems process acoustical information. Investigating the topographical encoding of basic auditory properties in the auditory cortex should provide useful information on the internal representations of key elements of complex stimuli.

The Present View of Auditory Cortex: Tonotopic Organization and Inter-animal Variability

Unlike many other regions of the brain, primary auditory cortex (AI) cannot be easily bounded on a strictly anatomical basis alone. Instead the location and extent of AI are defined by a combination of anatomical and physiological criterion. In the cat, AI, grossly, is located on the middle ectosylvian gyrus, and part of AI commonly resides between the dorsal tip of the anterior ectosylvian sulcus (AES) and the posterior ectosylvian sulcus (PES) (Fig. 1). Bordering AI on the anterior and posterior sides are the anterior (AAF) and posterior auditory fields (PAF).

In the ventral/anterior extreme of AAF low frequencies are represented. Characteristic frequency -- the frequency

at which a unit's minimum intensity threshold occurs --
increases along a smooth gradient in the dorsal/posterior
direction. After reaching Characteristic frequencies (CFs)
greater than about 60 kHz the CF progression reverses and
CF's begin to decrease posteriorly. This site of reversal in
a functional gradient marks the AI/AAF border. A second
reversal of the CF gradient, now towards decreasing CF,
occurs more posteriorly, often in the PES, and this reversal
demarcates the AI/PAF border.

Upon locating the middle ectosylvian gyrus,
characteristic frequencies must be mapped along the
anterior-posterior direction to delineate AI from AAF and
PAF. AI can be reliably identified by the direction of CF
progression (low frequencies rostral to high frequencies
caudal) and its location on the ectosylvian gyrus between
and/or slightly dorsal to AES and PES. Use of the CF
gradient is fundamental in defining AI in the cat because
sulcal patterns and the size and location of cortical fields
relative to them, is highly variable (Ades 1941; Rose 1949;
Kawamara 1971; Merzenich et. al. 1975). The depth and
dorsal/ventral extent of AES and PES is particularly
variable.

Historical Development of Brain Localization: The 19th Century

The road to a unified view of the location of auditory cortex as defined in Fig. 1 was long, bumpy, and occasionally controversial. Before even ascribing that there was an auditory sensory area in the cortex, a major philosophical obstacle had to be overcome. As early as 1825 Jean Baptiste Bouillaud, recognized that there was a correlation between anterior cortical (but not posterior) lesions and loss of speech capabilities. He concluded "the coordinating organ of speech (organe legislateur de la parole) resided in the anterior lobe of the brain" (Bouillaud 1825, quoted in Clark and Jacyna 1987, and in Head 1926). This finding, however, was not accepted because it was associated with the academically unpopular phrenology movement of Gall (e.g. Gall 1835). The seating of speech areas in the brain were slightly better accepted when presented in 1861 by Broca (Broca 1861a,b).

In the 1860's *action propre* brain theories such as Flourence's that the cortex, the medulla, and the cerebellum act as three large monoliths performing sensory, vital, and motor roles, respectively, were still very highly regarded. Contrasting brain localization theory, *action propre* brain theorists believed that the substance of each of these

monoliths was uniform; e.g. any part of cortex performed all sensory functions much like a hologram contains all information at all points. The idea of localization of cortical functions, however, made a huge leap forward with the work of Fritsch and Hitzig (1870). In experiments reportedly performed in Hitzig's house, they electrically stimulated the cortex of dogs and rabbits, and reported movements of localized muscles. Which, if any, muscles moved depended on where there stimulating electrodes were placed on the brain. These experiments provided the first motor maps, and while sharply attacked at the time, motivated several other investigators to use the relatively new technique of cortical electrical stimulation mapping.

The Concept of Sensory Cortex

Going one step beyond Hitzig and Fritsch, Ferrier (1875) attempted to extend brain localization theory to sensory functions. Ferrier performed cortical electrical stimulation experiments on monkeys, dogs, cats, jackals, rabbits, guinea pigs, rats, pigeons, frogs and fishes. In the monkey, electrical stimulation of only one of his twenty regions resulted in reported movements of the ears (Fig. 2A). "Pricking of the opposite ear, head and eyes turn to the opposite side, pupils dilate widely" was Ferrier's

(1876) noted response to electrical stimulation of site 14 (Fig. 2A). Ferrier, recognizing that the response to electrical stimulation closely resembled the behavioral response to a loud sound, hypothesized that this region might be an acoustic sensory area. Similar results were obtained for location-specific surface electrical stimulation in other species, including the cat (Fig 2B locations 8,14). In these experiments, Ferrier had corerctly located auditory sensory cortex. To help support his sensory hypothesis, Ferrier performed lesion experiments in the monkey and found that bilateral lesion of region 14 appeared to deafen his experimental animals; after lesions, they did not respond to sounds indicating the presence of food items out of their view.

Recording Electrical Activity in the Brain

While Ferrier had provided early evidence for sensory cortical regions in animal brains, direct evidence that the brain somehow reacted to sensory stimuli was being developed. Richard Caton set out to show that localized cortical areas changed electrical potential in response to sensory stimulation. There was no such thing as an electrical amplifier in the late 19th century so Caton had to devise a method to record minute electrical signals. He

used optical magnification by reflecting the beam of a

osyhydrogen lamp (they had no electrical lights either) off

the mirrored scale of a galvanometer onto a long wall: "A

graduated scale, some eight or nine feet in length, being

placed on the walls of the theatre, a beam of light from an

osyhydrogen lamp was thrown on to the mirror of the

galvanometer, and thence reflected to the scale" (Caton

1875a, quoted in Brazier 1988)). While successful in

confirming Ferrier's defined visual sensory area responded

to light stimulation (Caton 1875b), Caton (1877, cited in

Brazier 1988) apparently could not show that auditory cortex

responded to sound. In retrospect, a milestone in

neurophysiology had clearly been reached. The basis of

recording electrical activity in the brain had been

established. The first weak evidence of restricted auditory

responses in cortex was provided by Adolph Beck (1891) in

rabbits and Vasil Danilevsky (1891, cited in Brazier 1988)

in dogs (interpreted by Brazier 1988).

Before the turn of the century, unequivocal evidence of

an auditory sensory cortical area was provided by Vladmir

Larionev (1897; 1899, cited in Brazier 1988). Using tones as

a stimulus, Larionev demonstrated an area that responded

exclusively to sounds and that seemed to have a

topographical representation of the frequency of the tone

(Fig 3). By now brain localization had a pretty strong

standing, and investigators had a good estimate of the location of auditory cortex. During a similar time period Vogt (1898, cited in Bremer and Dow 1939) identified a region of early myelinization in the middle ectosylvian gyrus of the cat.

Early Evidence for Multiple Auditory Cortical Fields in the Cat

Early anatomical studies in humans, primates and cats indicated that there were cytoarchitectonic differences within auditory cortex. Campbell (1905) defined two distinct cytoarchitectural areas in the cat (Fig 4). He postulated that one region (roughly corresponding to modern AII and ventral AI) might receive its main input from the medial geniculate body and would be involved in sensory processing while the other area (roughly corresponding to AAF, PAF, and dorsal AI) would be involved in psychic function.

Evoked Potential Studies: Corroboration on the Approximate Location of AI

With the advent of the oscilloscope and amplifiers (along with other technical breakthroughs), a finer resolution could be obtained with neurophysiological

partially due to the use of a broad-band click stimulus used in these studies (see discussion of Chapter 3).

Auditory Cortex: Maybe it is Bigger?

In a partially coincident time frame to Ades (1941), Bremer and Dow (1939) and Kornmuller (1933), there was evidence (in addition to Campbell 1905) that auditory cortex could be quite large. A series of evoked potential studies (Gerard et al.1936) indicated that the cortical area expressing auditory responses was huge occasionally extending posteriorly to the posterior splenial gyrus and dorsally to the suprasylvian gyrus. Anatomical studies similar to those of Ades (1939) reported a larger auditory cortex in the ventral direction (roughly modern AI and AII). Woolard and Harpman (1939) ablated the medial geniculate body (MGB) and observed a larger area of cortical degeneration than identified by click-evoked potential response experiments (See Fig. 5). Also slightly after Ades publication, initial results of evoked potential studies with a different method of stimulation indicated a larger auditory area (Woolsey and Walzl 1941). By electrically stimulating restricted ranges of the osseous spiral lamina of the cochlea (corresponding to first order afferent fibres representing restricted preferred frequencies), Woolsey and

Walzl (1943) found a cochleotopic organization over a very large area in auditory cortex. They concluded that there were two separate cochleotopic organizations: a dorsal region that they called the "primary auditory cortex"; and a ventral one which the called the "secondary auditory cortex". In retrospect their primary field included parts of PAF and AAF and their secondary field undoubtedly included parts of VPAF (Fig. 6). Ades (1943) himself returned to the picture. He applied strychnine patches to cortex, which increased cortical activity by supressing cortical inhibition, and using evoked potentials defined a secondary area similar to the modern VPAF. Summing up the situation by 1943, Ades states, "At this point it may be pertinent to note that the only point of agreement that can be found in the feline temporal area [cortex] is on the location of the primary projection area."

Non-Primary Cortex Revisited: Getting Closer to Agreement

The next decade would see even more definitions of the totality of auditory cortex. Rose (1949) performed a thorough cytoarchitectonic study and defined four distinct regions (Fig 7). Roughly corresponding to modern AI, Rose's AI also extended roughly one third of the way down the ventral bank of the suprasylvian sulcus. The suprasylvian

fringe, whose potential auditory role was (and still is) undetermined, runs from the dorsal end of AI to approximately the fundus of the suprasylvian sulcus. Rose's AII roughly corresponds to modern AII and AAF. The "posterior ectosylvian area" as defined by Rose is roughly comprised of modern PAF and VPAF. In his article, Rose described in-detail the large variability of sulcal patterns and field boundaries that he observed across cats, and noted that key field boundaries , e.g., between AI and AII were not sharp, but were marked by transitions in cytoarchitectonic features that extended significant distances across the corrtex.

The strychnine patch method was applied by Hind (1953), who identified functional boundaries similar to those described by Rose (except in the depth of sulci, where the patch technique was impractical). These tonal stimulation experiments described a CF progression across auditory cortex similar to the modern view (Fig 7B). On the middle to ventral part of the posterior ectosylvian gyrus, high frequencies were represented. At the dorsal tip of the posterior ectosylvian sulcus, low frequencies were represented. A progression towards high frequencies was reported for AI which leaves a high frequency response generally at the dorsal tip of the anterior ectosylvian sulcus. Hind reports that there, finally, is a low frequency

response region in the ventral part of the anterior ectosylvian gyrus. While Hind's data roughly corroborate our knowledge of tonotopic organization within PAF, AAF, and AI, one more response area, another auditory area was reported on the suprasylvian gyrus dorsal to AAF (Lombroso et al 1956) (Fig 7C).

By the late 1950's compelling evidence of tonotopic organization in the auditory cortex had been strongly established (see also Tunturi 1950; 1952). The general location of the primary field, AI, was well-accepted, but there still remained much controversy about the location of other auditory fields.

Microelectrode Studies

With the advent of microelectrode recording techniques, a whole new world opened up. Many auditory cortical single neurons were found to be responsive to tones and selective for frequencies (Thomas 1952, Erulker et al. 1956). However early microelectrode studies of single neurons failed to display a similar strict tonotopic organization as previously encountered in evoked potential studies (Evans and Whitfield 1964, 1965; Goldstein et. al 1970). Unlike the successful evoked potential studies, the microelectrode studies tried to pool the locations of single neurons across

many animals. Goldstein and colleagues tried to achieve
pooling by creating a "standard cortex" which normalized
sulcal pattern across animals. These authors conclude from
their single unit data that there may be a weak tonotopic
organization of AI, but that this was fundamentally
different from the strong tonotopic organization of
subcortical structures. Contributing to their failure to
confirm strict cochleatopicity was their attempt pool data
across animals based on criteria strictly confined to gross
anatomical considerations.

Merzenich and colleagues (1975) circumvented the need
for pooling data by exploring multiple unit recordings. By
using the multiple unit technique time could be saved during
the experiments by eliminating the need to isolate and hold
units. The technique thus allowed for collecting data from
a large number of locations in each animal. By producing
extensive within-animal maps they succeeded in reaffirming a
strict tonotopic organization in a number of cortical fields
and in several species (Merzenich and Brugge 1973; review in
Merzenich et al. 1984). These findings have since been
verified with the most complete experiments performed in the
cat by Reale and Imig (1980) who also defined an area down
the ventral bank of the suprasylvian sulcus in some animals.
Demonstrations of tonotopicity in each individual animal
were extremely important in defining representations along

the roughly four to seven millimeters of rostro-caudal extent in AI. However AI is not one dimensional and most people believe this part of the brain is involved in more than simple single tone frequency discrimination.

The Isofrequency Domain of AI

By reconstructing the CF progressions along several parallel anterior to posterior lines, one can construct lines of equivalent CF and create isofrequency contours. In figures 1 and 9 the 3, 6, 12, 24, and 48 kHz isofrequency contours are identified in AI. Isofrequency contours of AI do not generally run perfectly in the dorsal ventral direction. Rather they run slightly slanted in the anterior-posterior direction so that one has to progress an electrode slightly posterior as the electrode is moved dorsally to stay on the contour. Along the center of AI a line angled between 0 and 30 degrees can usually approximate the isofrequency domain. At the dorsal extreme of AI the angle usually sharpens (see Figs. 1 and 9).

Up to 1988, little progress was made in the search for reliable representations in the isofrequency domain of the cat. Differences in binaural response properties had been seen in the dorsal-ventral direction, but for the most part these differences were not systematic. Similar binaural

responses seemed to be spatially clustered; however, they appeared relatively independent of cortical location (Imig and Adrien 1977, Middlebrooks and Zook 1983). One notable exception is that in the dorsal extreme of AI excitatory input from the ipsilateral ear appears to be the strongest (Middlebrooks and Zook 1983).

In a series of experiments conducted by Schreiner, Mendelson, Sutter and Grasse (Schreiner et. al 1988; Mendelson et. al 1988; Schreiner and Mendelson 1990; Schreiner et. al 1991; Mendelson et.al. 1991), it has recently been shown that several response characteristics of multiple unit recordings vary systematically within the isofrequency domain of AI. These properties include sharpness of frequency tuning (Schreiner et. al. 1988; Schreiner and Mendelson 1990), sharpness of amplitude selectivity (Schreiner et. al. 1988; 1991), responsiveness to broad-band stimuli (Schreiner et al. 1988; Schreiner and Mendelson 1990), responsiveness to frequency modulated stimuli (Mendelson et al. 1988;1991), and latency of response (Schreiner et. al 1988).

Various multiple-unit properties map across the isofrequency domain of AI. Several response properties show a continuous topographical distribution which has one maximum or minimum approximately at the center of the isofrequency domain (Figure 8A, B, D, E). Roughly in the

center of isofrequency lines, multiple-unit responses are most sharply tuned. A gradual and progressive broadening of tuning occurs in the dorsal and ventral directions. A similar distribution occurs for responsiveness to different modulation rates of 8 octave frequency modulated sweeps. Dorsally and ventrally multiple units respond best to sweeps with fast (greater than 125 octaves/second) modulation rate, while in the center they respond best to slower (less than 20 octaves/ second) sweeps. Similarly dorsal and ventral units respond best to upward sweeps and centrally to downward sweeps. With the sharpness of tuning gradient in mind, a new view of AI was introduced with defined differences in selective neuronal responses along its isofrequency axis (Fig. 9).

Several response properties, such as sharpness of intensity tuning, show double-humped topographical distributions with two "minima", and three "maxima" straddling the "minima" (Figure 8C, F). Occupying the two "minima" are units which only respond to a narrow range of amplitudes and which respond weakly to broad-band stimuli. One of these "minima" is roughly alligned with the region of AI which is sharply tuned for frequency, and the second minimum is approximately 3 mm dorsal to the first minimum.

The topographical representation of multiple-unit responses to these different stimulus parameters can be used

to predict how these neurons might respond to more complex biologically significant stimuli. It has been postulated that inhibitory mechanisms play an important role in all of the parameters, although very little data exists on inhibition in auditory cortex.

Other Species

While the development of knowledge of cat auditory cortex has been extensively described (since the cat is the animal model of these investigations), similar topographical order has been found in other mammals. In monkeys (Imig et al. 1977; Merzenich and Brugge 1973; Hind et al. 1958; Pribraum et al. 1954; Walzl and Woolsey 1943; Licklider and Kryter 1942), bats (summary in Suga 1989), ferrets (Kelly et al. 1986), rabbits (McMullen and Glaser 1982), squirrels (Merzenich et al. 1976), and guinea pigs (Hellweg et al. 1977), a central tonotopically auditory field surrounded by a "belt" of secondary fields has been described. In the echolocating mustached bat, the function of the different fields is thought to be related to specific functions of the bat's biosonar behavior (Fig. 10).

AI, with strict tonotopic organization, is probably involved in doppler shift frequency analysis of velocity. Doppler shift analysis is based on the fact that the

velocity of a sound source relative to a receiver affects the sound's frequency. For example, when a train blowing its whistle approaches you the frequency of the whistle increases as a function of the trains speed. Therefore, when the bat emits a reference tone at about 60 kHz, the relative velocity of an object can be discerned by detecting small shifts in the returning frequency. Neurons arranged in its tonotopically organized AI have such discrimination ability. The representation of frequencies behaviorally relevant to the bat have been shown to be magnified relative to other frequencies (Suga 1984). Within the isofrequency domain of AI, there is a map of preferred intensity of the stimulus (which can be used to help determine target size) (Suga and Manabe 1982).

Surrounding AI in the bat are several fields which are sensitive to combinations of stimulus parameters. Some of these areas contain neurons that are tuned to preferentially respond to tone-pairs corresponding to harmonics of the bat's ultrasonic chirp. CF's near the two separate harmonics are represented orthogonally in a CF-CF map (Fig 11). Using doppler shift analysis, a map of behaviorally relevant velocities can be derived for each CF-CF region. Other auditory cortical fields in the bat are tuned for a behaviorally important range of delays between emitted and

returned pulses. This timing map can be converted to a functional distance map.

Dissertation Studies

The experiments performed for this dissertation have been conducted to gain a better understanding of the physiological architecture of the isofrequency domain of the cat primary auditory cortex. The following chapters describe a revised characterization of the dorsal-ventral extent of AI (Fig 12) based on single neuron response properties. The experiments were performed to determine the topography of single unit responses to pure tones. The series of topographical studies previously performed by Schreiner, Mendelson, Sutter, and Grasse were all multiple-unit mapping studies. Multiple unit recordings provide a good measure of processing at a given site, roughly corresponding to a column, in the cortex. This dissertation addresses many important questions about how the neuronal elements that make up the multiple-unit response contribute to the functional topography of the primary auditory field. It implicitly addresses the question of whether single and multiple unit topographies differ. This study comprised 3 specific aims: (1) To determine the spatial distribution of functionally distinguishable single neurons in the

isofrequency domain of cat AI (Chapter 1); (2) to study the topography of the extent of excitatory frequency receptive fields (sharpness of frequency tuning) in the isofrequency domain of cat AI (Chapter 2); and (3) to investigate the spatial distribution of intensity coding properties within the isofrequency domain of AI of the cat (Chapter 3). Each chapter has been prepared in publication format and, thus, contains its own introduction and discussion.

A.

See legend about variabilty

AAF	Anterior Auditory Field
PAF	Posterior Auditory Field
VPAF	Ventral PAF
AI	Primary Auditory Cortex
AII	Secondary Auditory Cortex
VBSS	Ventral Bank of Suprasylvian **Sulcus**
SSS	Suprasylvian Sulcus
PES	Posterior Ectosylvian Sulcus
AES	Anterior Ectosylvian Sulcus
PSS	Pseudo-sylvian Sulcus

B.   **C.**

Rostral

Ventral
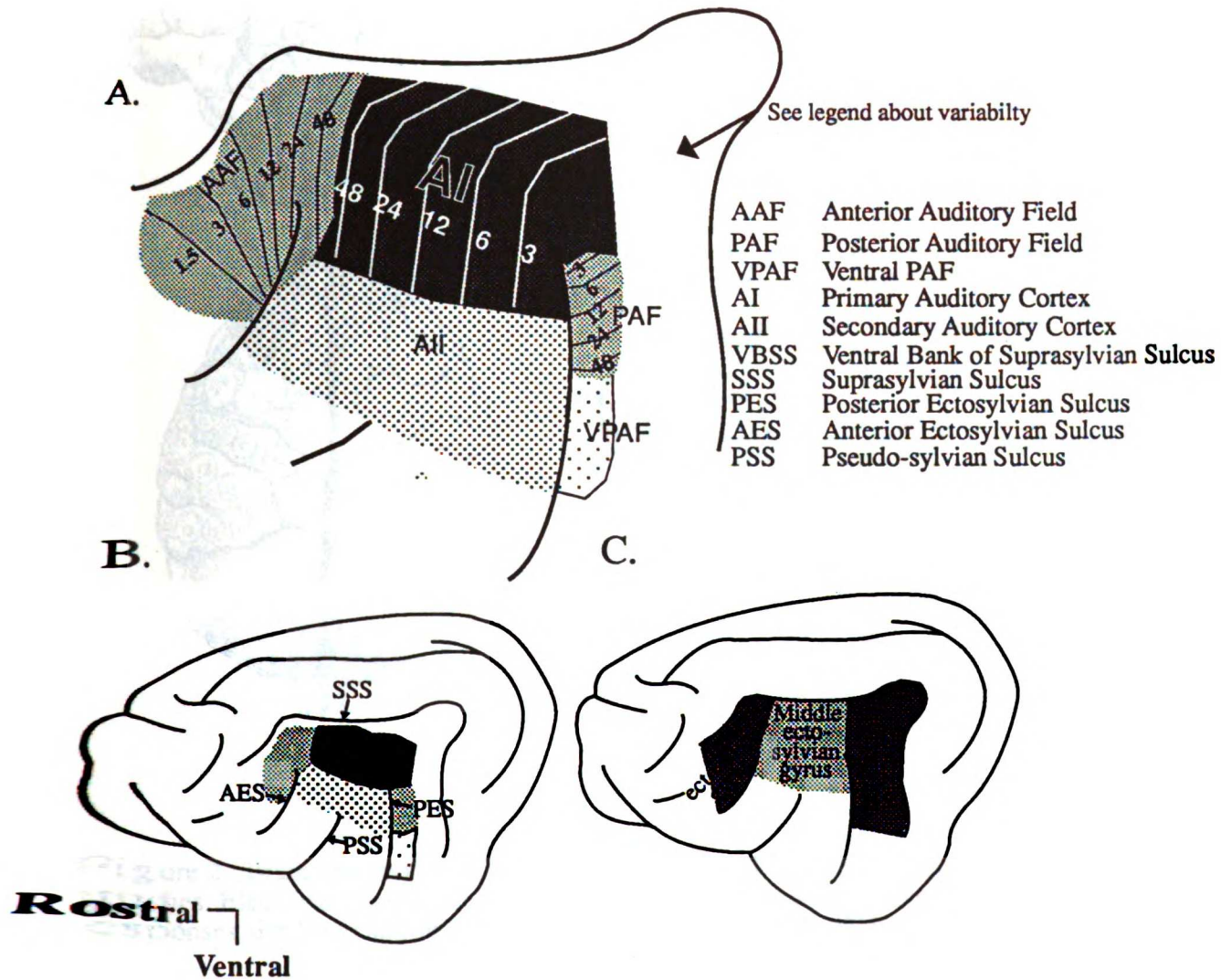
Figure 1: Schematized summary of the knowledge of the boundaries of auditory cortical fields before the most recent set of experiments by Schreiner, Sutter and colleagues. Extents and limits of fields are based on the data of Merzenich et al. 1975, and Imig and Reale 1980. It is important to emphasize variability in maps and sulcul patterns. Ocassionally AAF and/or AI can enter the ventral bank of the SSS. AAF can also reside entirely on the anterior ectosylvian gyrus with AI crossing over the AES. Similarly part of PAF can cross the PES and reside on the middle ectosylvian gyrus. Isofrequency contours (numbers represent frequency in kHz) are represented in AAF, AI and PAF. These, also, are highly variable and idiosyncratic for each animal. While they tend to be obliqued dorsal-ventrally, the contours can be substantially rotated. These lines almost always turn caudally in the dorsal part of AI. (B) shows the entire left hemisphere for the auditory cortex depicted in (A). Gyrus names are shown in (C).

A.
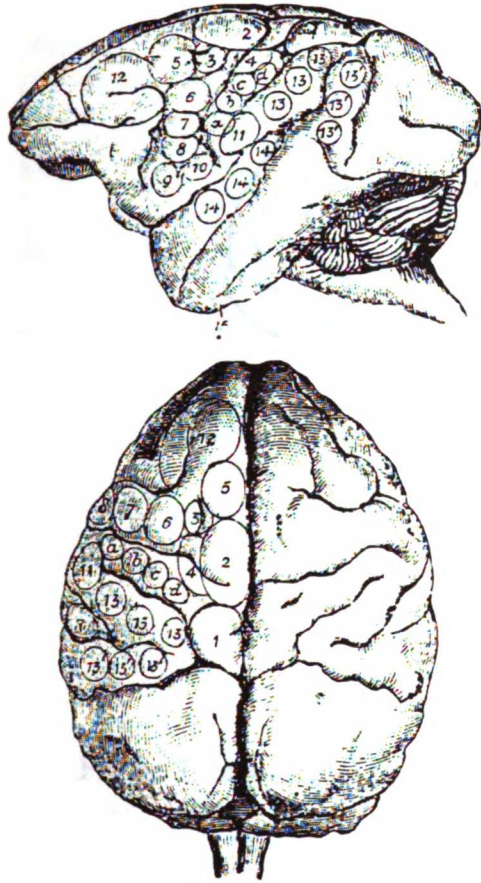
B.
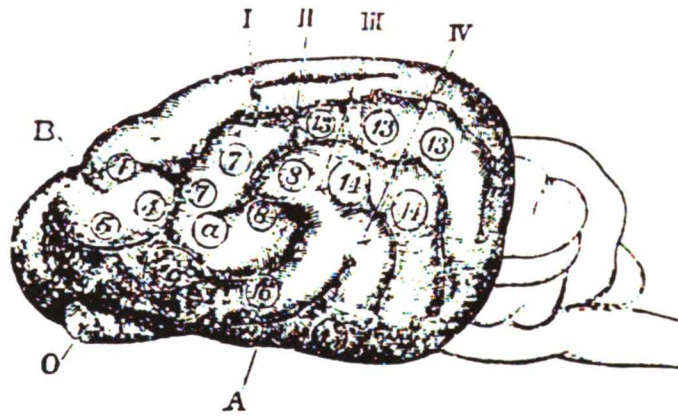
Figure 2 : Brain of a monkey (A) and a cat (B) from Ferrier's electrical stimulation studies. Electrical stimulation of area numbered14 was noted to evoke a behavioral responses similar to startle from a loud sound. Stimulation of site 8 also evoked that response in the cat. Note that areas 8 and 14 lie on anterior, middle, and posterior ectosylvian gyrus. (From Ferrier 1876).
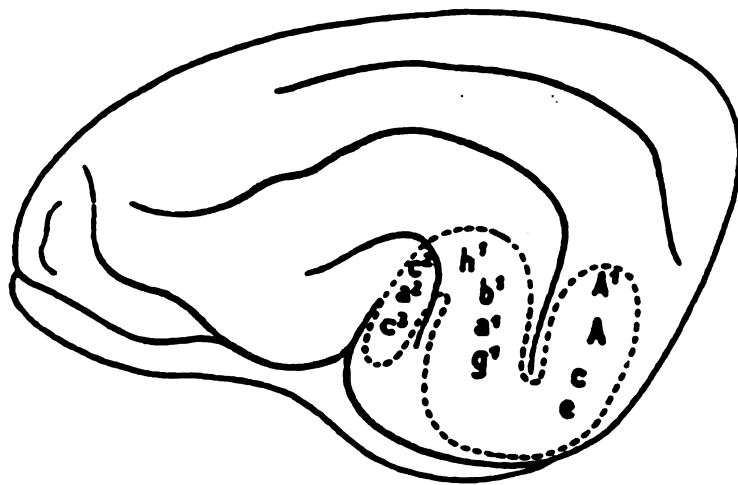
Figure 3: Maps for musical notes in the dog, taken from Larionev 1899
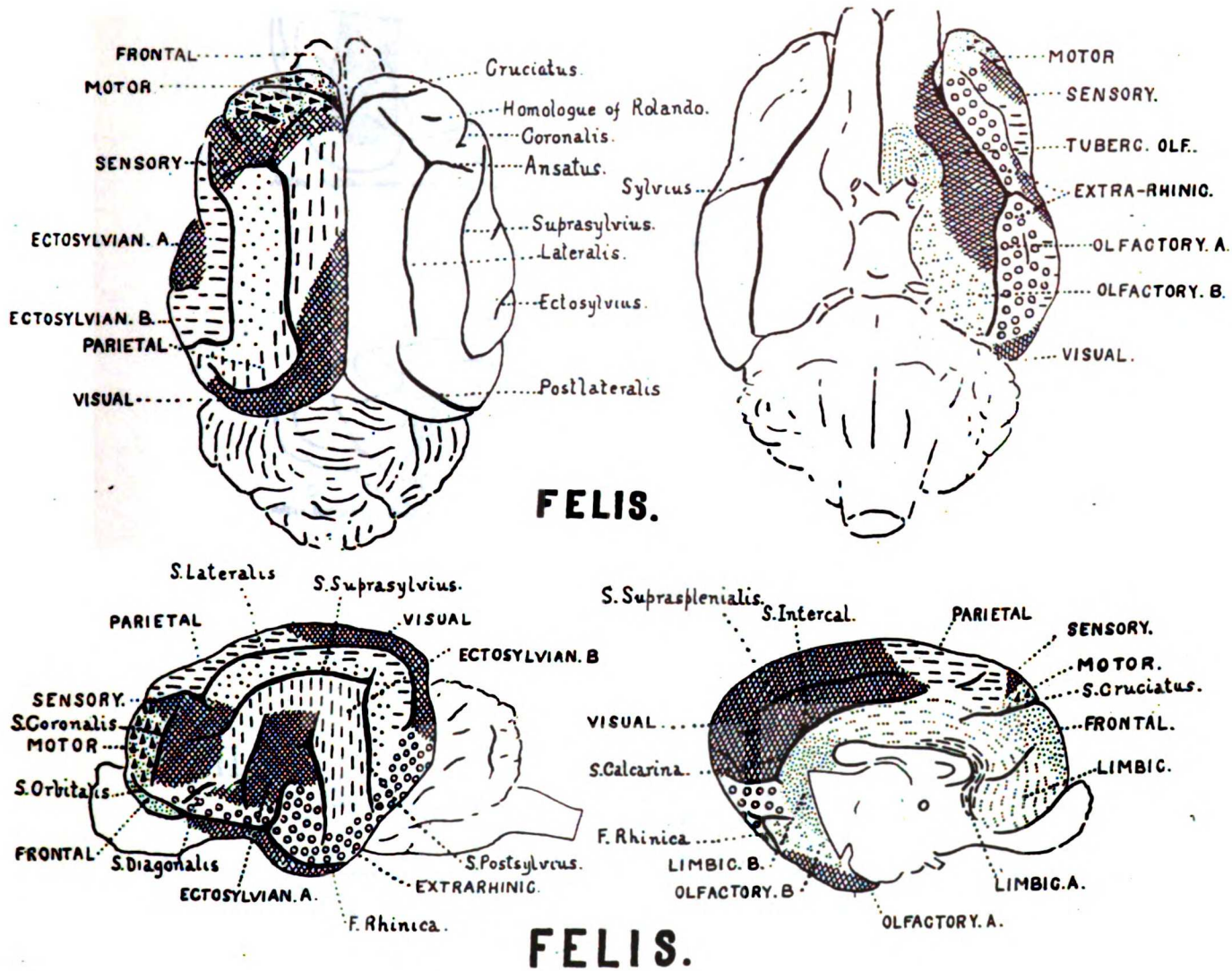
Figure 4: Cytoarchitecture of the cat as described by Cambell (1905). The area marked ectosylvian A was postulated to be "auditory sensory cortex"; the cortical zone marked ectosylvian B was postulated to be "auditory psychic cortex". (From Campbell 1905)

I.

II.
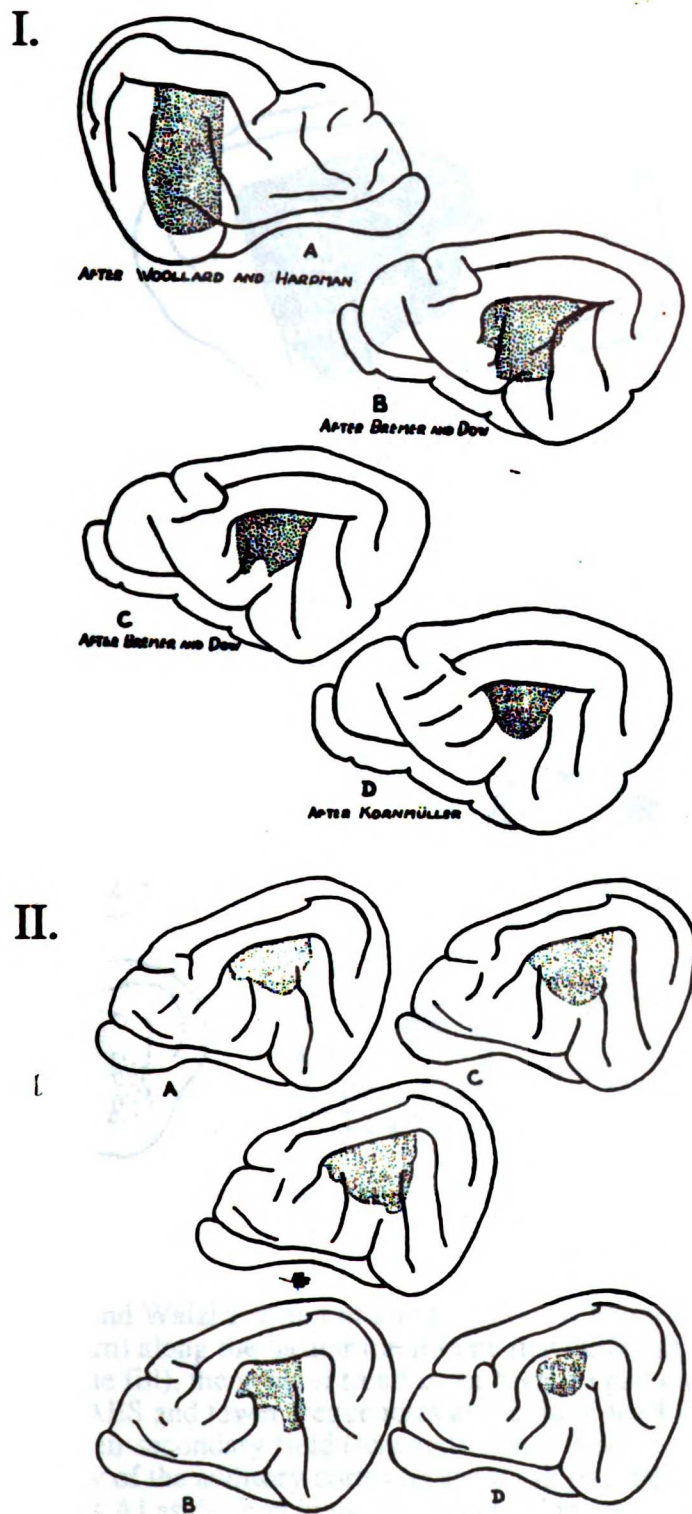
Figure 5: Relatively harmonious view of cat primary auditory cortex. Woolard and Harmon's (I.A), Bremer and Dow's (I.B, I.C), and Kornmuller's (I.D) data are summarized in (I). The results from 5 cases of Ades (1941) are shown in (II). Figures taken from Ades 1941.

A.
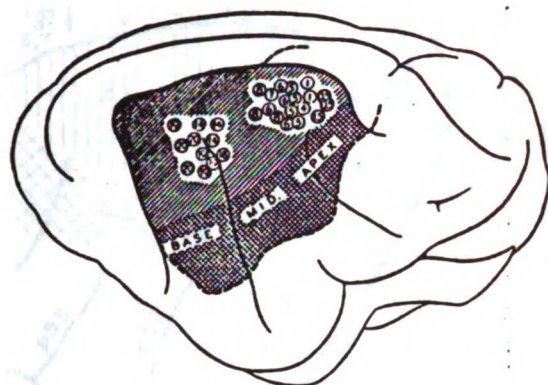
B.
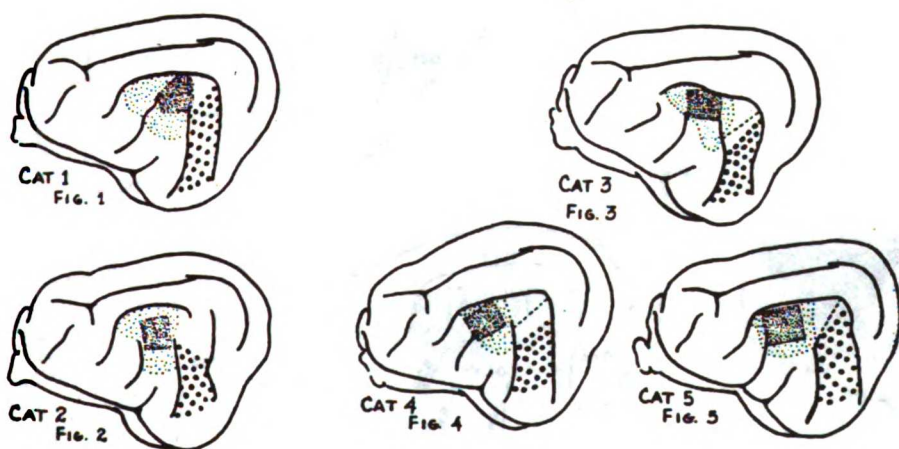
Figure 6:
(A) Woolsey and Walzl's notion of auditory cortex. Numbers correspond to the distance (in mm) along the basilar membrane that optimally excited that location. In AI (diagnal line fill), the general trend is for high frequencies to be represented at the tip of the AES and lower frequencies at the tip of the PES. This trend reverses ventrally in their secondary field (hatched). From Woolsey and Walzl 1943.
(B) Ades' view of the auditory cortex as shown in five different cats. The dark stippled area is AI as defined in evoked potential maps, and the light stippled zone is AI defined anatomically. The polka dot area corresponds to his secondary field. From Ades 1943.

ABBREVIATIONS

A. AI, first auditory area.
AII, second auditory area.
eca, anterior ectosylvian sulcus.
ecp, posterior ectosylvian sulcus.
Ep, posterior ectosylvian area.

pss, pseudosylvian sulcus.
ssa, ssm, ssp, anterior, middle, and posterior branches of the suprasylvian sulcus.
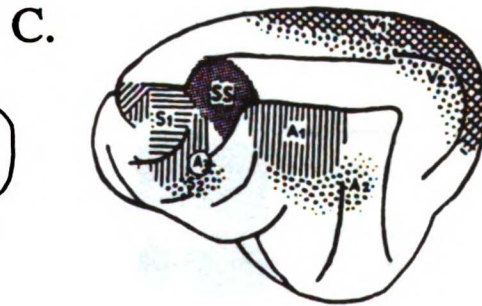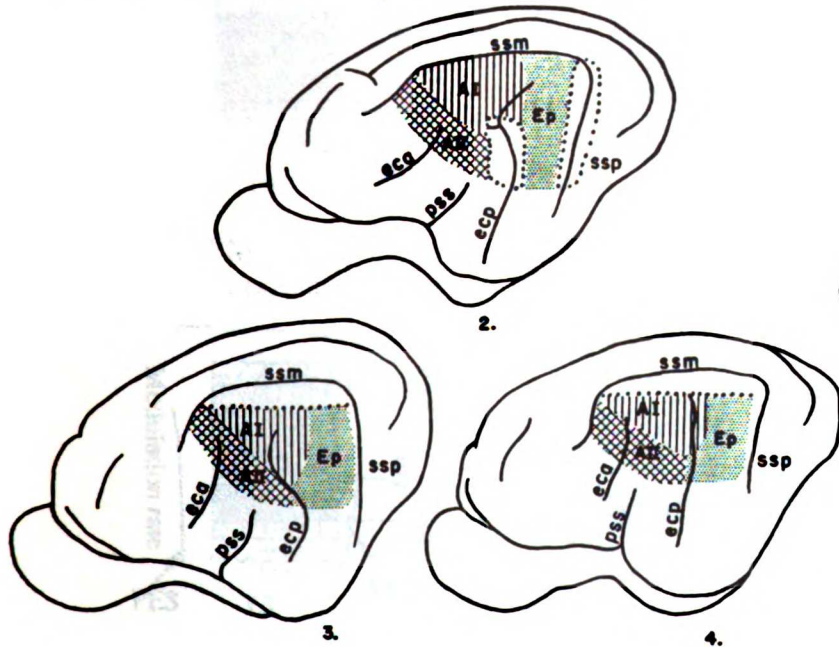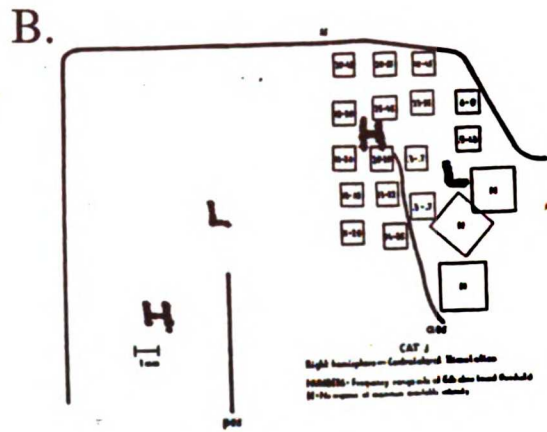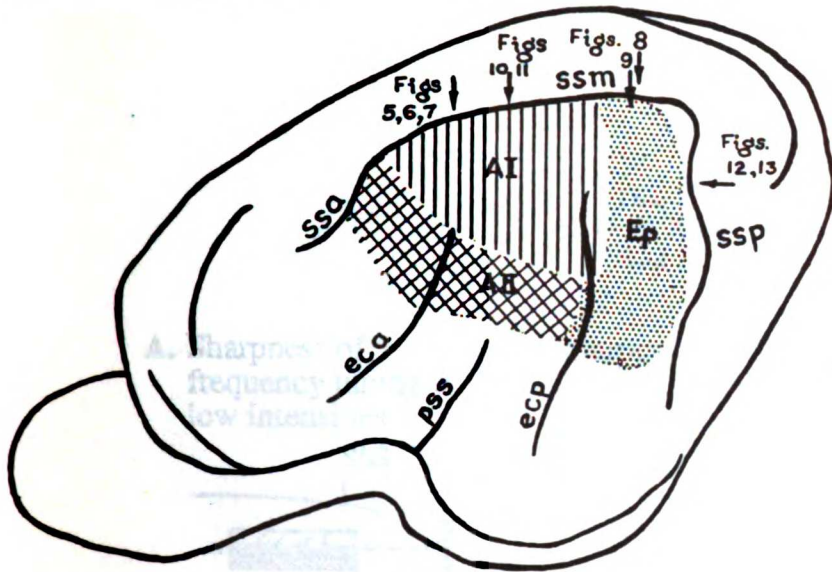
Figure 7:
(A) Rose's cytoarchitectural view of the auditory cortex. Rose's suprasylvian fringe area cannot be shown as it lies within the suprasylvian sulcus. Regions enclosed by dotted lines, or between dotted lines and sulci could not be analyzed because of the angle of sectioning. A summary case (1), plus three individual cases (2-4) are shown. (From Rose 1949.)
(B) Summary of the frequency organization as reported by Hind (1953). The letter "H" and "L" have been added to demostrate his stated conclusions. "H" means site represents high frequencies and "L" means site represents low frequencies. (Adapted from Hind 1953).
(C) Location of the suprasylvian gyrus (SS) response area as shown by Lombrosso (1956). SI, and SII represent the proposed somatosensory areas, and A3 represents a possible third auditory area. (Taken from Lombrosso 1956)
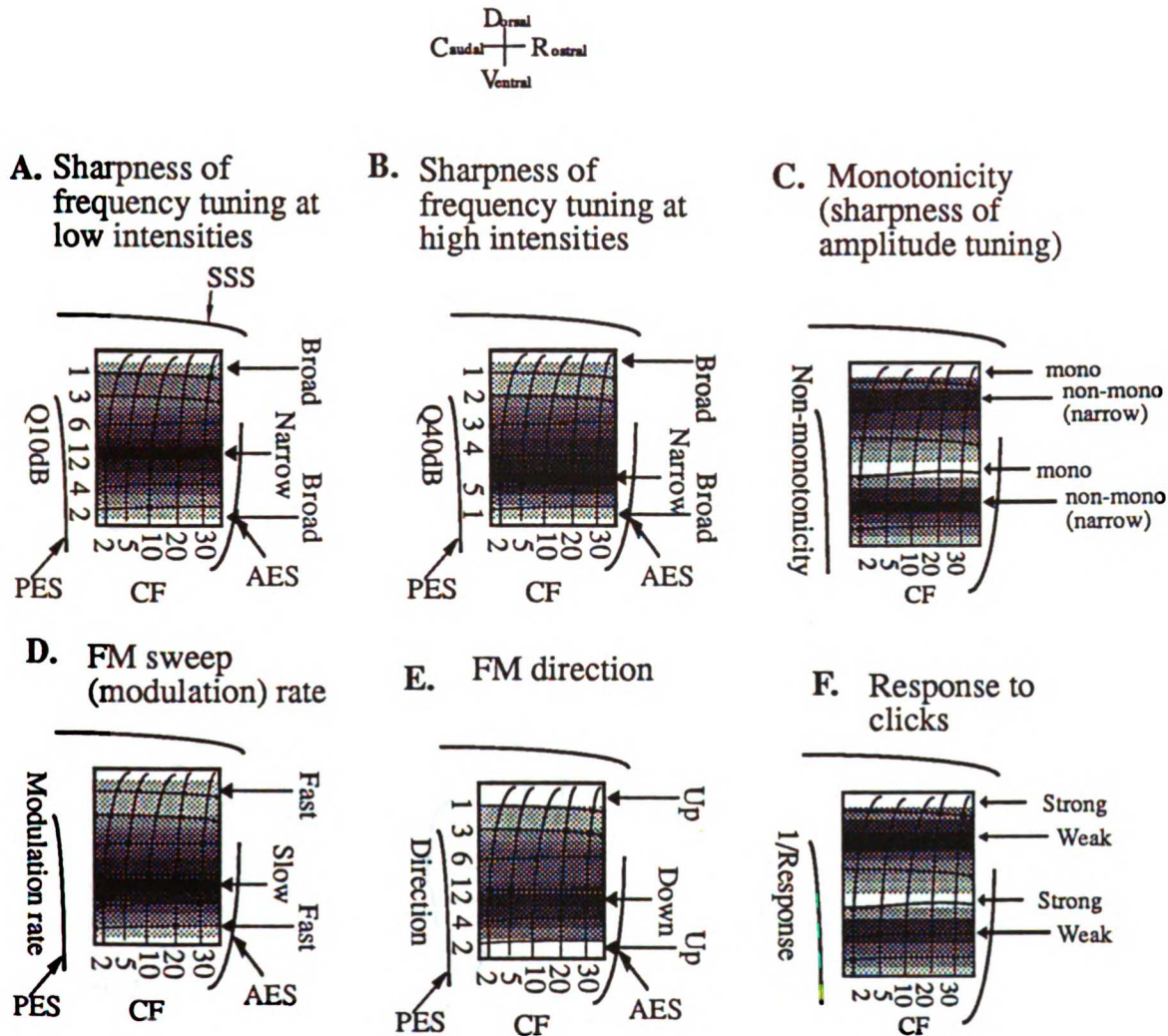
Figure 8: Summary cartoon of multiple unit results of Schreiner, Sutter, Mendelson and Grasse. Shading for each map represents the degree of the property listed to the left of the PES. Q10 map (A) reaches a maxima (Q10max) near the dorso-ventral center of AI. Just ventral of Q10max, Q40 (B) reaches a maxima (Q40max). In either direction from these maxima, responses of multiple unit recordings become more broadly tuned. Roughly lining up with Q40max, is a highly non-monotonic region (C). About 2 to 3 millimeters dorsal to Q40max there is a second non-monotnic region. Topography for FM properties (D,E) roughly follow Q-maps, and click response representation (F) is roughly inverse to non-monotonicity map (i.e., weak click responses are encountered in non-monotonic areas).
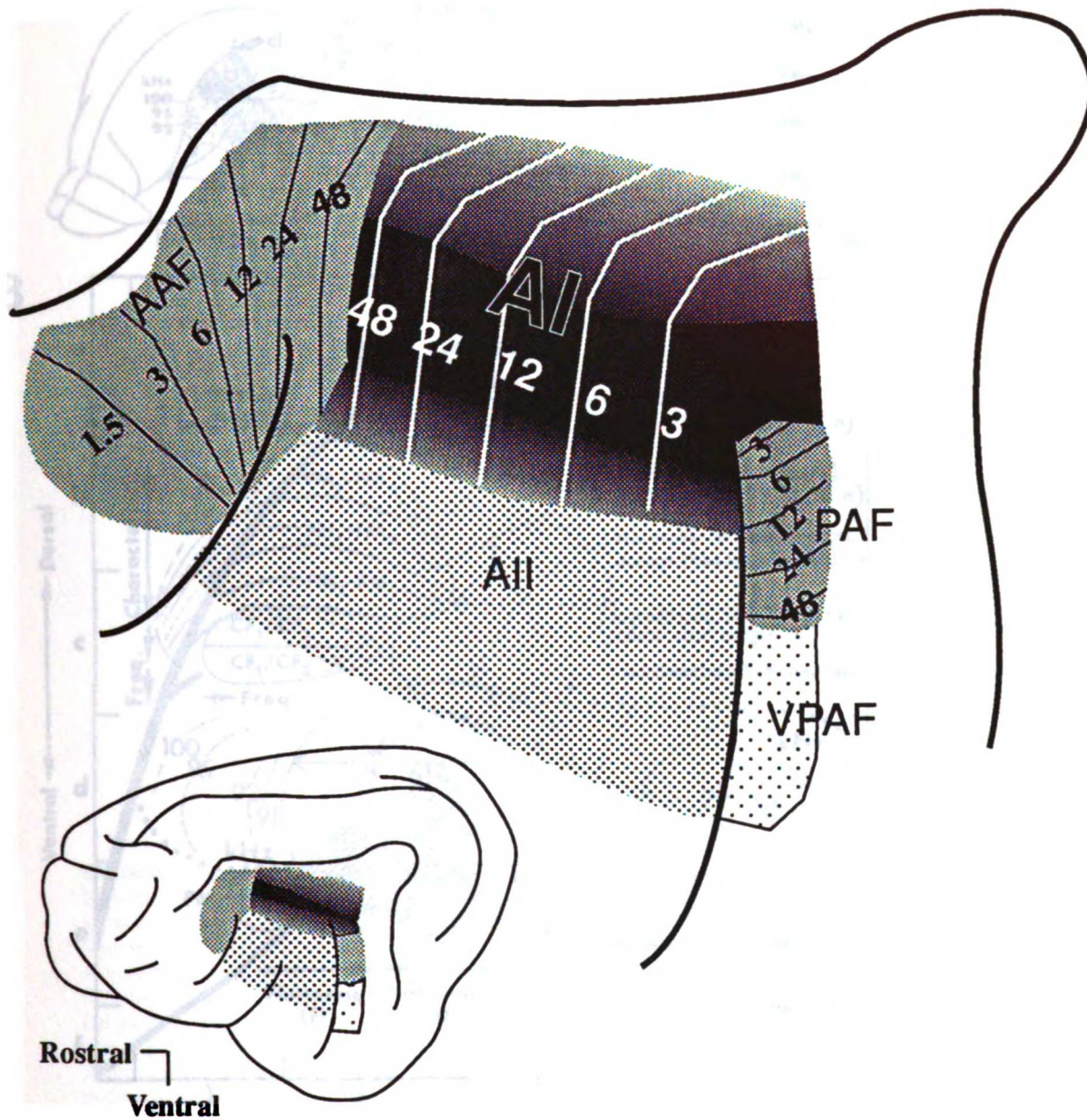
Figure 9: Scematic of improved view of cortex after the multiple unit experiments of Schreiner and colleagues (Shreiner et al. 1988 and Schreiner and Mendelson 1990). Shading within AI correponds to sharpness of frequency tuning. Dark regions are sharply tuned, whereas lighter shaded regions are more broadly tuned. In multiple unit maps, AI is marked by two gradients of sharpness of tuning. It should be noted (as in Fig. 1) that the precise location of AI in all directions is highly variable relative to sulcul pattern. Like CF, the representation of particular tuning sharpness is idiosynchratic across animals. While the general trend of sharp tuning in the center gradually giving wat to broader tuning dorsal and ventral is consistent across animals, the size of the sharply and broadly tuned areas varies considerably between individual cats (Schreiner and Mendelson 1990 and personal observation).
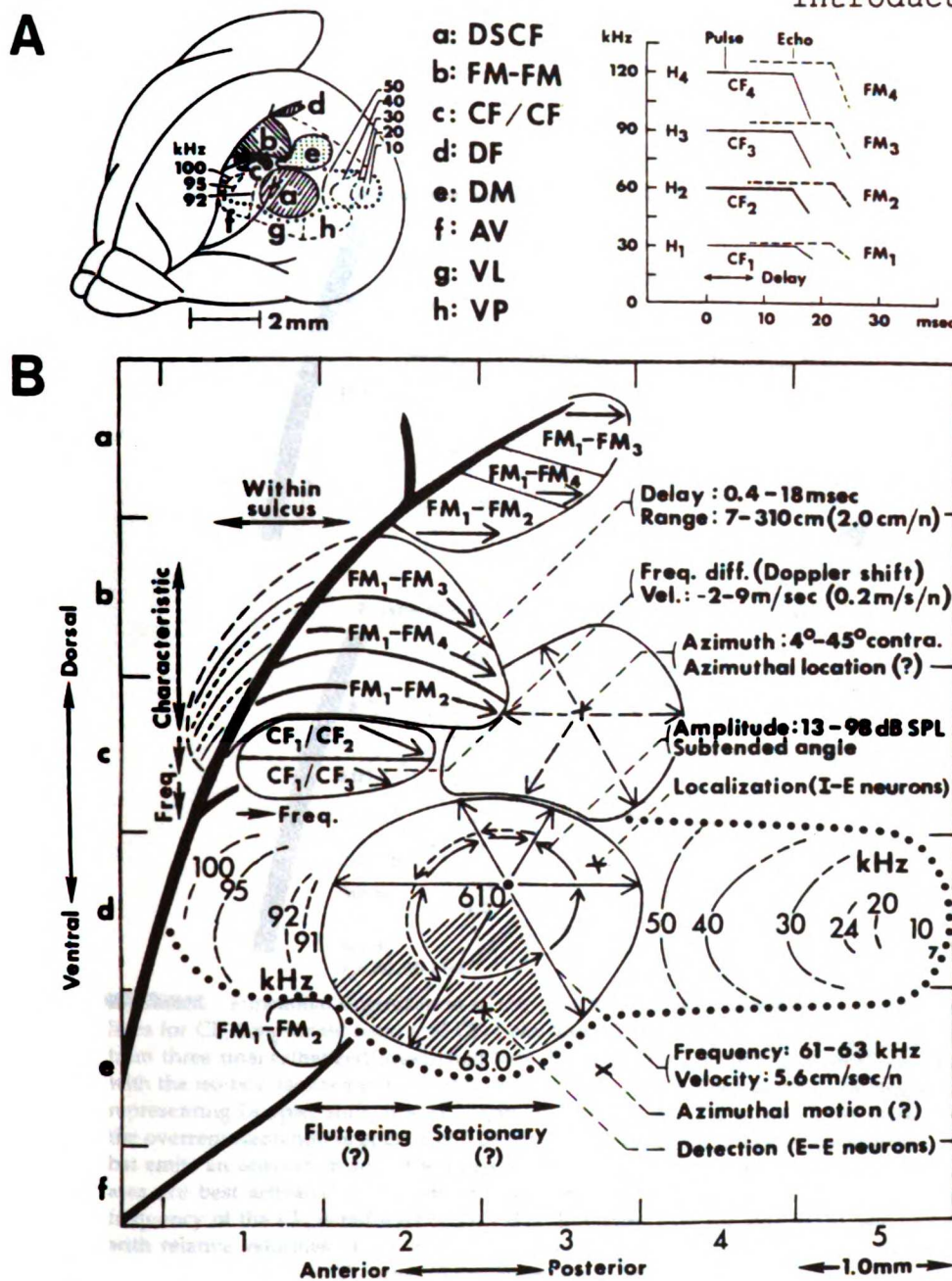
Figure 10:
(A) Left hemisphere of bat cortex. Area marked a-h represent separate areas. Right of figure shows cartooned spectrograph of bats emmitted pulse and doppler-shifted delayed echo.
(B) A doppler shift constant frequency area (DSCF) falls in the center of the tonotopically organized AI and is involved in coding information about the velocity and size of an object. A CF-CF area contains velocity maps for a range of fundamental frequencies (CF1) of echoranging signals (the bat can alter his fundamental frequency for behavioral reasons). FM-FM areas contain maps for time delays between emission and return. These delay maps can be converted to target distance maps. Comments in parenthesis connected to areas with dotted lines summarize information encoded in each functional cortical zone. (From Suga 1984).
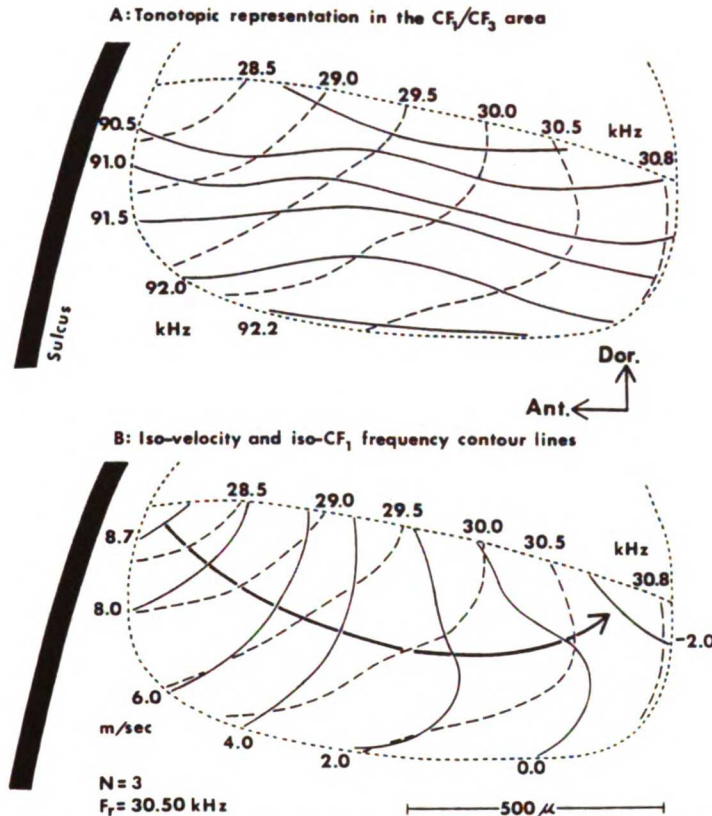
Functional organization of the CF₁/CF₃ area. A: Iso-best-facilitation-frequency contour lines for CF_1 (*long-dashed lines*) and CF_3 (*solid lines*). These contour lines are based on data obtained from three unanesthetized mustached bats. B: Isovelocity contour lines (*solid*) are shown together with the iso-best-facilitation-frequency contour lines for CF_1 (*long-dashed*). The long arrow is the axis representing Doppler shift, that is, target velocity (8.7 to −2.0 m/sec) in the radial direction. Note the overrepresentation of speeds of 0.0–4.0 m/sec. The figure indicates, for example, that when the bat emits an orientation sound with a CF_1 of 30.5 kHz (resting frequency), neurons in the CF₁/CF₃ area are best activated by targets moving with relative velocities of −1.2–2.0 m/sec. When the frequency of the CF_1 is reduced to 29.5 kHz, however, they are stimulated best by targets moving with relative velocities of 3.4–6.1 m/sec. Isovelocity contour lines similar to the above have also been found in the CF₁/CF₂ area. (From Suga et al., 1981.)

Figure 11:
(A) Dual frequency representation in bat CF₁-CF₃ area. One tonotopic axis is dedicated to the lower frequency (approximately 30 kHz) and the other to the higher frequency (approximately 90 kHz) of the two-tone combination necessary to drive neurons at given cortical loci..
(B) Conversion of higher frequency (CF₃) map to Doppler-shift velocitiy map. (Figure with legend taken from Suga 1984, Figure originally published by Suga 1981)
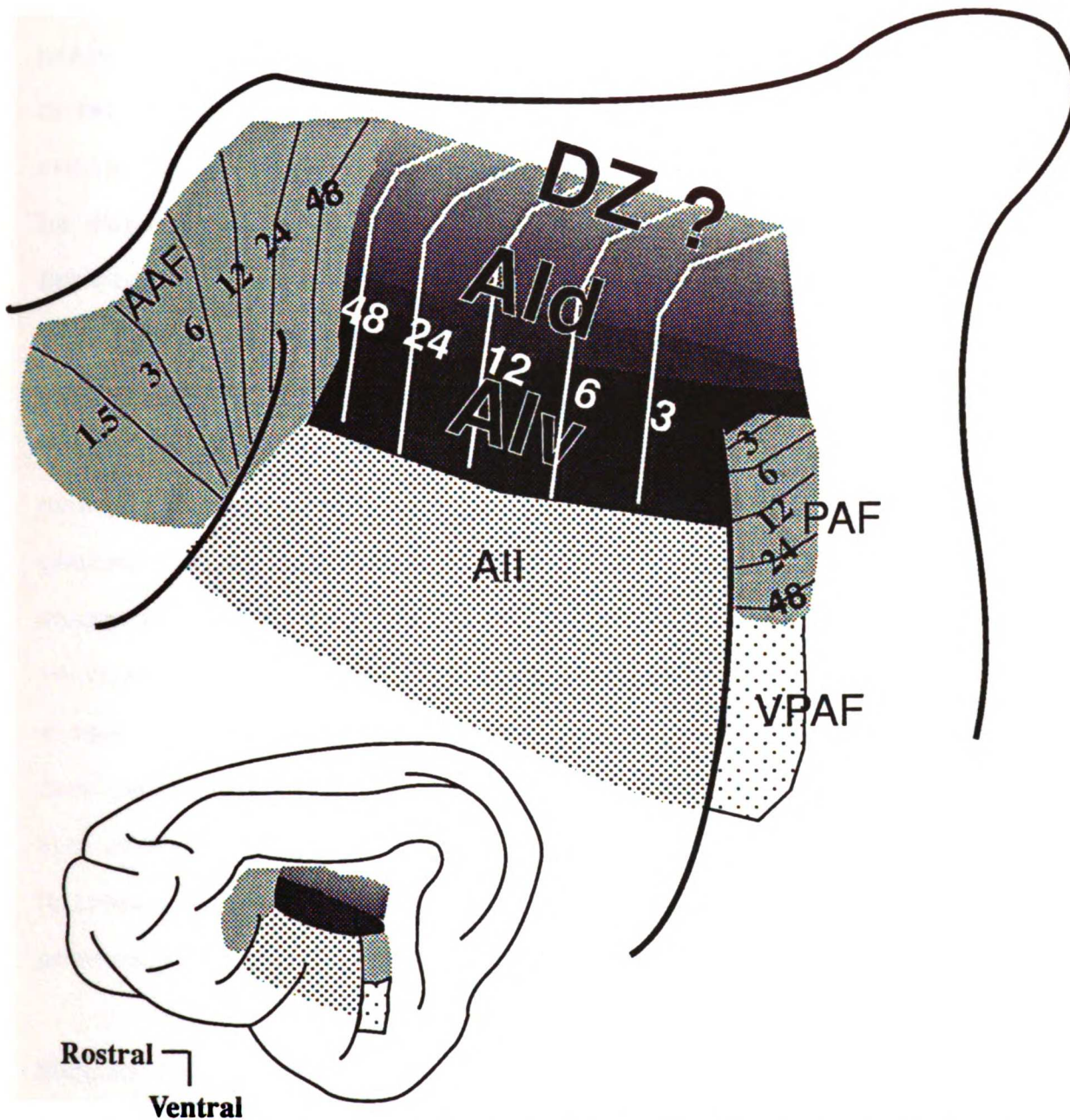
Figure 12: New view of AI as a result of dissertation experiments. Within AI darkness of shading represents sharpness of frequency tuning for **single neurons**. In ventral AI (vAI), there are predominantly sharply tuned neurons. At a region near Q-max (see previous figure), the tuning of single neurons start to follw a gradient towards broader tuning in the dorsal direction. The region with the gradient can be called dAI. The dorsal fringe of AI may give way to another auditory region to which the dorsal zone (DZ, named by Middlebrooks and Zook 1981) is a transition.

Methods

The main goal of this study was to determine the
properties and spatial locations of single neurons in AI. In
order to spatially localize single neurons in AI, some
reliable description of the dorsal-ventral extent of AI must
be obtained. The spatial distribution of the sharpness of
frequency tuning along the isofrequency domain as obtained
with the multiple-unit technique provides such a measure
(Schreiner et al 1988; Schreiner and Mendelson 1990). Our
experimental protocol consisted of the following series of
procedures: (1) surgical preparation of the animal; (2)
photographing the brain surface; (3) pre-mapping the
sharpness of tuning distribution (Q-map in chapter 1, BW map
in chapters 2 and 3); (4) recording from single neurons
whose location relative to the pre-map was known. Recording
from multiple units were only used for the pre-map and are
not addressed in the paper, except when specifically noted.
Unless explicitly stated to the contrary in the text, all
presented data will be from the single neuron data base.

Surgical Preparation

Experiments were conducted on 17 young adult cats.
Anesthesia was induced with an intramuscular injection of
ketamine hydrochloride (10mg/kg) and acetylpromazine maleate
(0.28 mg/kg). After venous cannulation, an initial dose of

sodium pentobarbital (30 mg/kg) was administered. Animals were maintained at a surgical level of anesthesia with a continuous infusion of sodium pentobarbital (2 mg/kg per hour) in lactated Ringer's solution (infusion volume: 3.5 ml/hour) and, if necessary, with supplementary intravenous injections of sodium pentobarbital. Cats were also given dexamethasone sodium phosphate (0.14 mg/kg, IM) to prevent brain edema, and atropine sulfate (1 mg, IM) to reduce salivation. The temperature of the animals was recorded with a rectal temperature probe and maintained at 37.5° C by means of a heated water blanket with feedback control.

The head was fixed, leaving the external meati unobstructed. The temporal muscle on the right hemisphere was then retracted and the lateral cortex exposed by a craniotomy. The dura overlaying the middle ectosylvian gyrus was removed, the cortex was covered with silicone oil, and a photograph of the surface vasculature taken to mark the electrode penetration sites. For recording topographically identified single neurons when brain pulsations were a problem, a wire mesh was placed over the craniotomy and the space between the grid and cortex was filled with a 1% solution of clear agarose. This approach diminished pulsations of the cortex and provided a fairly unobstructed view of identifiable locations across the exposed cortical surface.

Stimulus Generation and Delivery

Experiments were conducted in a double-walled sound-shielded room (IAC). Auditory stimuli were presented via calibrated headphones (STAX 54) enclosed in small chambers that were connected to sound delivery tubes sealed into the acoustic meati [Sokolich 1981, U.S Patent 4251686]. The sound delivery system was calibrated with a sound level meter (Brüel & Kjaer 2209) and a waveform analyzer (General Radio 1521-B). The frequency response of the system was essentially flat up to 14 kHz and did not have major resonances deviating more than +/- 6 dB from the average level. Above 14 kHz, the output rolled off at a rate of 10 dB/octave. Harmonic distortion was at least 55 dB below the primary (depending on the sampling rate and the settings of the antialiasing low-pass filter.)

Tones were generated by a microprocessor (TMS32010; 16 bit D/A converter at 120 kHz; low-pass filter of 96 dB/octave at 15, 35 or 50 kHz). The processor-related useful dynamic range of these stimuli was 78 dB, allowing a 3-bit amplitude resolution at the lowest intensity level. Additional attenuation was provided by a pair of passive attenuators (Hewlett Packard). Stimuli up to 110 dB SPL could be delivered through the speaker system. The duration

of the tone bursts was usually 50 msec, except when it was extended to 85 msec for long-latency responses. The rise/fall time was 3 msec. The interstimulus interval was 400 to 1000 ms.

Recording Procedure

Parylene-coated tungsten microelectrodes (Microprobe Inc.) with impedances of 1.0-8.5 MOhm at 1 kHz were introduced into the auditory cortex with a hydraulic microdrive (KOPF) remotely controlled by a stepping motor. All penetrations were roughly orthogonal to the brain surface. The recordings reported here were derived at intracortical depths ranging from 600 to 1000 microns, as determined by the microdrive setting. Neuronal activity of single units or small groups of neurons (2-6 neurons) were amplified, band pass filtered, and monitored on an oscilloscope and an audio monitor. Multiple unit recordings were employed to map the sharpness of tuning across AI. Recording multiple units allowed for collection of enough data to pre-map 10 to 30locations in a reasonable amount of time (less than 8 hours). Spike activity was isolated from the background noise with a window discriminator (BAK DIS-1). The number of spikes per presentation and the arrival time of the first spike after the onset of the stimulus were

recorded and stored in a computer (DEC 11/73). The recording window had a duration of 50 to 85 ms, corresponding to the stimulus duration and excluding any offset response.

Frequency response areas

Frequency response areas (FRA's) were obtained for each single unit. The method is similar to that originally used by Evans (1975; 1979). To generate an FRA, at least 675 different tone bursts were delivered to the animal. Tone bursts were presented in a pseudorandom sequence of different frequency/level combinations selected from 15 level values and 45 frequency values. Steps between consecutive levels were 5 dB, resulting in a dynamic range of 75 dB.

The frequency range covered by the 45 frequency steps was centered around the estimated characteristic frequency (CF) of the recording site and covered between 2 and 5 octaves, depending on the estimated width of the frequency tuning curve. Stimulus frequencies were chosen so that the 45 presented frequencies were spaced an equal fraction of an octave over the entire range. For most cases this provided 0.067 octave resolution over a total of 3 octaves.

To measure inhibition and facilitation, a two tone simultaneous masking paradigm was employed. The probe signal

was a CF tone burst presented at the minimum intensity
required to drive the neuron repetitively (usually 10-20 dB
above threshold). This constant tone burst was presented
simultaneously with a variable masker tone. The masker tones
were administered for 675 level/frequency combinations as
described for pure-tone FRA's.

Data Analysis

From the responses to 675 different frequency/level
combinations, an objectively determined frequency response
area (FRA) was constructed for every recording site. The
left side of Fig. 13 shows an examples of reconstructed
frequency response areas obtained in multiple (A) and single
(B) units in AI. The ordinate corresponds to the sound level
of the tone-burst stimulus, while the abscissa corresponds
to the frequency. All presented stimuli would be represented
by a 15 (ordinate) by 45 (abscissa) grid with equal spacing
and size of elements. Responses are represented at the point
of intersection of the intensity and frequency of each
presented stimulus. The length of the line at each
intersection is proportional to the number of spikes
discharged in response to the stimulus. No line for a given
point of stimulus presentation represents no response.
Usually each stimulus was presented once. If the resulting

FRA was not well defined, the process was repeated with the same 675 stimuli and the resulting evoked activity was added to the first. Occasionally FRA's were re-recorded approximately one to two hours after the original FRA (see table 3 in Chapter 1's DISCUSSION).

A frequency tuning curve (FTC) was extracted from the FRA using an objective method. For the response threshold, a computer program defined the iso-response criteria as the estimated spontaneous rate plus 20% of the peak rate. The true spontaneous rate was not measured, but was approximated by averaging the number of spikes from a 9 by 5 (45 point) region corresponding to the lower left most corner on the FRA. Controls with audio-visual response monitoring confirmed that this region was located outside the area of driven activity.

Response measures were calculated for each point on the FRA by weighted averaging with the eight nearest neighbors of the point. Responses directly above, below, right, and left of the response point were multiplied by 0.25. Responses to the 4 points diagonal to the response point were multiplied by 0.125. The response of the actual point was added to the eight weighted measures from above, and the resulting number was divided by 2.5 to give a spike count. This criterion was robust, yielding comparable tuning curves for the wide range of FRA's recorded. The range included

both high spontaneous multiple unit (Fig. 13A) as well as low spontaneous single neuron (Fig. 13B) recordings. From these objectively determined single tone frequency tuning curves (e.g., right side of Fig. 13) several response properties were measured.

a) Characteristic frequency (CF) = the stimulus frequency with the lowest sound pressure level necessary to evoke neuronal activity.

b) Strongest response frequency (SRF) = the stimulus frequency which evoked the greatest given response at a given intensity value.

c) Minimum threshold = lowest level associated with an activity in the frequency response area that is clearly stimulus evoked.

d) Q 10 dB = the CF divided by the bandwidth of the frequency response area 10 dB above the minimum threshold.

d) Q 40 dB = the CF divided by the bandwidth of the frequency tuning curve 40 dB above the minimum threshold. This measure and $Q_{10\ dB}$ were only used for forming the multiple-unit Q-map. (Multi-peaked multiple units were uncommon and not used in forming the Q-maps in chapter 1)

e) Bandwidth (BW_{**}) = the bandwidth (in octaves) of the response at a given sound pressure level above threshold. For multi-peaked units the entire bandwidth encompassing the

excitatory response (total bandwidth) was measured, as well
as the bandwidth of each individual peak.

f) Latency = The response latency, measured by
averaging the latent period to the first spike of a point on
the tuning profile with its two frequency neighbors
(directly right and left to the point) and the 3 latencies
to the same frequencies at the next highest level (directly
and diagonally above the point).. With this procedure,
latency versus level functions (10 dB resolution) were
derived. Two measures of response latency were determined
from these functions. Minimum latency is defined as the
shortest latency obtained for such a profile; L_{30} is the
response latency obtained 30 dB above a given peaks minimum
threshold.

g) monotonicity ratio = the number of spikes elicited
at the highest intensity level divided by the maximum
response of the neuron. Spikes are added over 1/4 octave of
frequency (usually 5 stimulus frequencies) and 15 dB of
intensity (usually 3 intensities) for a total of 15
repetitions per point (see chapter 3 Fig. 41).

Topographical Classification:

Topographical classification of responses is discussed
in detail for particular sections in which topography was

used. In general, a multiple unit map (usually of sharpness

of tuning to pure-tones -- Q or BW) was made within the

isofrequency domain. This map was then used as a reference

to pool single unit data across animals.
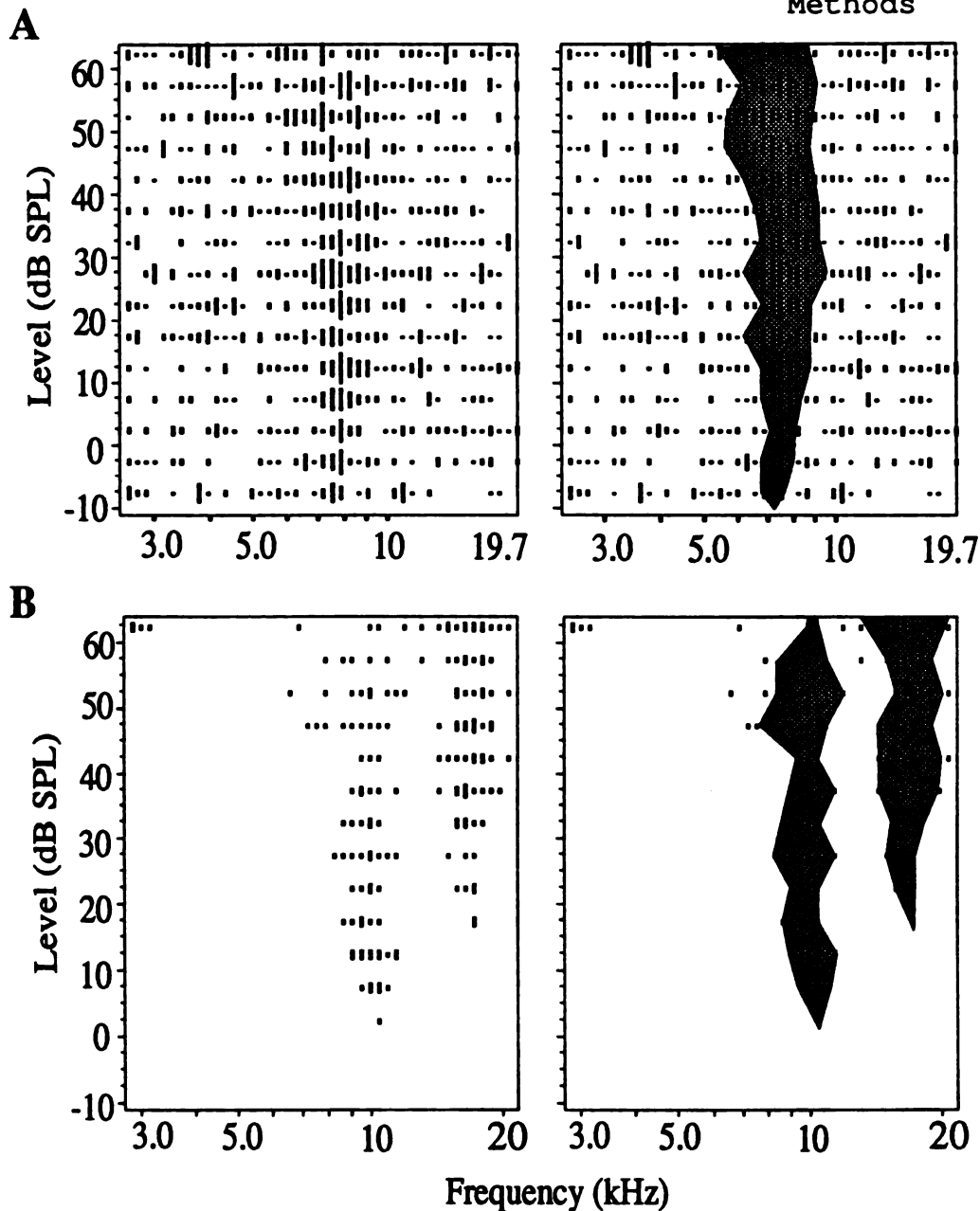
Figure 13: FRA's (left) and corresponding tuning curves (shaded area in right) for a multiple unit (A) and single neuron (B) in AI. The level and frequency axes correspond to stimulus parameters. Length of lines in the FRA are proportional to the numbers of spikes fired for the stimulus at frequency and level. No line for a given stimulus frequency combination signifies no response within a peristimulus time window. The frequency response areas are defined by 675 different stimuli for all single neuron and multiple units recorded in this study. Stimuli were presented at 15 different levels spaced 5 dB apart and at 45 frequencies equally spaced on a logarithmic scale. Tuning curves were determined by the objective isoresponse criterion of the spontaneous rate plus 20% of the maximum response. Responses above this criterion, were considered part of the frequency tuning curve. (A) is the single-peaked tuning curve for a high spontaneous multiple unit response and (B) is the multi-peaked tuning curve of a low spontaneous single neuron response.

CHAPTER 1

Physiology And Topography Of Neurons With Multipeaked Tuning Curves In Primary Auditory Cortex (AI) Of The Cat

SUMMARY AND CONCLUSIONS

1.   The physiology and topography of single neuron responses along the isofrequency domain of the middle and high frequency portions (CF's > 4 kHz) of the primary auditory cortex (AI) were investigated in the barbiturate-anesthetized cat. Single neurons were recorded at several locations along the extent of isofrequency contours,defined from initial multiple-unit mapping (Schreiner and Mendelson 1990). For each neuron a high resolution excitatory tuning curve was determined, and for some neurons high resolution two-tone tuning curves were recorded in order to measure inhibitory/suppressive areas.

2.   A physiologically distinct population of neurons was found in the dorsal part of AI of the cat. These neurons exhibited two or three distinct excitatory frequency ranges, while most neurons in AI responded with excitation to a single narrow frequency range. These were called multi-peaked neurons because of the shape of their tuning curves (Oonishi and Katsuki 1965). At frequencies between the excitatory regions, the multi-peaked neurons were inhibited or unresponsive.

3.   Multi-peaked neurons exhibited several distinct threshold minima in their frequency tuning curves. Most of the multi-

peaked neurons (88%) displayed two frequency minima, while the rest exhibited three minima.

4. The frequency separation between threshold minima was less than one octave in 71% of the double-peaked neurons recorded. Occasionally, the frequency peaks of these neurons closely corresponded to a response to second and third harmonics without a response to the fundamental frequency.

5. Multi-peaked neurons exhibited a wide range of total bandwidths (highest excitatory frequency minus lowest excitatory frequency expressed in octaves). Bandwidths of the isolated peaks within the same neuron were also quite variable.

6. Response latencies to tones with frequencies within each peak of a multi-peaked neuron could vary considerably. In 71% (17) of the neurons, tones corresponding to the high frequency peak (CF_h) elicited a longer response latency (4 msec or longer) than those corresponding to the low frequency peak (CF_l).

7. Inhibitory/suppressive bands, as demonstrated with a two-tone paradigm, were often present between the peaks. Typically, neurons with excitatory peaks of similar response latencies showed an inhibitory band located between the peaks.

8. Ninety percent of the topographically localized multi-peaked neurons were in the dorsal part of AI (more than 1 mm

dorsal to the maximum in the sharpness of tuning map). While these neurons were restricted to dorsal AI, only 35% of neurons in this region were multi-peaked.

9. Multi-peaked neurons could show decreased response latencies and thresholds to two-tone combinations.

10. These results suggest that the subpopulation of multi-peaked cortical neurons, located in the dorsal part of AI, may be sensitive to specific spectro-temporal combinations in the acoustic input. If so, these neurons may physiologically parallel combination sensitive neurons found in bats (Suga et al. 1979) and may be involved in complex sound processing.

INTRODUCTION

Neurons that preferentially respond to combinations of spectral parameters are potentially useful for the integration and classification of acoustical signals with complex harmonic, formant, or resonance structures. Most neurons in the auditory cortex of cats (Oonishi and Katsuki 1965; Goldstein et. al 1968; Abeles and Goldstein 1970, 1972; deRibaupierre et. al 1972; Phillips and Irvine 1981) and monkeys (Funkenstein and Winter 1973; Pelleg-Toiba and Wollberg 1989) possess response areas centered around a single frequency. In these studies, however, a small percentage of neurons was recorded that responded to several distinct frequency ranges, separated by non-excitatory frequencies. These neurons have been called "multiple peak" (Oonishi and Katsuki 1965) or "multi-peaked" (Abeles and Goldstein 1972) neurons because their frequency tuning curves display two or more clearly separated frequency threshold minima. Multi-peaked neurons represent a separate functional class of cells and are potential candidates for neurons that process complex sounds.

In echolocating mustached bats, *Pteronotus parnellii*, neural responses with two distinct frequency peaks have been reported (Suga et al. 1979,1983; Suga and Tsuzuki 1985). These neurons respond best to the presentation of a stimulus

with energy restricted to both frequency regions of the two peaks in the tuning curve. These multi-peaked neurons can encode the velocity of a biosonar target through analysis of Doppler-shifted echoes, and are topographically organized within a restricted area in the mustached bat's auditory cortex (Suga et al. 1979,1983).

Although there is extensive literature on the properties of single-peaked neurons in the auditory cortex of non-echolocating mammals such as the cat and monkey, little is known about the properties and spatial distribution of multi-peaked cortical neurons in these species. In the past, knowledge of functional organization in the cat's primary auditory cortex (AI) has been limited to the well-established tonotopic organization in the rostro-caudal dimension (Merzenich et al. 1975; Reale and Imig 1980) and to the topographic organization of binaural response properties (Imig and Adrien 1977; Middlebrooks et al. 1980). More recently, the dorsal-ventral extent of AI has been defined by a gradient in multiple-unit sharpness of frequency tuning or bandwidth (Q-map)(Schreiner et al. 1988, Schreiner and Mendelson 1990). At the dorsal and ventral ends of AI, multiple-unit recordings are broadly tuned. Clusters become more sharply tuned, showing an increase in Q_{10dB} and Q_{40dB}, as electrode penetrations progress toward the center of the dorsal-ventral extent of the isofrequency domain of AI. A

combination of tonotopic and excitatory bandwidth
organization now provides a more detailed physiological
framework to explore the functional organization of AI.

In this study, experiments were performed to explore the
properties and spatial distribution of isolated single
neurons with multi-peaked tuning curves across the dorsal-
ventral extent of cat AI. A multiple-unit Q-map was obtained
to physiologically define the dorsal-ventral extent of AI so
that the position of single neurons within the isofrequency
domain could be reliably measured . A preliminary disclosure
of some of the results presented in this paper has appeared
in abstract form (Sutter and Schreiner 1989).

RESULTS

A total of 116 single neurons from 8 cats were analyzed for this study. Twenty-four (20.7%) of the 116 neurons had multi-peaked tuning curves. Multi-peaked classification was based on FRA analysis that was performed blindly with respect to neuron location. Neurons were classified as multi-peaked if two or more frequency regions to which the neuron responded were separated by a frequency range that elicited no driven activity. To eliminate any possibility of sound system artifact (see DISCUSSION) two criteria were employed: (1) the thresholds of at least two of the peaks had to differ by less than 40 dB, and (2) separation between the peaks had to be maintained for levels greater than 15 dB above the neuron's intensity threshold.

Neurons whose FRA showed multiple response maxima within a complex but continuous frequency receptive field were classified as single-peaked. One such neuron responded best to tones between 4 and 6 kHz, and also responded well to tones between 8 and 10 kHz (Fig. 14). The response to tones between 6 and 8 kHz was weaker. This neuron, however, was not classified as multi-peaked because the firing rate within this complex FRA never fell below the response criterion used to estimate the FTC (Figure 14B). This neuron failed to meet the second standard for multi-peaked classification; that is,

the separation of the peaks was not maintained at intensity levels greater than 15 dB above the threshold.

The neuron whose FRA is depicted in Fig. 13B fulfilled both criteria for multi-peaked classification. The non-responsive area between the peaks was maintained from 15 to 60 dB above the neurons threshold, meeting criterion (2), and the thresholds of the two peaks were less than 40 dB apart, meeting criterion (1).

A large variety in the shapes of multi-peaked tuning curves were observed. The tuning curves of all the encountered multi-peaked neurons are shown in Fig. 15. While most multi-peaked neurons had two distinct peaks, 3 neurons had 3 peaks (Fig, 15 G, H ,I). In some neurons each peak was sharply tuned (less than 0.4 octaves at 30 dB above threshold, panels A-I, K). Occasionally, sharp tuning was accompanied by non-monotonic rate-level functions (D, E), although non-monotonicity was not restricted to sharply tuned neurons (J). These highly non-monotonic neurons displayed circumscribed FRA's and FTC's since they failed to respond to stimuli presented at high intensity levels. Several neurons (P, S-V, X) displayed a broad, low threshold, low frequency peak accompanied by a narrower, high threshold, high frequency peak. Characteristic frequencies of the peaks of some neurons (E, F) were similar, while others (K) were

widely separated. While all multi-peaked neurons displayed distinct multiple CF's, they did not exhibit uniform frequency tuning breadth, intensity threshold properties, or CF ratios.

Frequency Separation of Peaks

The CF's of the individual peaks of a multi-peaked neuron were usually within an octave of each other. For some neurons, the CF's of the peaks approximated the second and third harmonics of a fundamental frequency to which the neuron did not respond (Fig. 16A). This neuron (also see Fig. 15B) was exceptional in that the tip of its tuning curve shifted sharply towards lower frequencies, although in almost all other neurons the CF and the strongest response frequency (SRF) 10 dB above threshold were within 0.1 octaves of each other. Therefore, SRF rather than CF is used in the following discussion of the neuron depicted in Fig. 16A. At a level of 10 dB above threshold, the tuning curve displayed SRF's at 26 and 38 kHz, respectively. The ratio of the peaks, SRF2/SRF1, was 1.46, which is close to the ratio of 1.5 characterizing second and third harmonics. Figure 16B shows a multiple-unit tuning curve that was recorded at the same location in the cortex. To obtain this plot, the window

discriminator was adjusted to allow three neurons to be

recorded at once. The multiple-unit response

contained the previous frequency response areas plus a new

response area corresponding to the fundamental frequency of

approximately 13 kHz.

Multi-peaked neurons showed a wide range of CF ratios,

but most peaks (71% in neurons with 2 peaks) were within an

octave of each other (Fig. 17). For all multi-peaked neurons,

the median CF ratio was 1.56 with the 25th and 75th

percentiles at 1.46 and 2.16, respectively (see Table 1 : for

percentiles of all other presented median values see Tables 1

and 2). A ratio of 1.5 roughly corresponds to second and

third harmonics in a harmonic complex. In the three neurons

with three distinct peaks, the CF ratios (CF_h/CF_m : CF_m/CF_l :

CF_h/CF_l) were 1.27:1.31:1.67, 1.56:1.35:2.10, and

1.34:1.37:1.84.

Relative Thresholds of Peaks

On the average, CF_h displayed a slightly higher

threshold than CF_l, although there was a wide range of

relative threshold values. The distribution of the difference

in response threshold (threshold difference = threshold to

CF_h tones minus threshold for CF_l tones) for all neurons with

two peaks displays this difference (Fig. 18). The mean

threshold difference was 4.0 dB with a standard deviation of
16.5 dB. The median threshold difference was 5.0 dB (Table
1). The threshold ratios (CF_1-threshold/ CF_m-threshold/ CF_h-
threshold, where the CF_1 threshold is assigned a reference

value of 0 dB) for the three triple-peaked neurons was
0/15/25, 0/0/-20, and 0/15/15.

Sharpness of Tuning

Each peak of the FTC can be assigned a bandwidth value.
It is apparent that the sharpness of tuning for the peaks
containing CF_1 (BW_1), CF_h (BW_h), or CF_m (BW_m) varied

considerably (Fig. 15). In general, each of the individual
bandwidths within multi-peaked neurons (BW_1, BW_h, and BW_m)

was comparable to the bandwidths of single-peaked neurons.
The histogram in Fig. 19a depicts the distribution of

bandwidth values for all individual peaks within multi-peaked

neurons. Bandwidth values were derived 30 dB above the

threshold, as determined from the FTC for individual peaks,

and are expressed in octaves. For several peaks (1 low, 1

middle, and 3 high frequency peaks) bandwidth could not be

determined since, at 30 dB above the peak's threshold, there

was already substantial overlap with the response area of a

neighboring frequency peak.

The median for BW_l, BW_m, and BW_h combined was 0.27 octaves (Table 2). The corresponding median $Q_{30 \ dB}$ value would be approximately 5. For single-peaked neurons , the median bandwidth was 0.35 octaves (Fig. 19B). This corresponds to a median $Q_{30 \ dB}$ value of approximately 3 to 4. While the median bandwidth for single-peaked neurons was greater than BW_l, BW_m, and BW_h for multi-peaked neurons, the difference was not statistically significant (p= 0.11, Mann-Whitney test).

The distribution of "total excitatory bandwidth" for multi-peaked neurons was highly variable (Fig. 19C). This measure reflects the low and high frequency excitatory threshold for the entire FRA, and includes the non-responsive frequency range between individual peaks. This measure was significantly broader than the bandwidth of single-peaked neurons (p = 0.0001, Mann-Whitney). The median total bandwidth for multi-peaked neurons was 1.17 octaves (Table 2). The median BW_l was 0.27 octaves, while the median BW_h was 0.23 octaves (Table 1). This difference was not statistically significant (p = 0.21 paired T-test).

Response Latency

Latencies to CF_h tones were usually longer than latencies to CF_l tones. Latency versus level plots at the

CF's of each peak for four representative multi-peaked

neurons are displayed in Fig. 20. The neuron, whose latency

vs. level plot is shown in Fig. 20A, had a relatively short

latency, while those of Figs. 20B and 20C had longer latency

responses. At 30 dB above threshold, these three neurons had

longer latencies for the CF_h tones. In the neuron whose

latency vs. level function is shown in Fig. 20C, however, the

latencies to CF_l and CF_h tones approached an identical

minimum latency asymptote at high intensities. In contrast,

the latency plots shown in Figs.20 A and B remained separated

and parallel at all tested intensities. Some neurons had

similar latencies for CF_l and CF_h over a wide range of levels

(Fig 20D). For this neuron, with a peak separation of 0.57

octaves the latency was approximately 1 to 2 msec shorter for

CF_h than for CF_l.

Of the two latency measures, minimum latency and latency

30 dB above threshold, the latter measure proved to be the

most reliable and valid measure. The use of minimum latency

was not desirable because stimuli were presented over a 70 dB

range. Minimum latency usually occurred at the higher

intensity levels, and often at those intensities the boundary

between individual peaks could not be clearly determined.

Seventeen (70.8%) of the multi-peaked neurons had a

longer latency to CF_h tones, as measured by L_{30}, than to CF_l

tones. Seven of 24 neurons (29.2%) had the reverse

relationship. The mean latency difference (CF_h tone latency minus the CF_l tone latency) was 4.1 msec. with a standard deviation of 6.8 msec. The median latency difference was 2.7 msec (Table 1). The latency difference between peaks was statistically significant (p=0.0067, paired T-test).

Multi-peaked neurons tended to have longer latencies than single-peaked neurons (compare Figs. 21 A and B). For CF tones of all the peaks of multi-peaked neurons, the median latency was 19.6 msec (Fig. 21A). The median latency for CF_l tones was 18.7 msec, and for CF_h tones, 22.6 msec. (Table 1). For single-peaked neurons (Fig. 21B), the median latency was 16.5 msec (Table 2). The longer latency of multi-peaked neurons was statistically significant (p=0.0051, Mann-Whitney test).

Habituation to Repetitive Tones

For neurons in which CF_h tones elicited a long latency response (greater than 25 msec), the response to higher CF tones was more subject to habituation than was the shorter latency CF_l response. With repetitive stimulation (1/second), a neuron's threshold to the CF_h tones would often increase.

Most multi-peaked neurons showed some habituation to repetitive presentation of a constant probe tone. Occasionally this could result in an inability to drive the

neuron repeatedly. The inhibitory characteristics of the neuron could not be reliably determined in these cases (5 neurons), since the applied two-tone paradigm required a large number of presentations (675) of an excitatory (probe) tone. Often the habituation effect was more subtly recorded as an increase in the latency to the constant probe tone, compared to the latency recorded in the random order single tone tuning curve (Fig. 24B).

Two-Tone Suppression

Complete two-tone response properties were obtained for 14 multi-peaked neurons. Two-tone inhibition/suppression was defined by a 50% reduction of the activity generated by the probe tone alone in the habituated state. When the habituated rate was less than 2 spikes per frequency/amplitude bin, the activity was averaged (weighted) across 9 neighboring frequency and amplitude conditions to assess two-tone suppression properties. Figure 22 shows the single- (A,D) and two-tone (B,E) FRA's of two single neurons. For each neuron, probe tone activity was completely eliminated in the frequency/amplitude region between the peaks. In the neuron depicted in Fig. 22E, a low frequency inhibitory/suppressive sideband completely eliminated the probe-tone-driven activity, while in the example in Fig. 22B only a weak low

frequency suppression area is present. The low frequency suppression area in B was confirmed in another two-tone FRA under the same conditions with finer frequency resolution (not shown).

Thirteen of the fourteen neurons with two-tone response areas exhibited an upper and/or lower suppressive sideband(s) outside the excitatory range. Ten (71.4%) neurons showed inter-peak inhibition/suppression, defined as an inhibitory/suppressive area located between two excitatory peaks. Some inhibitory areas seemed to be carved out of a broader excitatory area (Fig. 22), whereas other inhibitory areas appear to be more classical inhibitory sidebands (Fig. 22 and 23). Several neurons exhibited relatively complex spectral properties in their inhibition (Figs. 22 and 23). These neurons could display multiple high or low frequency inhibitory bands (Fig. 23C), "sidebands" that did not abut the excitatory area (Fig 22C), or highly non-monotonic inhibition (Fig. 23 B and D). At high intensity levels, the neuron shown in Fig. 23B had strong upper and lower sidebands surrounding a narrow single-peaked excitatory area; at lower intensities, however, inter-peak inhibition was apparent resulting in a multi-peaked excitatory area.

Relation of Inter-Peak Latency Differences to CF Ratio and Interpeak Inhibition

The latency differences observed between responses to CF tones from the low and high frequency peak were found to relate to other response properties of a neuron. Neurons with a wider separation of CF peaks had longer latency differences, favoring the high frequency peak, than those neurons with narrow separation of peaks. Neurons with a CF ratio of 1.70 or greater (N=11) had a median latency difference of 7.3 msec, i.e., the high frequency peak had on the average a longer response latency. Only one of these neurons displayed a latency difference favoring the low frequency peak. Neurons with CF ratios below 1.7 (N=13) had a median latency difference of 1.1 msec, i.e., the average response latency was only slightly longer for CF_h tones. Six (46%) of these neurons had latency differences favoring the low frequency peak. The variation in mean latency differences for narrowly and broadly separated peaks was statistically significant (p= 0.0059, Mann-Whitney).

The presence of inhibitory/suppressive sidebands might also relate to the observed latency differences. The four neurons that displayed no inter-peak inhibition had latency difference values of 3.3, 10.0, 12.6, and 16.2 msec (mean 10.5 msec). The mean latency difference for neurons with

inter-peak inhibition (4.7 msec, N=10) was considerably
smaller.

Two-Tone Enhancement

Eleven (78.6%) of the fourteen multi-peaked neurons for
which a two-tone FRA was derived displayed areas with
relative enhancement during two-tone stimulation. These
additional responses did not appear or were extremely weak in
the single-tone tuning curve, but were clearly expressed in
the two-tone response area. They were not facilitatory by
classic definition, because the combination of tones in the
partially habituated state of the two-tone paradigm did not
necessarily drive the neurons better than the single tone
alone in the unadapted state or the sum of the two tones in
the adapted state. The applied two-tone paradigm could not
measure unadapted response without an extremely long
interstimulus interval (greater than 10 seconds), and
consequently long recording periods (greater than 2 hours)
would be needed to collect a 1-repetition FRA. Instead
response regions with enhanced activities were identified by
an increase in the adapted probe-tone response attributed to
the second tone.

Rather than displaying an increased probability of
firing, the responses to the combined tones could show a

decreased latency compared to the constant tone response in the adapted state. As the intensity of the enhancing tone increased, the latency decreased further (Fig. 24).

Enhancement effects were not restricted to multi-peaked or dorsal area neurons. For example, a neuron from the dorsal third of AI that was classified as single-peaked showed two-tone enhancement in a separated frequency area, outside the normal tuning curve (Pure-tone FRA in Fig 25A, Two-tone FRA in Fig. 25B). The outlined region in Fig. 25C represents the single-tone excitatory tuning curve. The dark area represents a low frequency suppressive sideband and the white areas represent regions of two-tone enhancement. Many neurons (9/14) displayed a lowering of the threshold of the non-probe frequency upon two-tone stimulation (Fig. 26). In combination, these effects are suggestive of integrative or combination-sensitive response behavior.

Topography of Tuning Sharpness

In six of the eight experiments, the dorsal-ventral extent of AI along the isofrequency domain was physiologically characterized to provide a common reference for recording sites across animals. The reference system for the topographical experiments was based on the observation that the integrated excitatory bandwidth of multiple-unit

tuning curves changes systematically across the isofrequency domain of AI (Schreiner et al. 1988; Schreiner and Mendelson 1990). The dorsal-ventral alignment of the recording sites roughly approximated the orientation of isofrequency contours. In those cases where the isofrequency lines were not perfectly aligned with these coordinates, the distance relative to a rotated coordinate system was measured. The necessary rotation angle did not exceed 20 degrees.

In all six topographical maps the maximum Q-values were near the approximate dorso-ventral center of AI. Figure 27 shows a representative example of the distributions of $Q_{10\ dB}$ and $Q_{40\ dB}$ along an isofrequency contour of approximately 7 kHz in the primary auditory cortex. The locations of the penetration sites relative to sulcal pattern for these Q-maps are represented as black points in Fig. 28B. The numbers along the curves in Fig. 27A correspond to the multiple-unit tuning curves indicated in Fig. 27B. The AI/AII border was indicated by abrupt changes in CF topography, an increase in response thresholds, and/or average $Q_{10\ dB}$ values below 3 (Schreiner and Cynader 1984).

To aid in defining the spatial location of $Q_{40\ dB}$ and $Q_{10\ dB}$ maxima, a fifth order polynomial curve was fit to the data points (Fig. 27A, stippled curve). The location of the maximum of the Q-values (Q-max) was defined as the average of the locations of the individual $Q_{40\ dB}$ and $Q_{10\ dB}$ maxima;

this maximum was 3.6 mm from the most dorsal recording site
in Fig. 27. The AI/AII border was less than 2.5 mm from the
Q-max in those cases in which the border could be
unequivocally identified. Auditory responses were encountered
up to 4 mm dorsal to the Q-max in AI.

In the area of AI more than approximately 2 mm dorsal to
the Q-max, isofrequency contours turned more caudally and
multiple-unit recordings were more broadly tuned than in the
center of AI. In this region, responses were often best
driven by binaural stimulation. Neuron clusters often
responded best to white noise and responded with longer
latencies than classical AI (up to 45 msec longer). While the
majority of multiple-unit recordings in this area displayed
these properties, short latency and sharply tuned neuron
clusters were occasionally encountered. Additionally,
multiple-unit clusters that were inhibited by the ipsilateral
ear also could be found in this dorsal region of AI.

Topography of Multi-peaked Neurons

Multi-peaked neurons were topographically restricted to
the more dorsal regions of AI (Figs. 28 and 29). That
dorsally located neurons were more likely to be multi-peaked
than ventrally located neurons was apparent in each
individual experiment. The locations of recording sites

relative to the sulcal pattern and Q-maximum for two
representative experiments are shown in Fig. 28. Pooling
topographical data across animals raised several problems.
Dorsal and ventral anatomical landmarks were not consistent
across animals. The AI/AII border alone is not a reliable
reference, because the dorsal-ventral extent of AI is highly
variable with lengths from 4 to 7 mm (Reale and Imig 1980).
Similarly, sulcal patterns were not used because previous
studies had found that sulcal patterns in the auditory cortex
vary greatly between individual cats (Reale and Imig 1980;
Merzenich et al. 1975; Kawumara et al. 1971).

To avoid these problems with the anatomical localization
of recording sites, a physiological characterization of the
dorsal-ventral domain of AI was used as a common frame of
reference for pooling data. The multiple-unit $Q_{10 \ dB}$ and $Q_{40 \ dB}$ gradients across AI were used as the physiological
criteria. Data were pooled across animals by aligning the Q-
maxima of the individual cases. Although the dorso-ventral
extent of the observed Q-gradients varied over several
millimeters, normalizing the length of the pooled maps was
not necessary to identify the topographical domain of multi-
peaked single neurons.

All multi-peaked neurons were located dorsal to the most
sharply tuned part of AI, and all but one were more than 2 mm
dorsal to this central landmark (Fig 29). When the extent of

AI was divided into three regions, the central 2 mm (from -
1.0 to 1.0 mm in Fig. 29), dorsal and ventral, all but one
multi-peaked neuron fell in the dorsal region. 35 percent of
the neurons in the dorsal region were multi-peaked; 3 percent
of the neurons in the central region were multi-peaked; none
of the neurons in the ventral portion were multi-peaked. It
is concluded that neurons with multi-peaked tuning curves
form a functionally distinct subpopulation in the dorsal
third of AI.

DISCUSSION

Most neurons in the peripheral and central auditory system have a single, clearly definable frequency with the lowest response threshold, the characteristic frequency (CF). In contrast, multi-peaked neurons with two or more response threshold minima of similar value, separated by frequencies with substantially higher thresholds, were recorded in the dorsal aspect of AI. The existence of multi-peaked neurons in the auditory cortex of bats (Suga et al. 1979, 1983; Suga and Tsuzuki 1985) and cats (Oonishi and Katsuki 1965; Goldstein et al. 1968; Abeles and Goldstein 1970, 1972) has been demonstrated previously. This study was performed to examine in more detail the physiological properties and spatial distribution of multi-peaked single neurons in the primary auditory cortex of cats.

Among the main findings reported here are: (1) the frequency separation of the multiple CF peaks was usually less than one octave; (2) the median ratio between the highest and lowest CF peak was 1.56, which roughly corresponds to a second and third harmonic of a fundamental frequency that itself is not excitatory to the neurons; (3) multi-peaked neurons generally had longer latencies than single peaked neurons; (4) latencies between peaks within the same neuron were highly variable, with the higher frequency

peak most often having a longer latency; (5) the bandwidth of individual peaks of multi-peaked neurons was similar to that of single-peaked neurons; (6) two-tone suppression/inhibition was often observed between the peaks; and (7) areas of response enhancement, defined by a two-tone paradigm, were often systematically related to the multi-peaked frequency response area as obtained for a single tone. All of the multi-peaked neurons were found in the dorsal aspect of AI, as defined relative to the spatial distribution in sharpness of multiple-unit tuning curves. Multi-peaked neurons were interspersed with single-peaked neurons, thus providing further evidence for a functional and spatial segregation of response characteristics within AI. Before discussing possible functional implications of multi-peaked neurons in the cat, however, the physiological validity of the multi-peaked frequency response areas obtained in this study should be assessed.

Validity of Multi-Peaked Response Areas

Four arguments support the interpretation that the multi-peaked neurons seen in this study are not an artifact, e.g., created by the frequency transfer function of the sound delivery system. First, calibration of the system revealed frequency-dependent amplitude variations not larger than +/-

6 dB. This should result in "indentations" of threshold tuning curves of not more than 12 dB. Threshold increases observed between neighboring frequency peaks were, in almost all cases, larger than 30 to 40 dB. Second, the minimum threshold distribution of the obtained multi-peaked CF's did not differ from the threshold distribution of single-peaked neurons and did not show a strong frequency dependence. Third, in several cases single-peaked neurons were recorded that had a low threshold CF that fit into the gap between excitatory bands of a nearby recorded multi-peaked neuron. Fourth, although the harmonic distortion product for a tone was at least 55 dB below the primary (depending on the sampling rate of the output signal and the setting of the antialiasing low pass filter), the usually small threshold difference between peaks essentially rules out this source of artifact in the generation of multi-peaked neurons. Nevertheless, peaks that were more than 40 dB higher than the minimum threshold of a neuron were disregarded for this analysis.

The strict criteria applied to rule out a sound system artifact might have caused us to underestimate the number of multi-peaked neurons. Several cells were rejected because of the criterion that the thresholds of the peaks had to be within 40 dB of each other, including one neuron in the ventral part of AI.

Consistency of FRA Measurements

Because the reported results are based on FRA's obtained with only a few repetitions of a large number of signal conditions, some discussion of the method's robustness is in order. It should be noted that a similar method has been used in the inferior colliculus (Caird and Klinke 1987), and that the method is similar to the repeated raster frequency scan method used by several other cortical investigators (Goldstein et al. 1968; Wollberg and Newman 1972; Funkenstein and Winter 1973; Pelleg-Toiba and Wollberg 1989). The FRA method in this study uses a pseudo-random order of presenting frequencies, while the earlier raster methods present frequencies in ascending order. The response variability of our method is similar to that observed with the repeated raster method (Goldstein and Abeles 1975).

Temporal variation in neuronal responsiveness combined with the use of one presentation for each frequency/level combination introduced a slight variation in the quantitative parameters extracted from the FRA's. Table 3 shows the variation of the measures for all thirteen peaks in which catch trials were performed after a full battery of tests were run on the neuron. This assessment of measurement variability can be considered an exaggeration for two

reasons: (1) the second measure was performed after extensive two-tone testing, and thus the responsiveness of the neurons could have changed due to 675-2025 presentations of the probe tone and/or the passing of 1 to 2 hours; and (2) unlike the first measurement, which was repeated until a well-defined FRA was obtained, the second measurement was only performed once, even if more repetitions were needed to completely define the FRA. Even this overestimated variability should have little effect on the presented results, however. Variability did not shift mean values but could only slightly increase the variance of distributions.

When a unit's responsiveness was weak, the FRA response method was repeated until a well-defined FRA was obtained. One neuron required five repetitions of the complete tone sequence. Additionally, when a multi-peaked neuron displayed narrow frequency separation (Fig. 22D), an additional FRA was recorded to verify the separation of the peaks.

Advantages of the employed pseudo-random signal presentation, such as many frequency-amplitude combinations and a potential decrease in habituation, are traded off against few presentations per stimulus condition. The effective number of presentations was increased by smoothing algorithms that incorporated very similar signal conditions into the response estimate of a given frequency/level combination. Nine-point weighted averaging increased the

number of effective presentations per point by 2.5 fold at
the expense of some frequency resolution (less than one
neighbor or 0.067 octaves per side). Similarly, 6-point
averaging of latency calculations allowed us to increase the
effective number of stimulus presentations for this method by
six-fold, at the expense of 5 dB of amplitude resolution.

Interpretation of Simultaneous Two-Tone Paradigm

Since most neurons in the primary auditory cortex of the
pentobarbital-anesthetized cat display only low levels of
spontaneous discharges, measuring inhibitory effects requires
elevating the neuronal activity with a probe stimulus and
observing the influence of a second signal on that activity.
Traditionally, a CF probe tone is used in the "two-tone
paradigm" either following (forward masking) or concurrent
(simultaneous masking) with a second variable (masker) tone.
Inhibition/suppression is said to be present when the masker
tone reduces the response to the probe tone below the
response generated by the probe alone.

Both forward and simultaneous masking are limited in
determining the origin of inhibition/suppression. For
simultaneous masking paradigms, mechanical effects at the
level of the basilar membrane result in two-tone suppression
(Rhode 1977) that is projected into the central auditory

system. In addition, neural inhibition originating from all intervening stations of the auditory pathway may be reflected in the cortical response.

The interpretation of the origin of inhibition obtained with forward masking is also hampered by several constraints, including effects of adaptation, habituation, duration of inhibition, and influences from offset responses. For this initial study, we chose to examine inhibition and enhancement to stimuli with temporal overlap, common in both communication and localization cues. In this investigation, we were not concerned with determining the origin of the inhibition or facilitation, as neither physiological method, on its own, can be used to study cortical effects in isolation.

Percentage of Multi-Peaked Neurons Encountered in AI

Most investigators of cat auditory cortices have reported the presence of multi-peaked neurons (Oonishi and Katsuki 1965, Goldstein et al. 1968, Abeles and Goldstein 1970,1972; DeRibaupierre et al. 1972; Reale and Imig 1980; Phillips and Irvine 1981). The rate of occurrence varies, however, ranging from 2% (Phillips and Irvine 1981) to more than 30% (Oonishi and Katsuki 1965) of the recorded samples. On the basis of our results, the discrepancies between the

percentage of multi-peaked neurons found in different studies could be largely attributed to the location of sampled regions of the auditory cortex. Many early recordings may have included areas now believed to be outside of AI, while more recently the dorsal region of AI may have been undersampled, since some of the response characteristics do not parallel "classical" AI properties.

Multiple unit mapping experiments of the frequency organization of the auditory cortex (Merzenich et al. 1975, Reale and Imig 1980) have established the unreliability of anatomical landmarks for the localization of AI, and have, instead, suggested that strict physiological criteria (e.g., a reversal in the CF gradient) be used for the determination of the rostral and caudal boundaries of AI. In contrast, similarly unequivocal physiological criteria for the ventral and dorsal boundaries of AI have not been developed. Recent studies that examined in more detail dorsal and ventral portions of AI (Middlebrooks and Zook 1983; Schreiner and Cynader 1984; Schreiner and Mendelson 1990; Mendelson et al. 1988) have described several physiological characteristics that when taken together may serve that purpose. A common observation of these studies is that classical physiological characteristics of AI, i.e., strict cochleotopic organization, sharp tuning, and short latencies, gradually give way to less-strict cochleotopic organization, broader

tuning curves, and longer latency responses in the dorsal and ventral regions of AI. The lack of a precise definition of the dorsal-ventral extent of AI may have led to over-conservative estimates of the physiologically-defined extent of AI, confining it to the more sharply tuned, shorter latency areas, and excluding any region with more diverse response patterns at the margins of AI.

Properties of Dorsal AI

The multi-unit mapping performed in the current study confirmed most of the findings of previous studies regarding the physiology of the most dorsal region of AI. Middlebrooks and Zook (1983) refer to this region as "the dorsal zone of AI" (DZ). These authors showed that DZ ranges from approximately 1 to 2 mm in dorsal-ventral extent. Whether this region should be considered a separate cortical area or a part of AI, however, has not been resolved. The progression of physiological properties toward this region (Schreiner et al. 1988; Schreiner and Mendelson 1990) appears to be gradual over several millimeters. Anatomical evidence shows that the projections from medial geniculate body to DZ overlap with those to AI (Middlebrooks and Zook 1983) and may also be gradual over a few millimeters (Brandner and Redies 1990). Cytoarchitectural characteristics attributable to DZ

gradually change over a transitional area of more than one millimeter (Winer 1984). The relatively small size of DZ and the continuance of weaker CF topography indicate that this region may be a transitional zone between AI and other auditory areas within the suprasylvian sulcus. On the basis of the physiological organization of the ectosylvian gyrus, we cannot unequivocally state whether this region should or should not be considered part of AI. For the purposes of this paper we consider it part of AI, since no clear, sharp functional border was evident separating it from classical AI. Experiments performed in the current study included recordings from DZ; however, not all of the encountered multi-peaked neurons were from that area. The probability of encountering a multi-peaked neuron seems to increase gradually approaching the dorsal third of AI and beyond, mirroring the decrease in the sharpness of tuning gradient (Schreiner et al. 1988; Schreiner and Mendelson 1990).

Consistent with the findings of earlier studies (Middlebrooks and Zook 1983; Reale and Imig 1980), the present study revealed that isofrequency lines turned caudally, and multi-unit recordings were broadly tuned and often best driven by binaural stimuli in the dorsal area of AI. Response latencies of multiple unit clusters were often longer than those of neurons in the center of AI, consistent with previous observations (Schreiner et al. 1988). The

shortest latencies were similar to the shortest latencies in the rest of AI, but the longest latencies could be longer by as much as 40 msec.

In the present study, dorsally located neuron clusters often gave better responses to white noise than to tones. In general, the single neuron topography roughly corroborated the multiple unit results; however, some of the neurons in dorsal AI that were not multi-peaked were more narrowly tuned than the unit clusters.

In addition to those mentioned above, several other factors can lead to sampling bias against recording neurons in the most dorsal regions of AI. This region's CF topography is weakly defined and the neurons in this area are often difficult to drive with monaural contralateral tones. They generally have little or no spontaneous activity under pentobarbital, and thus cannot be found without a search stimulus; however, they are very susceptible to habituation, or possibly affected by anaesthesia, and are difficult to drive repeatedly (sometimes even at a rate of 1 repetition per 3 seconds). Lastly, some penetrations in dorsal AI could not produce an auditory evoked response, even with multiple unit recording. This was especially the case closer to the dorsal end of the ectosylvian gyrus.

Characteristics of Multi-peaked Neurons

The current description of properties of multi-peaked neurons are in close agreement with the earlier descriptions given by Abeles and Goldstein (1970, 1972). Although these authors did not analyze the CF ratios of peaks, their graphs reveal that most of their best frequency ratios were between 1 and 2, in close agreement with the data presented in this paper. In addition, they reported the existence of inhibitory regions between the multi-peaks. The current data differ substantially from the properties of multi-peaked neurons reported by Oonishi and Katsuki (1965). They found most CF ratios of the peaks to be between 2 and 3 and reported only weak and occasional inhibition in multi-peaked neurons. The most probable cause for the discrepancy between these studies is the difference in the definition of AI, and hence a difference of recording locations, possibly including the anterior auditory fields (see Fig. 5 of Oonishi and Katsuki 1965).

Comparison to Bat Studies

A similar organization to that described in this paper has been demonstrated in the bat's auditory cortex, which have single-peaked tuning curves for the majority of AI

neurons. AI is surrounded dorsally by several physiologically and functionally distinct areas. One of these, the CF/CF area, contains multi-peaked tuning curves (Suga et al. 1979,1983). Although those neurons have functional characteristics related to the bat's echolocation sounds, several physiological properties are similar to those of the cat, described in this paper. The multi-peaked CF/CF area neurons display more habituation than neurons in other bat auditory cortical areas. The higher frequency peak of CF/CF neurons is usually more sharply tuned to frequency than the low frequency peak. Upon two-tone stimulation, the intensity threshold of CF/CF neurons for the second (non-probe tone) frequency range lowers and the response latency shortens. More recently, Suga and Tsuzuki (1985) have demonstrated that inhibition is clearly and consistently expressed between the peaks.

One important property of bat CF/CF neurons has not been explicitly tested in cats: facilitation/ combination selectivity. Bat CF/CF neurons demonstrate clear two-tone facilitation. Responses to two-tone combinations, where the tones are at the CF's of the peak's, are greater than the sum of the response to the two tones alone. Although two-tone responses were obtained in this study, the cat data failed to confirm (or reject) the presence of clear facilitation in cats. Among possible reasons for the absence of clear two-

tone facilitation in this study are the status of anesthesia
and the lack of using different temporal relationships
between the two tones. This study does find two-tone
enhancement above the rate of the probe tone presented alone,
however, suggesting at least the potential presence of
facilitation.

Several differences between cat and bat multi-peaked
neurons might be accounted for by species-specific auditory
system adaptations to cortically magnify the representation
of the bat's biosonar signal. Suga and colleagues's CF ratios
for multi-peaked neurons were usually 2.0 and 3.0, with very
few neurons containing CF ratios of 1.5 (CF3/CF2 neurons).
This adaptation for harmonic responses results from the roles
of CF/CF neurons in coding Doppler shift magnitude (for more
details see Suga et al. 1983; Suga 1989). They did not report
in detail single-tone latencies of each peak because the
latencies were long and inconsistent; however, they report
many CF/CF neurons were broadly tuned to the temporal
presentation of the two frequencies.

From the properties of multi-peaked tuning curves in
cats and bats, several general hypotheses may be posited
regarding response properties of multi-peaked neurons in
regions of mammalian cortex: (1) most multi-peaked neurons
display more habituation and longer latencies to tones than
classical AI cells; (2) responsiveness within a multi-peaked

neuron is facilitated or enhanced by two-tone stimuli with energy restricted to the peaks (this facilitation can be expressed as an increase in firing rate, a lowering of the peaks intensity threshold, or a shortening of response latency, and is often non-monotonic); (3) bandwidth sharpening may occur between the peaks by inhibitory processes; and (4) these multi-peaked neurons are topographically restricted to an area adjacent to the part of AI with narrow frequency tuning curves . In the cat this region at least partially overlaps with dorsal AI paralleling the general spatial location of multi-peaked neurons seen in bats.

On the basis of bat behavior, two more speculative *hypotheses* can be made that require further studies in the cat. (5) The bandwidths between the peaks can vary over a wide range and probably relate to the sound signals being analyzed by the auditory system, and, (6) temporal relationships between peaks are systematic and probably reflect temporal relationships of the signals being analyzed. Lastly if these hypothesis are general mammalian features, one must explore whether in other mammals -- in which AI isofrequency lines are not oriented in the dorsal-ventral dimension -- a multi-peaked region abuts AI in a way that systematically relates to physiology.

Hypotheses (5) and (6) cannot be proven until combination-selectivity to behaviorally useful stimuli is demonstrated for multi-peaked neurons in the cat. Pure-tone physiological properties that might relate to appropriate stimulus combinations include latency differences and frequency separation of responses to CF_l and CF_h tones. In the remainder of this section, we will elaborate on interpretational limitations of these recorded physiological properties and discuss how these single tone properties might relate to a functional role for multi-peaked neurons.

Latency Differences and Input Source of Multi-Peaked Neurons

CF_h tones usually elicited longer latency responses than CF_l tones. These latency differences must be generated by mechanisms other than travel time differences on the basilar membrane because delays initiated by travel along the basilar membrane result in longer latency responses for low frequency tones. Additionally, it has been observed that habituation effects differentially effect CF_l and CF_h tones. Longer latency CF_h tones habituate more strongly than CF_l tones. The latency and habituation differences between the responses to CF tones of the different peaks can be explained by either inhibitory effects or differential input. An inhibitory region (possibly inter-peak inhibition) that overlaps the

excitatory area of the high frequency peak on the FTC could

increase habituation and the response latency to tones with

frequencies in the overlapping area. These influences may be

exaggerated by the use of pentobarbital which can enhance

inhibitory effects.

Alternatively, frequency selective differences in

latency and habituation could be explained by convergent

input from two different populations of neurons. The high

frequency input could conceivably come from a pathway that

includes more synapses than the pathway that supplies input

to the low frequency peak. Pentobarbital might differentially

effect the two pathways.

This study provides evidence that both mechanisms may be

involved in generating multi-peaked FRA's. Inhibition is

often prominent between peaks arguing in favor of dividing

the excitatory input into segregated response areas. Inter-

peak inhibition, however, was only observed in 10 of 14

tested multi-peaked neurons. Latency and habituation effects

can argue for either hypothesis. Both multiple excitatory

input and central inhibitory input are probably involved in

the formation of multi-peaked neurons. Apparently, there are

two extremes of involvement. Some multi-peaked neurons

display wide separation of peaks, little or no inter-peak

inhibition, and large latency differences suggesting that

multiple inputs are expressed. In contrast, some neurons have

narrowly spaced peaks, strong inter-peak inhibition, and similar latencies, suggesting that inhibitory splitting of the FRA is involved. Which subcortical and cortical processes are involved has yet to be determined.

Relation to Spectral Properties of Naturally Occurring Sounds

While the purpose of this paper is to describe the physiological and topographical properties of multi-peaked neurons, some discussion about the relationship of the neurons' response properties to those of behaviorally useful stimuli is in order. Potential harmonic properties of multi-peaked neurons have been demonstrated. Cortical locations with clearly expressed harmonic input (Fig. 16) are particularly intriguing. While the multiple unit FRA indicates that the neuron cluster might be well-suited to analyze a 13 kHz harmonic series, there are elements (single neuron) in the same local network that may be suited to encode portions of the harmonic complex, i.e., without the fundamental frequency. These response properties provide evidence that some locally available inputs (in this case the fundamental frequency of a harmonic complex) might not be expressed in the output of cortical cells. The currently available evidence is not conclusive, however. These neurons

have not been shown to be combination-selective (facilitatory) for harmonic complexes.

In contrast to the bat, the lack of clearly identified behaviorally useful stimuli for the cat that match the physiological properties of these neurons renders an interpretation more difficult. Most neurons studied in these experiments had high CF's, and the fundamental frequencies that potentially could be encoded would generally have to be greater than 5 kHz. The fundamental frequencies of cat and kitten isolation and deprivation calls are usually between 0.5 and 2 kHz (Wantanabe and Katsuki 1974; Haertel 1975; Brown et al. 1977; Haskins 1979; Shipley et al. 1988). Fundamental frequencies above 3 kHz are rare. Only a few spectrographic studies have considered high frequency (> 8 kHz) components of cat and kitten vocalizations (e.g., Haertel 1975, Romand and Ehret 1984). While these studies reported vocalizations components up to 50 kHz, they did not demonstrate harmonic structures with fundamental frequencies above 5 kHz; however, it cannot be completely ruled out that some cat/kitten vocalizations do contain high frequency harmonic complexes.

Potential prey such as rodents have been shown to generate narrow-band vocalizations with frequencies that closely correspond to the CF's of multi-peaked neurons encountered in this study (e.g., Anderson 1954; Ehret 1980;

Nitschke 1982; Haack et al. 1983). While rodents commonly
emit high frequency (5 to 100 kHz) calls, bird vocalizations
with fundamental frequencies above 10 kHz are rare (Marler
1977). Therefore, it appears that rodent vocalizations might
be a good stimulus to use with the high frequency multi-
peaked neurons.

Several of the lower CF neurons (Figure 15 E, F, J, Q, R
and W) could be encoding elements of naturally occurring
vocalizations. For all neurons with 2 CF-peaks below 10 kHz,
the range of peak separation was 1.4 to 2.3 kHz. This is
within the range of fundamental frequencies of isolation and
deprivation calls. Four of the six neurons have CF pairs
roughly corresponding to second and third harmonics. One of
the six had a CF separation corresponding exactly to fourth
and fifth harmonics. These lower frequency multi-peaked
neurons would be excellent candidates to study with naturally
occurring isolation and deprivation calls.

Another functional objective for multi-peaked neurons
could be the encoding of monaural spatial localization cues.
The pinnae of cat's selectively attenuate certain frequencies
of sound depending on the source's spatial location (Musicant
et al. 1990). Because many multi-peaked neurons respond well
to broad-band stimuli and display distinct excitatory (and
inhibitory) frequency regions, they may be particularly well

suited to detect spectral notches in broad-band stimuli. such as that reported by Musicant and colleagues.

Significance of Latency Differences

This study demonstrates latency differences between responses to CF_l and CF_h tones, however, temporal/delay selectivity to two-tone presentation was not studied. In the bat, facilitatory responses of multi-peaked neurons were not strongly affected by relative delays of the components (Suga et al. 1979; 1983). Whether this is also the case in the cat remains to be determined. Consequently, a functional interpretation of the delay differences can only be cursory.

In the acoustical biotope, delay components are present in a variety of sounds, including modulations and transitions in vocalizations, sound reflections, and moving sound sources. The delays between responses might not relate to temporal selectivity, however, but may simply reflect relative delays created within the auditory system. For example, it has been shown that response delays systematically vary over more than 20 msec. within the isofrequency domain of the central nucleus of the inferior colliculus (Schreiner and Langner 1988). It is conceivable that the observed range of latency differences in multi-peaked neurons is a reflection of the integration of

responses from different portions of the same projection or from different projection sources.

Possible Functions of Multi-Peaked Neurons in Dorsal AI

In considering a functional role for dorsal AI, one cannot rule out the possible importance of acoustic environment and plasticity. In the somatosensory (Clark et al. 1988) and visual (Blasdel and Pettigrew 1979; Stryker and Strickland 1984) cortex the response properties of cortical neurons can be greatly altered so that the representation of temporally coincident stimulation of the receptor surface is magnified. Similarly, temporal coincidence or patterns in the stimulation of different basilar membrane segments might be reflected in multi-peaked neurons. Therefore, naturally occurring temporal-frequency interplay in the cat's environment might effect or create the observed responses of multi-peaked neurons in the primary auditory cortex. Temporal coincidence of different spectral regions are common in communication sounds (formants, harmonics, transitions) as well as sound localization tasks using outer ear transformations (Musicant et al. 1990), and characterizing common sound sources.

That neurons in the posterior-dorsal region of AI respond to noise and clicks, but less to tones (Merzenich et

al. 1975, Reale and Imig 1980) suggests that the dorso-posterior region performs some spectral integration (summation). Occasionally, we encountered neurons in AI that responded well to two-tone stimulation, but not to single tones. More commonly, neurons were encountered that showed a new tuning area upon two-tone stimulation that was not apparent from single-tone stimulation. These data support the hypothesis that dorsally located neurons could be tuned to respond best to specific spectral combinations.

We can reasonably hypothesize that the dorsal part of AI is being used as a highly tuned pre-processor of complex spectral information. This pre-processed information can be used for diverse behavioral functions. This includes, in the high frequency region, sound localization using pinna spatial transformations (Musicant et al. 1990), and the localization and identification of complex sounds, including possibly echoes. Sounds of interest to cats in the lower frequency range include species-specific communications (Haertel 1975), sounds generated by prey and humans and sounds from inanimate sources common to the cat's natural environment.

Since there appears to be a gradient in the complexity of excitatory spectral tuning (Schreiner and Mendelson, 1990) and latencies (Schreiner et al. 1988), refining and integration of spectral tuning and selectivity might occur progressively in the dorsal direction within AI. If this were

true, the lack of recognized auditory responsiveness of cortex as one approaches and enters the suprasylvian sulcus (e.g. Merzenich et al. 1975; Middlebrooks and Zook 1983) might be due to the use of inappropriate stimuli and/or anaesthetic state.

Concluding Remarks

This study reports the presence and topography of neurons that are potential candidates for analyzing complex sounds. The physiological properties of neurons in dorsal AI as described in this paper might provide a framework for the creation of highly specialized, behaviorally significant filters of information in the spectrally complex acoustic environment of mammals. Further studies are necessary to test the temporal sensitivity of these neurons to two-tone combinations, and the responsiveness of these cells to behaviorally relevant stimuli.
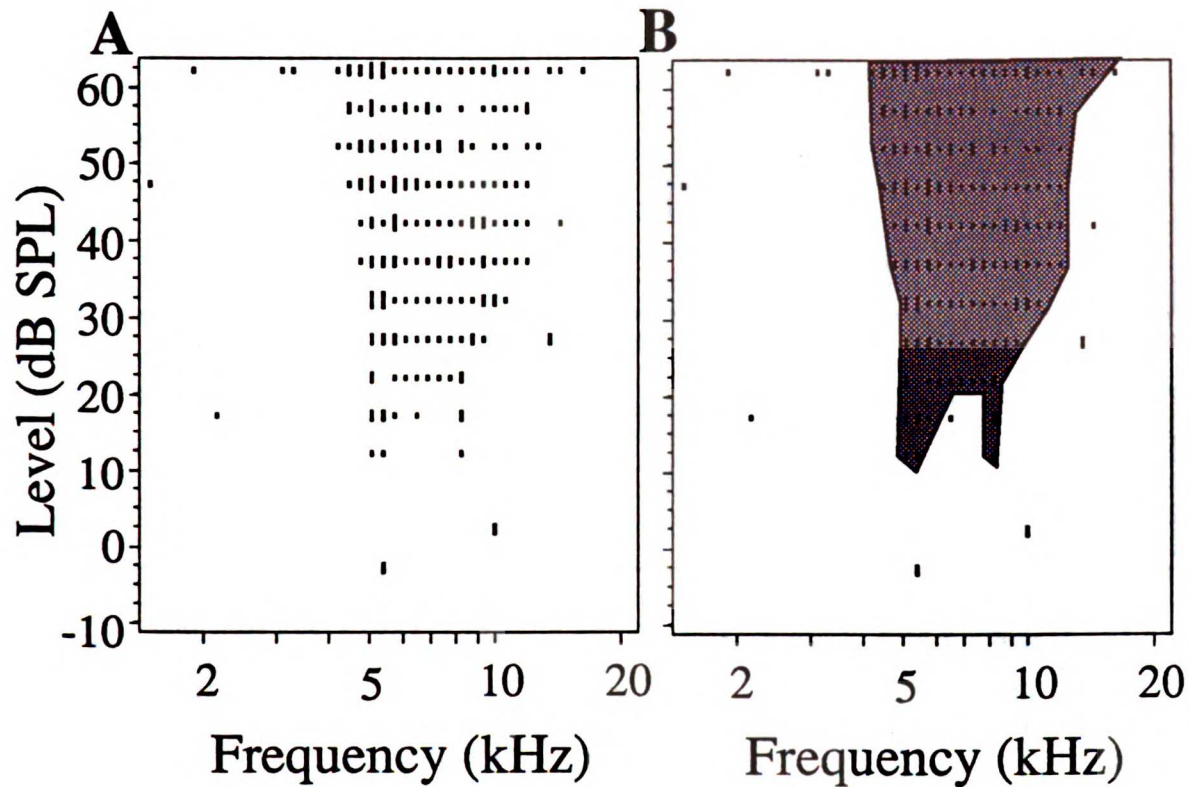
Figure14:
(A) Frequency response area (FRA) for a single-peaked neuron with complex internal structure. This neuron responded best to 5 kHz (longer lines) with weaker response areas between 6-9 kHz and 11-12 kHz. Amplitude of responses from 9-11 kHz were between the weak and strong responses.
(B) Dark shaded area represents the objectively determined tuning curve of the same neuron using an isoresponse criteria of the spontaneous rate plus 20% of the maximum firing rate.
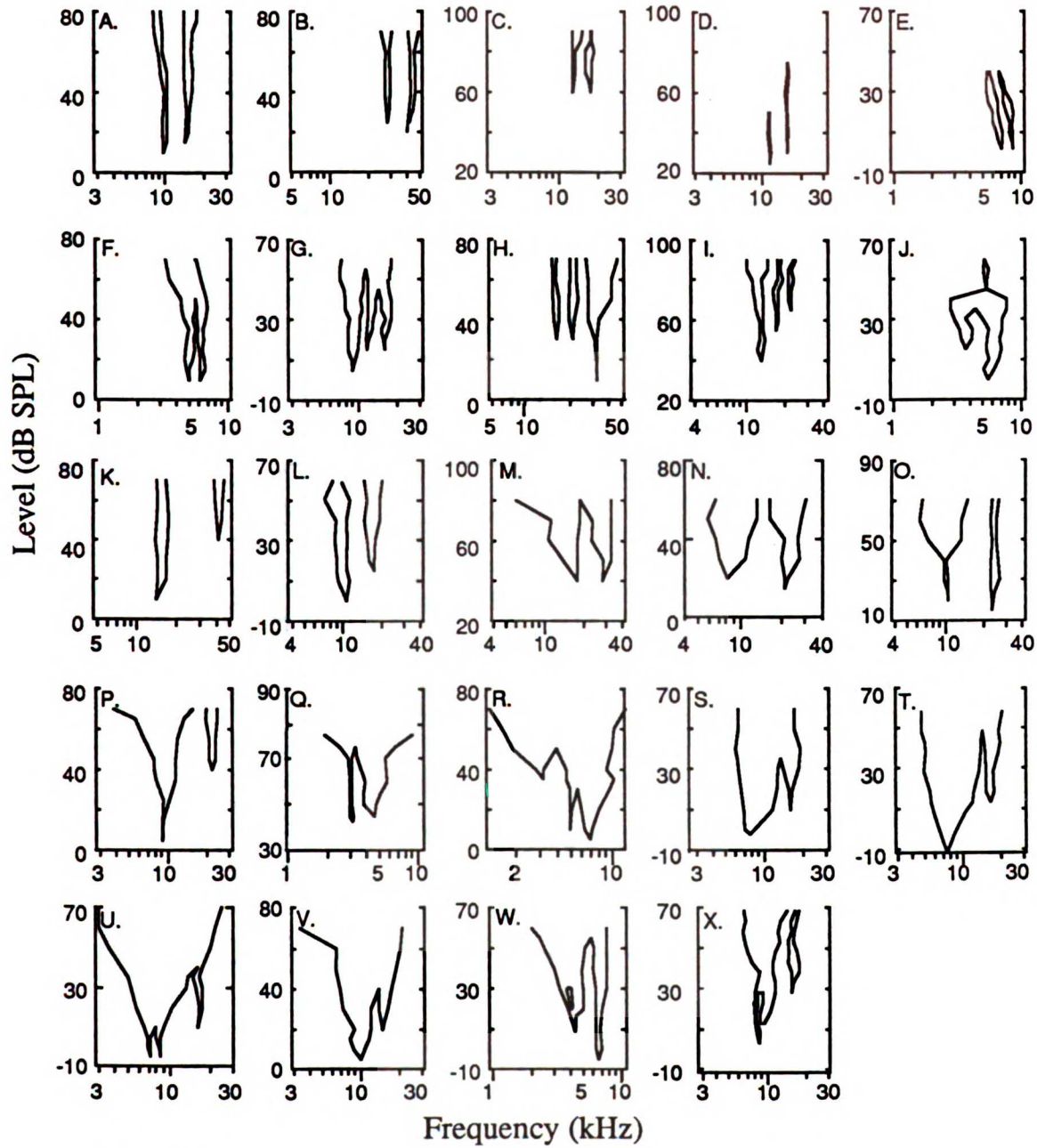
Figure 15
Frequency tuning curves for the 24 recorded multi-peaked neurons. All tuning curves were plotted for 1 decade of frequency and an 80 dB amplitude range to aid direct visual comparison.
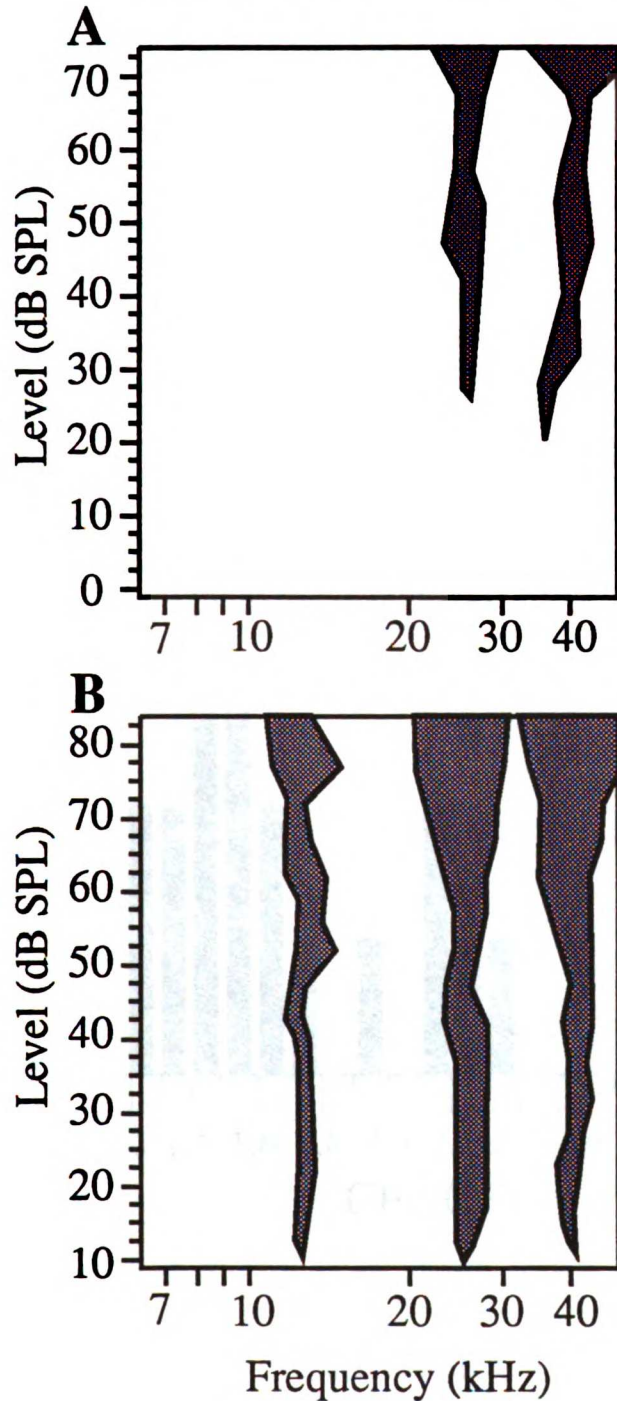
Figure 16:
(A) Frequency tuning curve for single neuron that responded to second and third harmonics of a missing fundamental. This neuron's tuning curve is also depicted in panel B of Figure 3.
(B) Frequency tuning curve for multi-unit recording at the same location showed a response to two harmonics plus the fundamental frequency to which the largest amplitude single neuron (in A) did not respond. Note, that the thresholds are lower for the multiple unit responses.
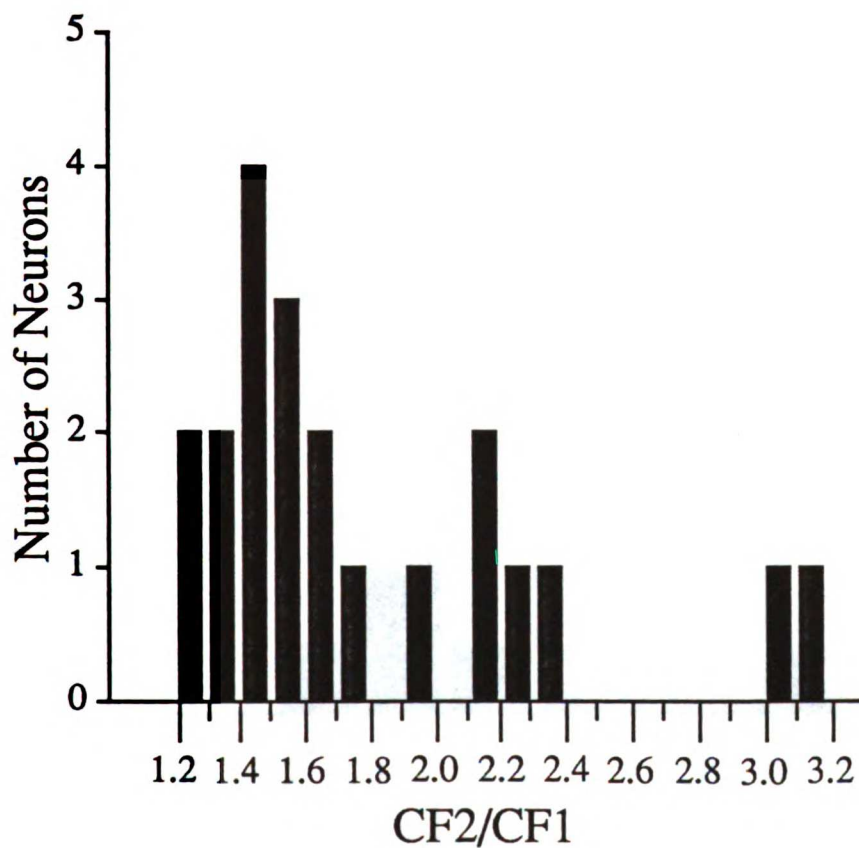
Figure 17:
Histogram of the ratios of CF's between peaks in the same neuron. CF ratio = CF of high frequency peak divided by the CF of the low frequency peak. The median CF ratio is 1.56. A CF ratio of 1.5 would correspond to CF's that were second and third harmonics of a missing fundamental frequency.
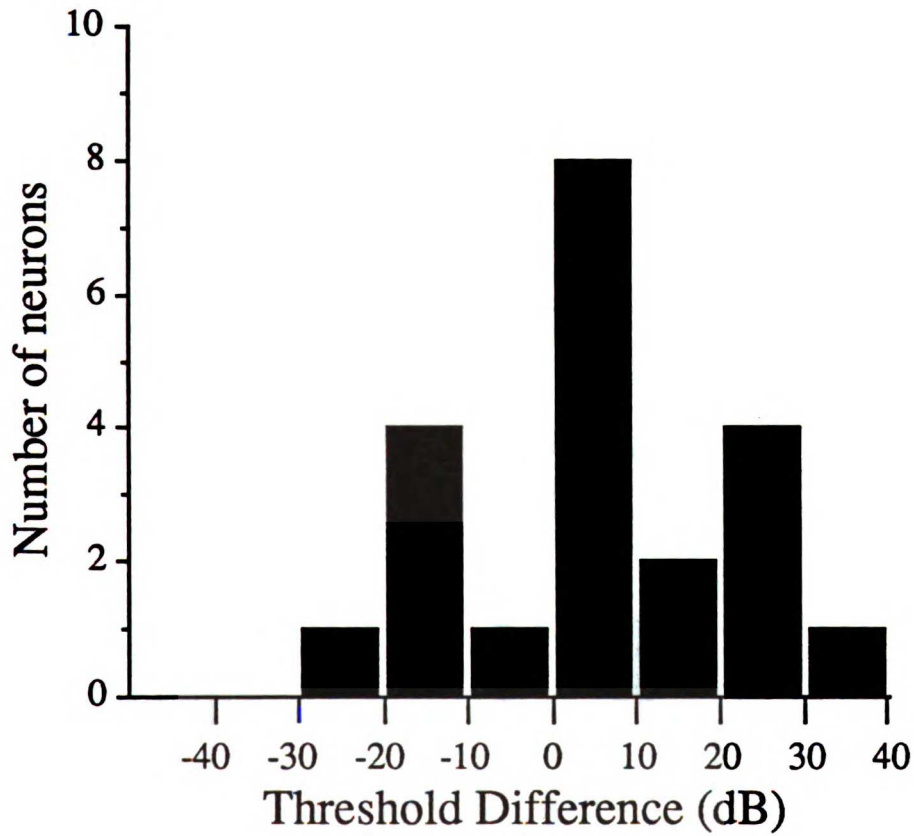
Figure 18:
Histogram of threshold differences between peaks within multi-peaked neurons.
Threshold difference = high frequency peak threshold - low frequency peak threshold.
Negative values correspond to a higher threshold for the lower frequency peak.
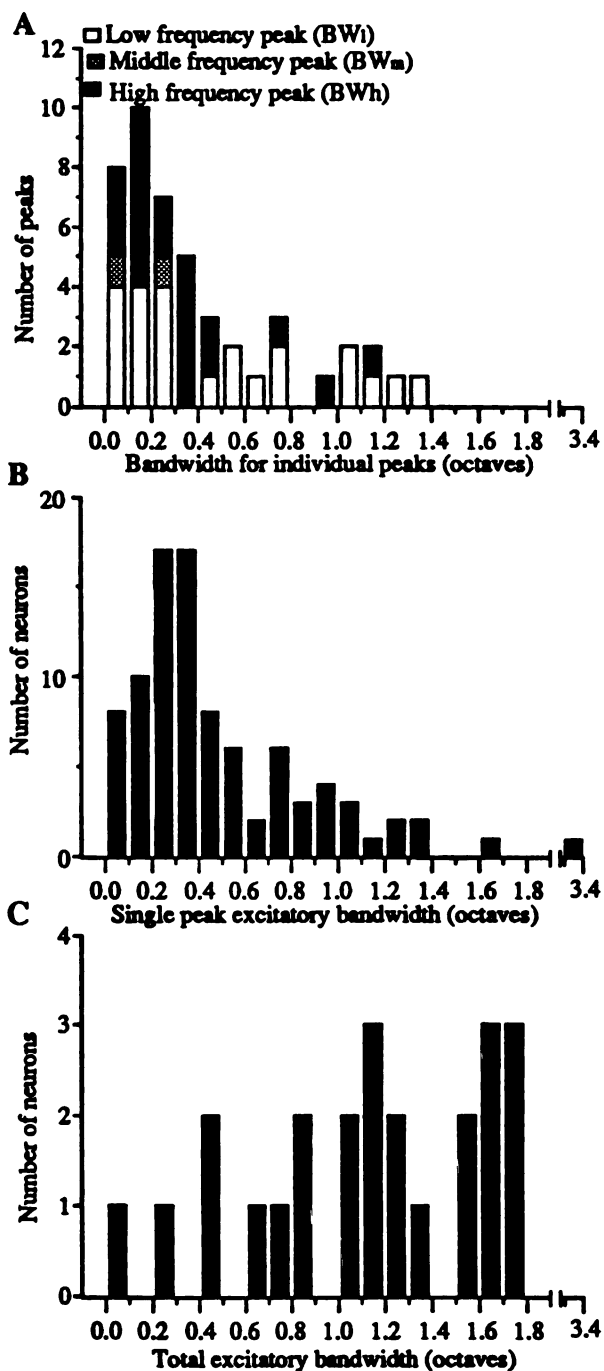
Figure 19:
(A) Histogram of bandwidths (in octaves) for all peaks in multi-peaked neurons. White bars in the stacked bar graph correspond to bandwidths of low frequency peaks, stippled bars correspond to middle peaks, and black bars correspond to bandwidth of high frequency peaks.
(B) Histogram of bandwidths for all single-peaked neurons.
(C) Histogram of total bandwidth for multi-peaked neurons. The total bandwidth is the complete excitatory bandwidth for multi-peaked neurons, including the region of no response between the peaks.
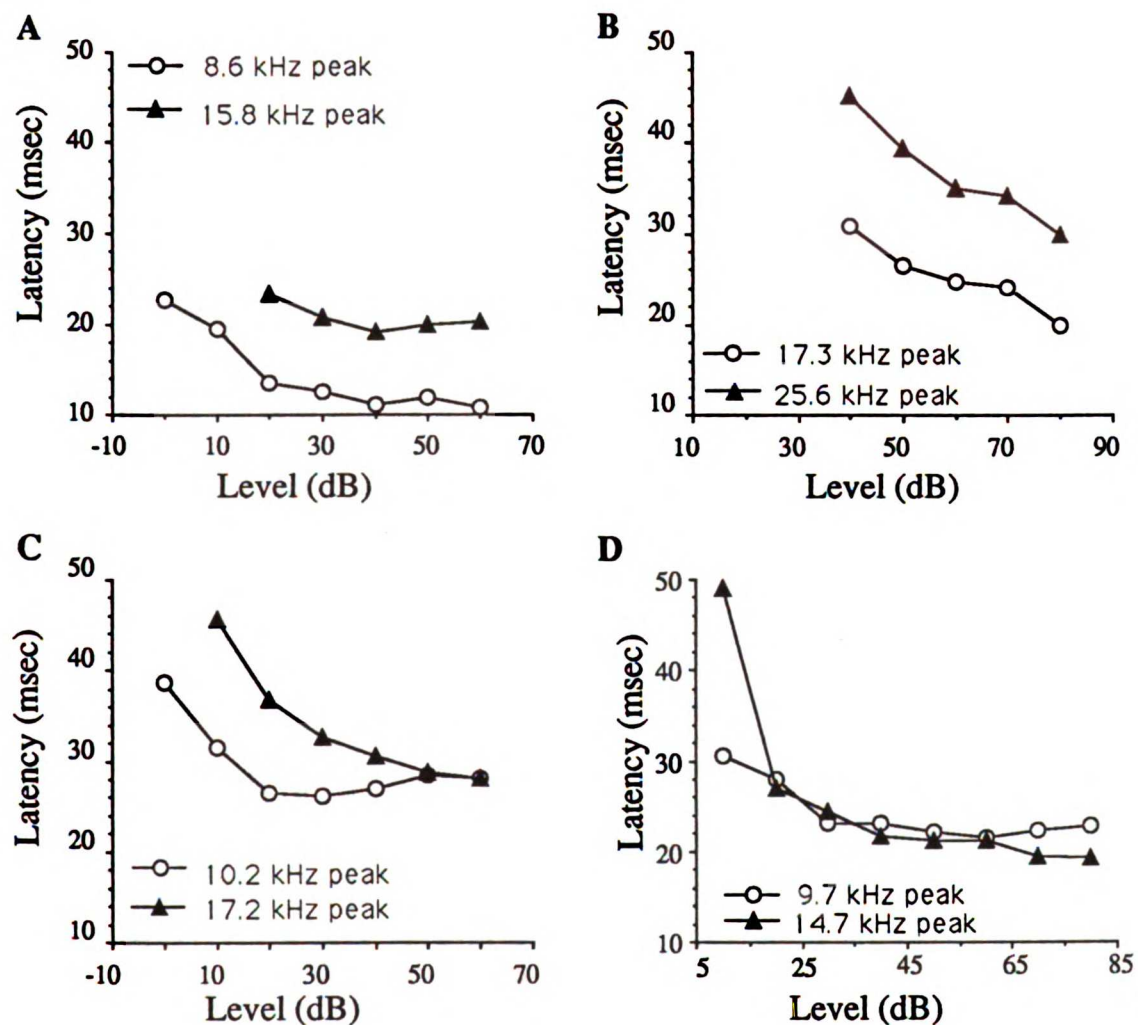
Figure 20:
Latency versus intensity level function for four multi-peaked neurons. Filled triangles are data points for the CFh tones and open circles are data for the CFl tones.
(A),(B) Two neurons in which CFh tones elicited a longer latency response than the CFl tones at all tested intensities.
(C) Neuron in which the high frequency peak had a longer latency than the low frequency peak over 40 dB. The latencies converge to a common asymptote at higher intensity levels.
(D) Neuron with similar latencies between the two peaks.
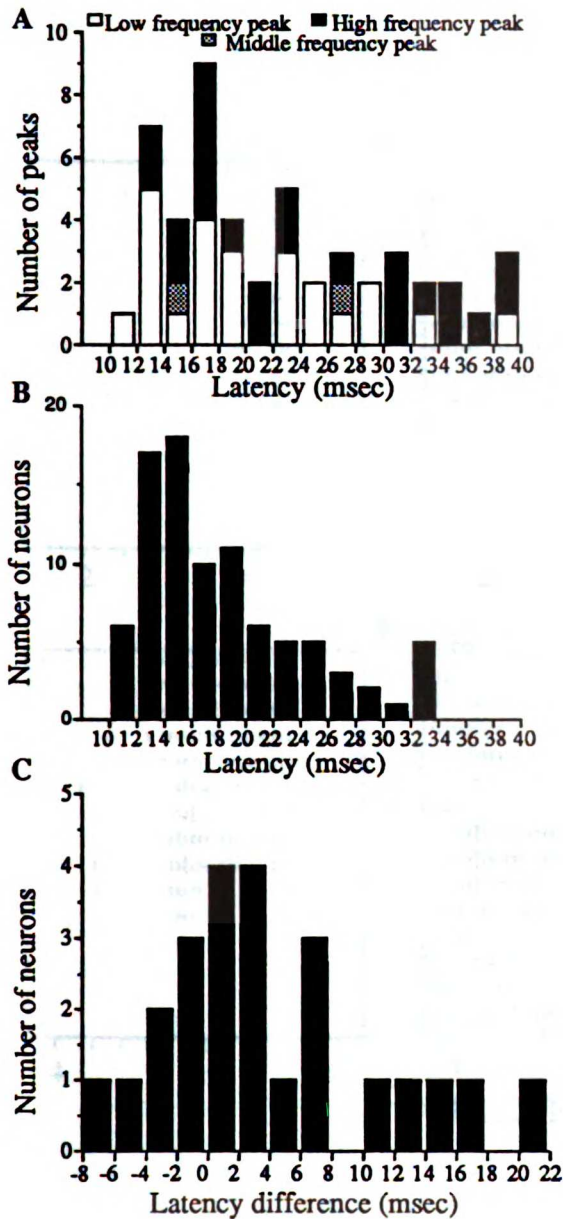
Figure 21:
(A) Histogram of the latency 30 dB above threshold for each individual peak within multi-peaked single neurons. White bars correspond to bandwidths of low frequency peaks, stippled bars correspond to middle peaks, and black bars correspond to bandwidth of high frequency peaks.
(B) Histogram of latency 30 dB above threshold for all single-peaked neurons.
(C) Histogram of latency difference 30 dB above each individual peak's threshold. Latency difference = high frequency peak latency - low frequency latency. Negative values correspond to a longer latency for the low frequency peak.
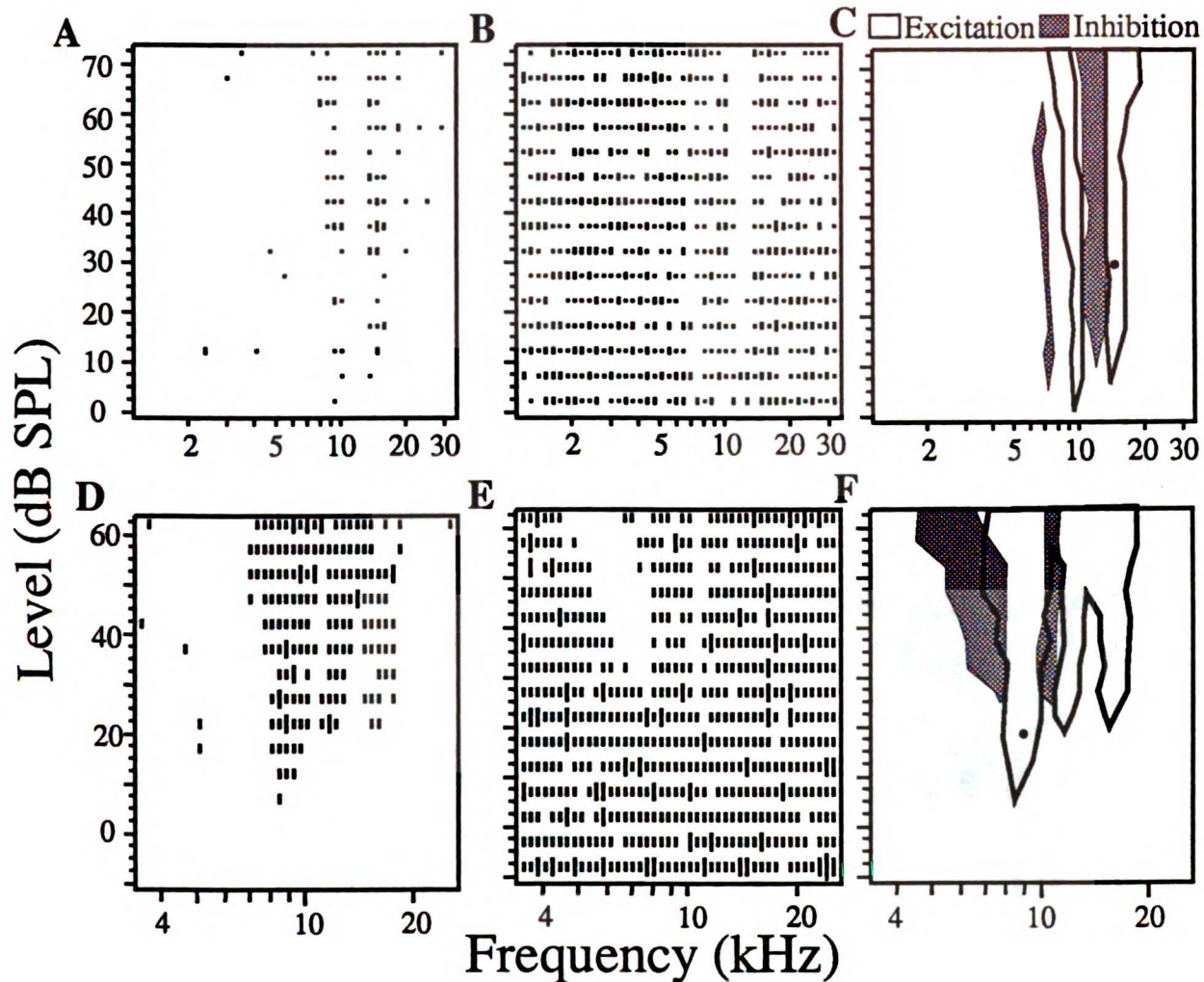
Figure 22:
Single tone (A,D), and two-tone (B,E) FRA's for two single neurons. For the two-tone FRA's, a CF tone (probe tone) was repeatedly presented to drive background activity. A second masker tone was presented for the 675 different frequency-amplitude combinations shown. A reduction of the background activity by 50% was defined as sufficient evidence for suppression/inhibition. In (C,F) a simplified tuning curve representation is shown. Outlined, non-filled areas correspond to regions of excitation from the single-tone FRA. This is equivalent to the excitatory frequency tuning curve (FTC) of the neuron. The filled circle in the excitatory FTC signifies the frequency and amplitude of the probe tone. Dark shaded areas correspond to inhibitory regions derived from the two-tone FRA. In (C) the inhibitory areas were determined from the 2-tone FRA in (B) and a 2-tone FRA with an expanded frequency range (not shown)
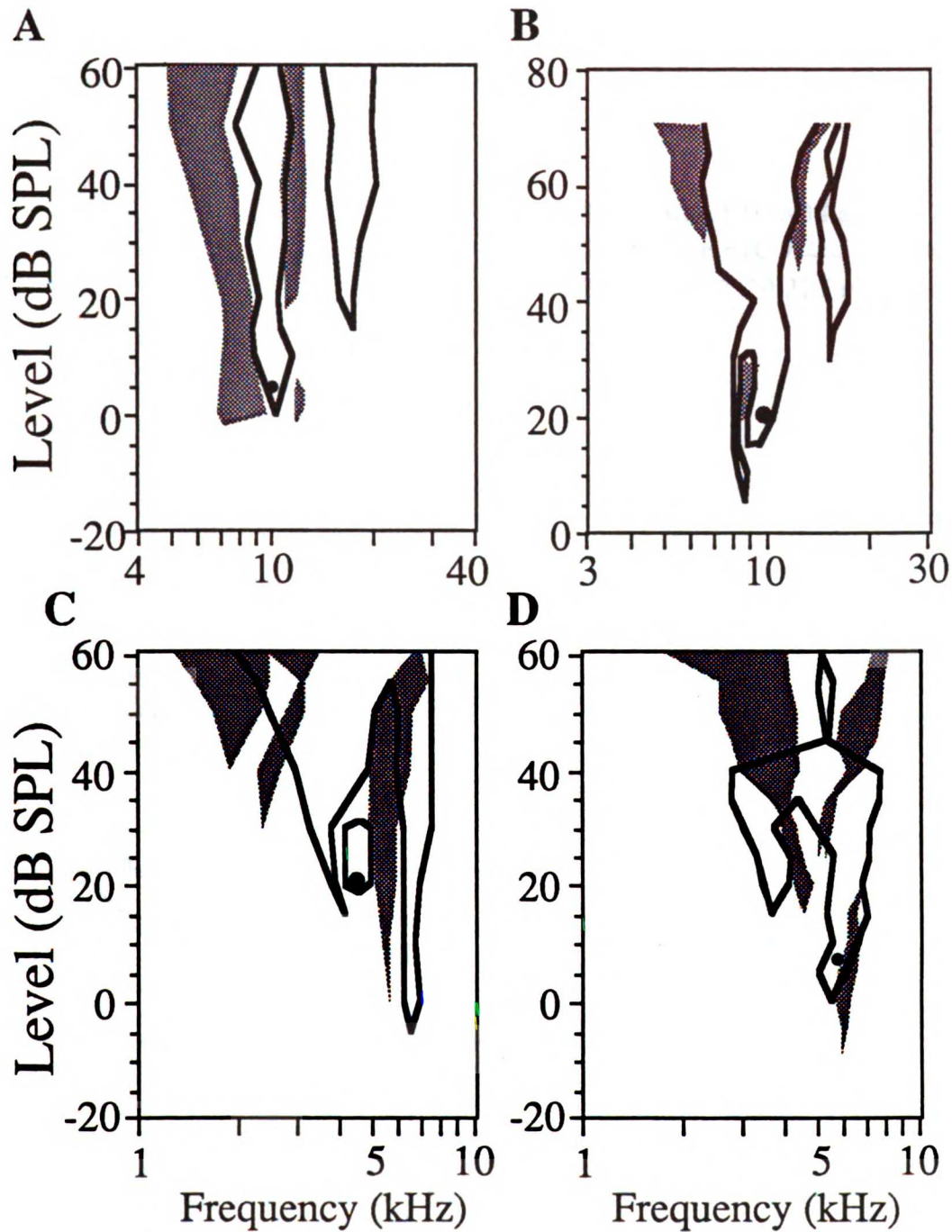
Figure 23:
Frequency tuning curves for four multi-peaked neurons with central inhibition. Dark shaded areas represent suppressory/inhibitory regions. Clear outlined areas are excitatory regions. Filled circles represent probe tone location.
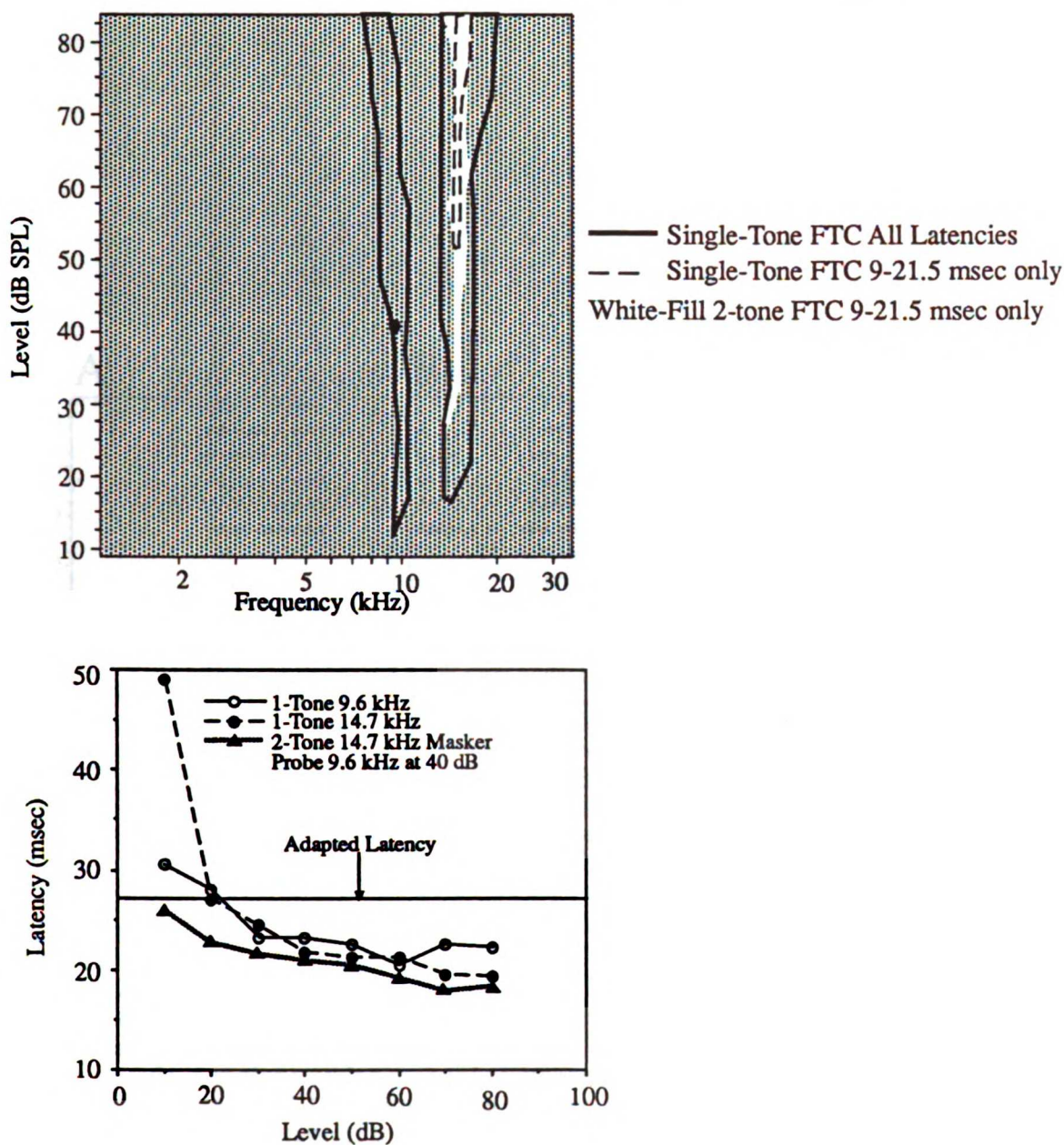
Figure 24:
Top: Tuning curve depicting latency facilitation. Solid outlined area corresponds to the single tone FTC for this neuron. Dashed outlined area around 14-15 kHz corresponds to frequencies and amplitudes of stimuli which elicited response latencies between 9 and 21.5 msec. White shaded area corresponds to frequencies and amplitudes which elicited 9-21.5 msec latencies in the two-tone case with the probe tone at 9.6 kHz and 40 dB (Black dot). In the two-tone case the intensity threshold for shortest latency responses (9-21.5 msec) of this neuron decreases by 20 dB. Inhibitory areas are not displayed in this plot (see Fig. 10C).
Bottom: Latency versus level plot for same neuron. Open circles with a solid line depict the latencies for a 9.6 kHz tone. Filled circles connected by dotted lines depict latencies to 14.7 kHz tones. The filled triangles connected by stippled lines depict the latencies for the two-tone condition (probe 9.6 kHz at 40 dB, masker 14.7 kHz with variable intensities corresponding to the abscissa). Note that the two-tone case always elicits a shorter latency than either tone presented alone. Also note that the adapted latency (solid line) is more than 4 msec longer than the unadapted tone (9.6 kHz at 40 dB)
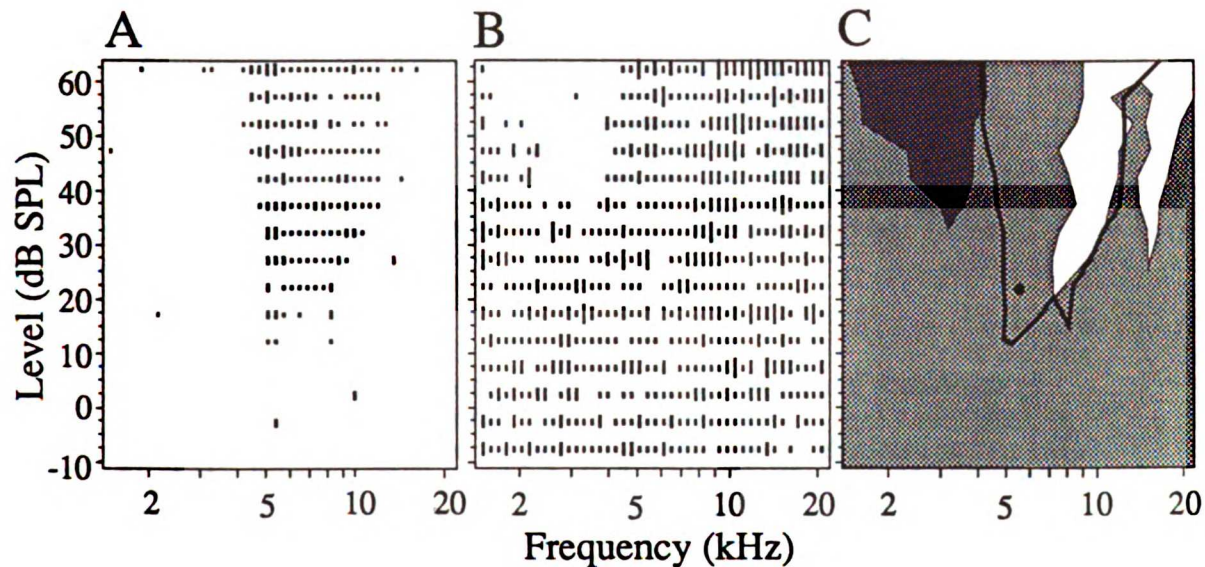
Figure 25:
Single-tone (A) and two-tone (B) FRA's for a neuron that shows two-tone enhancement. A tuning curve representation is shown in (C). The white shaded area corresponds to regions with enhanced responses. The dark shaded area corresponds to the inhibitory region. The outlined area with no fill corresponds to the excitatory FTC. The dark circle corresponds to the probe tone (5.5 kHz, 20 dB). At 50 dB the masker tone suppressed responses ranging from approximately 2.0 to 4.0 kHz and enhanced responses from 8.5 to 12 kHz and 15.0 to 18.0 kHz. The criterion to determine the enhanced region was conservative (200% of the adapted rate) and, thus, excluded some regions which might reflect enhancement effects.
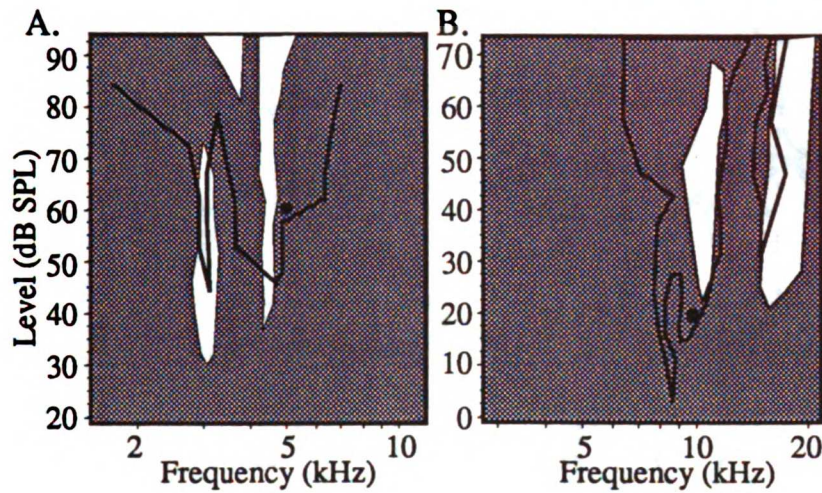
Figure 26:
Tuning curves for two neurons that displayed lowering of thresholds in two-tone cases. Black outlines depict single-tone FTC, and white shading depicts two-tone facilitatory regions. Inhibition is not depicted in this graph. Black dots indicate frequency and amplitude of probe tone. Note the lower threshold of three of the enhanced response regions.
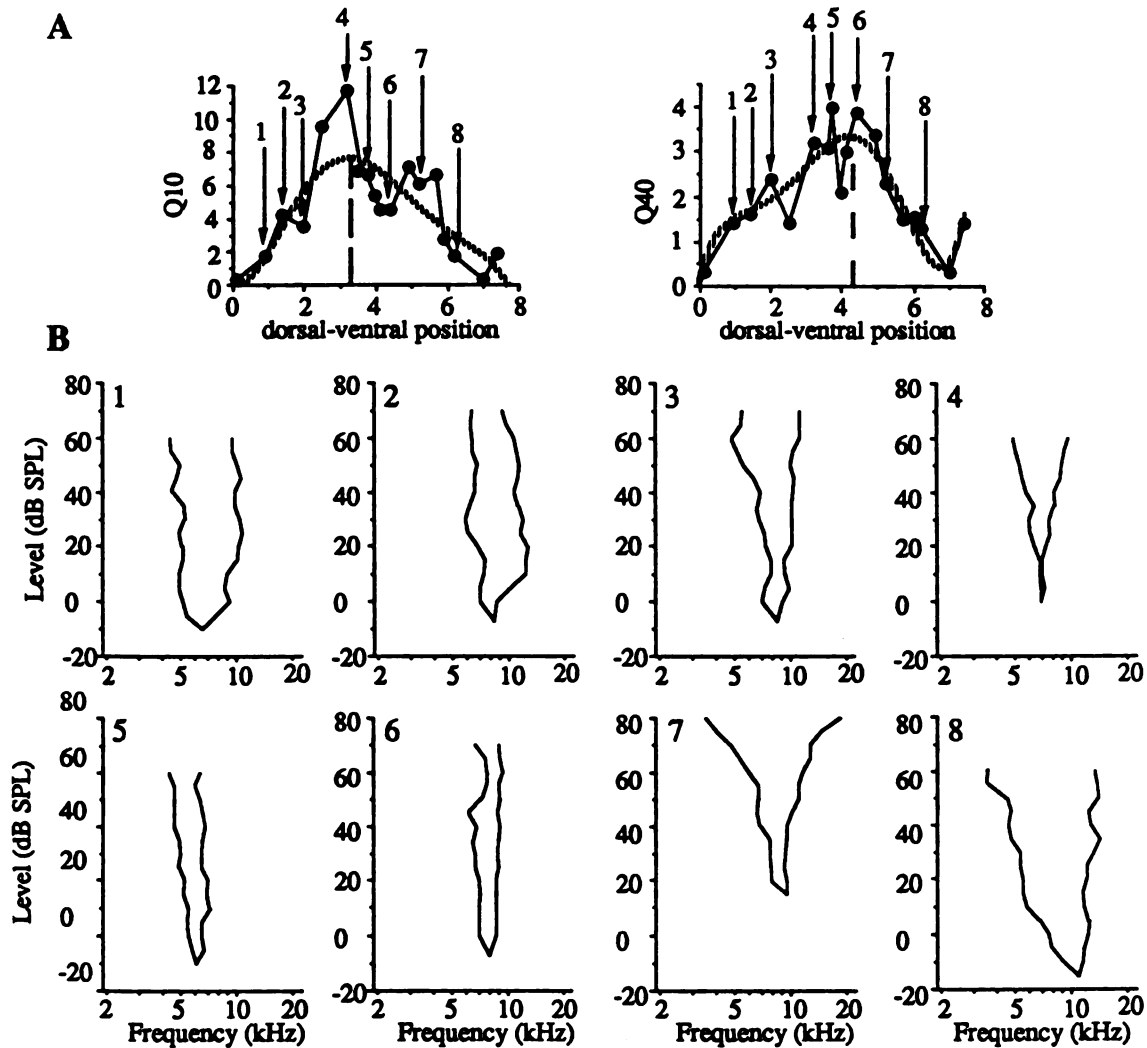
Figure 27:
Demonstration of the gradient in sharpness of tuning (Q-map) in AI of one representative animal.
(A) Plot of Q10 dB and Q40 dB versus location. Zero mm. corresponds to the most dorsal, acoustically driven recording site. Vertically stippled curves show 5th order polynomial fits to the data points. Dashed lines correspond to position of the maximum of this fit. Numbers with arrows indicate tuning curves shown in (B).
(B) Tuning curves from selected data points in (A). Numbers in upper left hand corner of the tuning curves correspond to the numbers of the points in (A). Lower numbers (1-3) correspond to dorsal multiple units and high numbers (7-8) correspond to ventral units. All tuning curves are plotted on the same frequency and amplitude scale.

★ No Response   O Single Unit Single-peaked

● Multiple Unit Mapping Point   ✹Single Unit Multi-peaked
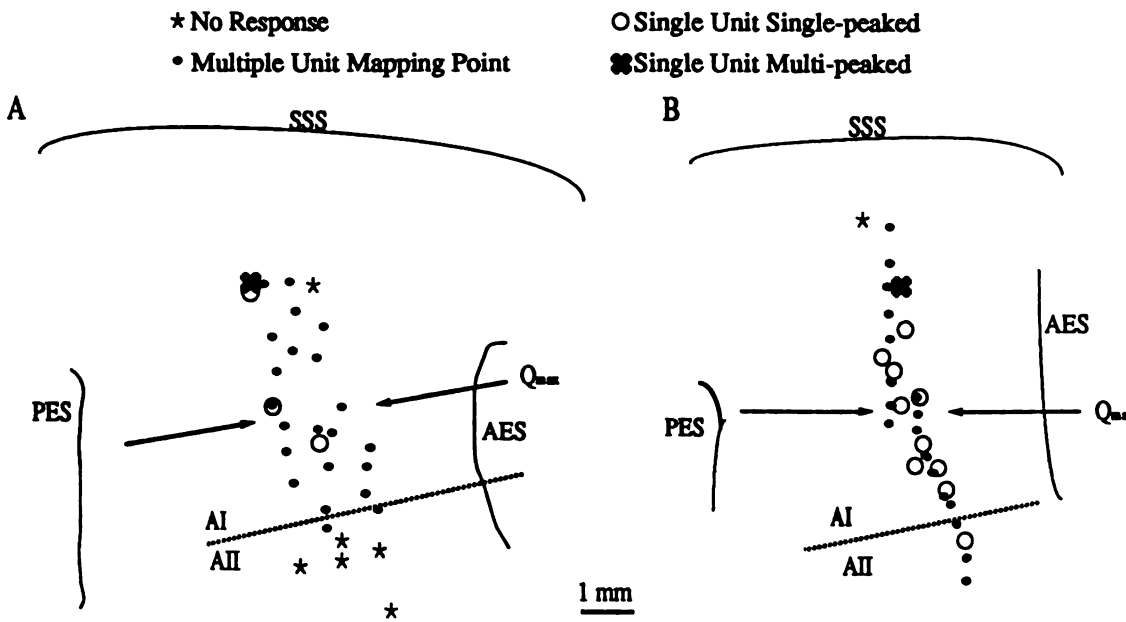
Figure 28:
Graph showing location of recording sites for two representative examples. Multi-peaked single neuron locations are represented by an X. Black dots represent multiple unit penetration sites for recording Q-maps. Open circles represent locations of single-peaked single neuron recordings. In (A) the location of the multi-peaked neuron was the same as that for a single neuron. The two symbols are offset to aid in visualization. SSS: suprasylvian sulcus, PES: posterior ectosylvian sulcus, AES: anterior ectosylvian sulcus, AI: primary auditory cortex, AII: secondary auditory cortex.
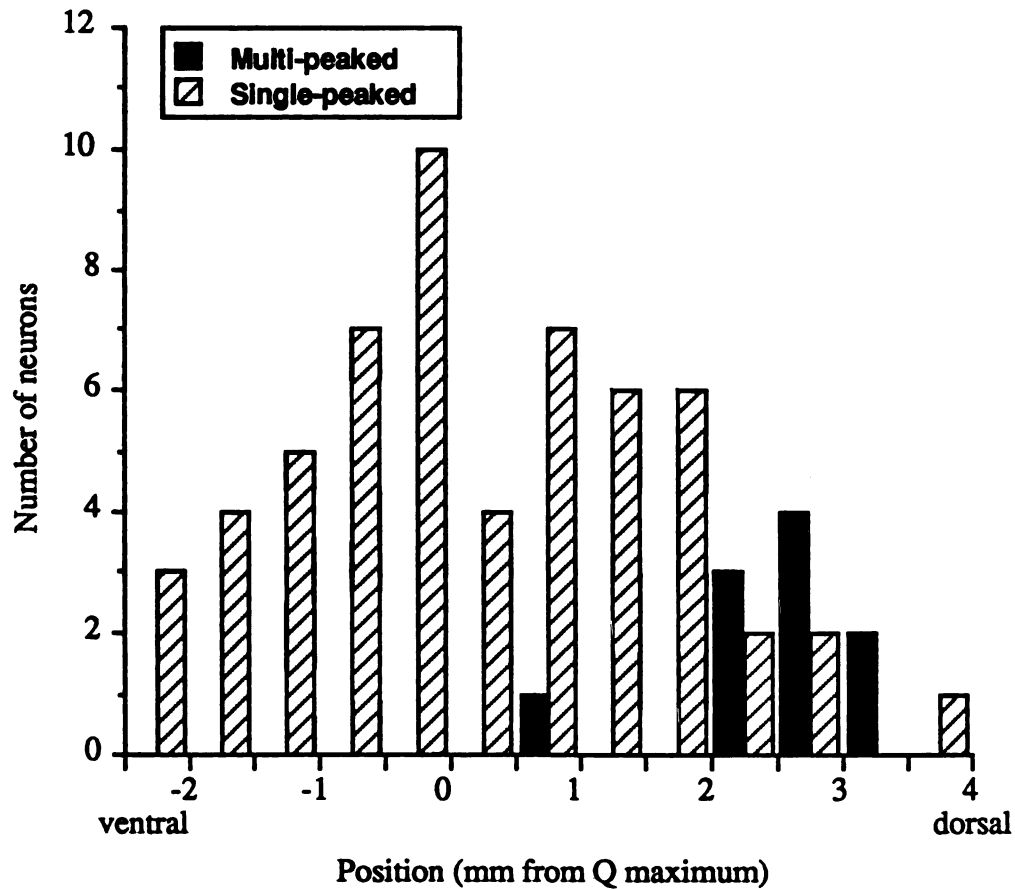
Figure 29:
Histogram showing locations of single (N=57) and multi-peaked neurons (N=10) pooled across animals. Zero millimeters was the common reference point for pooling across animals, corresponding to the location of the Q-map maximum for each animal. Negative values were located ventral to the center and positive values were dorsal to the center. Stippled bars show distribution of single-peaked neurons and black bars show the distribution of multi-peaked neurons.

Table 1   Comparison of Differences in Properties of Low and High Frequency Peaks

| | Difference Function * | | | Low Frequency Peak | | | High Frequency Peak | | | p †† |
| | Percentiles | | | Percentiles | | | Percentiles | | | |
	n §	25th	Med	75th	n	25th	Med	75th	n	25th	Med	75th	
Latency (msec)	24	-0.15	2.70	7.50	24	14.30	18.70	24.90	24	16.50	22.60	32.30	0.0067
Bandwidth (oct)	21	-0.41	-0.04	0.12	23	0.15	0.27	0.72	21	0.13	0.23	0.40	0.2100
CF Ratio†	21	1.46	1.56	2.16									
Threshold (dB)	21	-7.50	5.00	7.30									

* Value of high frequency peak minus value from low frequency peak (except for CF ratio).

† CFl/CFh

†† Paired T-test between 2 peaks

§ Triple-peaked neurons were excluded from CF Ratio and Threshold

Table 2 :   Comparison of Distributions for Single-Peaked and Multi-Peaked Neurons

	Multi-peaked neurons				Single-peaked neurons				p †
		Percentiles				Percentiles			
	n *	25th	Med	75th	n	25th	Med	75th	
Latency (msec)	50	16.30	19.60	27.90	91	13.70	16.50	21.50	0.0051
Bandwidth (oct)	46	0.13	0.27	0.59	91	0.24	0.35	0.70	0.1100
Total BW (oct)	24	0.79	1.17	1.57	91	0.24	0.35	0.70	0.0001

* Values from all three peaks (low, medium, and high) included

† p values for Mann-Whitney tests

Table 3   Repeated Measures of Response Consistency *

	For Peaks Tested †			Difference ††	
	Range	Mean	SD	Mean	SD
CF (kHz)	4.7-15.9	8.30	3.13	-0.09	0.27
Threshold (dB)	0 to 30	7.00	8.62	1.15	6.18
Bandwidth (Octaves)	0.06 to 0.76	0.33	0.20	-0.05	0.13
Latency (msec)	12.1 to 40.1	20.00	6.76	-0.68	1.77

* Trial 1 was normal data. Trial 2 occurred after all battery of tests were

performed. N=13 neurons

† Values for all 26 (pre and post) trials

†† Mean and Standard deviation for difference distribution. Difference =

(trial 2 value) - (trial 1 value)

CHAPTER 2

Functional Topography of Cat Primary Auditory Cortex:

Sharpness of Frequency Tuning for Single Neurons

SUMMARY AND CONCLUSION

1) The spatial distribution of the sharpness of tuning of single neurons along the isofrequency domain of primary auditory cortex (AI) was studied. The sharpness of tuning gradient obtained with multiple unit recordings was used as a frame of reference for the locations of single neurons. The frequency selectivity or 'integrated excitatory bandwidth' of multiple units had been shown to vary systematically along isofrequency contours in AI (Schreiner and Mendelson 1990; Sutter and Schreiner, 1991). The most sharply tuned unit clusters were found at the approximate center of roughly dorso-ventrally oriented isofrequency contours. A gradual broadening of the integrated excitatory bandwidth in both dorsal and ventral directions was consistently seen.

2) The multiple unit measures of the bandwidth pooled across several animals and expressed in octaves 10 dB (BW10) and 40 dB (BW40) above response threshold were similar to those described within individual cases in cats. As in the individual animals, the bandwidth maps were V-shaped with minima roughly located at the center of the dorsal-ventral extent of AI. The location of the minimum in the multiple unit bandwidth map (most sharply tuned area) was used as a reference point to pool single neuron data across animals.

3) For single neurons, the dorsal half of the BW40 distribution showed a gradient paralleling that for multiple units. For single and multiple units, bandwidth increased at a rate of approximately 0.27 octaves per millimeter from the center of AI toward the dorsal fringe. By contrast, the ventral half of AI showed no clear BW40 gradient for single units. At 40 dB above thresholds, most encountered ventral neurons were sharply tuned. At the same time, the multiple unit BW40 showed a gradient similar to the dorsal half with 0.23 octaves per millimeter increasing from the center toward the ventral border of AI.

4) For single neurons, BW10 showed no clear systematic spatial distribution in AI. Neither the dorsal nor ventral gradient was significantly different from zero slope although the dorsal half showed a trend toward increasing BW10s. In Contrast to the responses of single neurons, both dorsal and ventral halves of AI showed BW10 slopes for multiple unit samples confirming a "U" or "V-shaped" map of the integrated excitatory bandwidth within the isofrequency domain.

5) Based on the distribution of the integrated (multiple unit) excitatory bandwidth, AI was parcelled into three regions: the dorsal gradient, the ventral gradient, and a central narrowly tuned area. In ventral AI, single units were significantly more sharply tuned than were multiple units for BW10 and BW40. In dorsal AI, single units were not

statistically different from multiple units for BW40. In central AI, single units were significantly sharper for BW40, but not BW10.

6) The combined single and multiple unit results suggest that AI is composed of at least two functionally distinct sub-regions along the isofrequency domain based on the bandwidth properties of tuning curves of component neurons. The dorsal region (AId) exhibits a gradient of BW40 expressed in single and multiple unit measurements, and can contain broadly tuned single-peaked as well as multi-peaked neurons (Sutter and Schreiner, 1991). In the ventral region (AIv), single neuron responses are predominantly narrowly tuned at 40 dB above threshold, but there is progressively wider scatter of the frequency ranges of narrowly tuned neurons represented at progressively more ventral AI locations. The transition between these areas is delineated by a reversal in the BW40 gradient for multiple units.

INTRODUCTION

Recent studies of cat auditory cortex have demonstrated topographic order within the functional organization of the isofrequency domain of the primary auditory cortical field (AI) (Schreiner and Cynader 1984; Schreiner and Mendelson 1990; Schreiner et. al. 1991; Mendelson et. al 1991; Sutter and Schreiner 1991) that goes beyond the previously described organization with respect to binaural response properties (Imig and Adrian 1977; Middlebrooks et al. 1980; Reale and Kettner 1986). Several response parameters including sharpness of frequency and amplitude tuning obtained from multiple unit recordings were found to be nonrandomly distributed along the dorso-ventral dimension of AI. These findings are suggestive of systematic functional organization(s) in the isofrequency domain of AI of the representations of basic signal properties, among them signal intensity and spectral complexity (Schreiner and Mendelson 1990, Schreiner et al. 1991, Sutter and Schreiner 1991a, Shamma and Fleshman 1990). The functional interpretation of topographies based on multiple unit recordings is, however, limited and can only represent an approximation to the actually performed cortical processing. Therefore, the properties of single neurons underlying those integrated measures of cortical activity have to be analyzed and related to the multiple unit findings in order to understand more

fully aspects of physiological and functional organization of AI.

Studying the spatial distribution of single neuron response properties across larger portions of AI has proven to be a difficult task for a number of reasons. Characterizing enough single neurons in one experiment to construct a reliable physiological map is difficult in a cortical field of the extent of cat AI. Sulcal patterns and vasculature cannot be used to pool topographical data across animals since they display tremendous variability between cats (Merzenich et. al. 1975). Additionally, the cytoarchitectonic boundaries of AI are not sharply enough expressed (e.g., Rose 1949, Winer 1984) to guide a precise alignment of individual fields. Consequently, single unit studies that used anatomically based pooling strategies failed to fully support basic organizational principles obtained with integrated measures such as a strong cochleotopicity of AI (e.g., Evans and Whitfield 1964, Goldstein et al. 1970).

An alternative to using anatomical landmarks is the use of the spatial distribution of physiological features that may provide information about the proper spatial alignment of fields from several individual cortices. The most basic choice is the use of the cochleotopic frequency gradient, reliably determinable with multiple unit recordings

(Merzenich et al. 1975, Reale and Imig 1980, Schreiner and Mendelson 1990), to determine the rostro-caudal extent of the field and to identify locations within the rostro-caudal dimension of the field. However, a second parameter is necessary to align locations along the dorso-ventral extent of AI, i.e. approximately along its isofrequency domain. The clustered distribution of binaural response characteristics along the dorso-ventral extent of AI is quite variable from animal to animal (Imig and Brugge 1978; Middlebrooks et al. 1980; Imig and Reale 1981; Schreiner and Cynader 1984; Reale and Kettner 1986) and cannot serve as a basis for a spatial normalization or alignment of AI from different cortices.

A recent study of the spatial distribution of the integrative excitatory bandwidth along the dorso-ventral dimension of AI (Schreiner and Mendelson 1990) revealed an area of sharp tuning in the isofrequency domain flanked by ventral and dorsal gradients of decreasing sharpness. This spatial distribution of the integrated excitatory bandwidth in AI (Schreiner and Mendelson 1990) appears to be similar from animal to animal and may serve as a topographical frame of reference to compare and pool data from different animals. In a previous report, this approach was successfully utilized to determine the spatial distribution of a subpopulation of auditory cortical neurons, namely neurons with multi-peaked tuning curves, in the dorso-ventral dimension of AI (Sutter

and Schreiner 1991a). By pooling data across animals, a sufficient number of topographically identifiable neurons with multi-peaked tuning curves was obtained to derive a statistically secure estimate that their locations were essentially confined to the dorsal part of AI. This paper explores the property and topography of sharpness of tuning of single neuron responses along the dorso-ventral extent -- approximating the isofrequency axis -- of cat AI. Single neurons were located relative to gradients in integrated excitatory bandwidth as determined with multiple unit recordings. Potential contributions of single neurons to multiple unit maps will be discussed. Some results have previously been presented in abstract form (Sutter and Schreiner, 1991b).

RESULTS

Results are based on a total of 147 multiple units and 109 single units from 9 cats in which multiple unit bandwidth maps with sufficient detail were collected. On the average, multiple unit maps were derived from approximately 15 fairly evenly spaced recording locations. From multiple unit recordings, three parameters were extracted. First, the AI/AII border was determined in accordance with criteria suggested by Schreiner and Cynader (1984). The criteria are based on a reliable shift of three multiple unit physiological properties: (1) an abrupt increase in thresholds by 15 or more dB, (2) Q-10dB values below a certain CF-dependent value, and (3) a blurring of the CF topography. Single neurons falling within functionally defined AII were not included in these analyzed data. Second, the orientation of the isofrequency gradient within AI was determine. Third, the distribution of the integrated excitatory bandwidths derived 10 and 40 dB above minimum response thresholds were reconstructed. Usually, responses to pure tones could not be recorded more dorsal than about 2 millimeters ventral to the suprasylvian sulcus. For a few cases, neurons with responses to pure tones were recorded up to about 1.0 millimeters from the suprasylvian sulcus.

A large array of bandwidths for multiple and single units were encountered in this series of experiments

corresponding to ranges seen for Q-10dB and Q40-dB for multiple units (Schreiner and Mendelson 1990), and Q-10dB (Phillips and Irvine 1980) and bandwidth (Abeles and Goldstein 1970) for single neurons .

Topography of Integrated Excitatory Bandwidth

For topographical characterization, electrode penetrations orthogonal to the cortical surface were placed to closely approximate the orientation of isofrequency contours. For most of AI, these contours can be fitted with a straight line deviating slightly from the dorsal-ventral direction with the dorsal end slanting posteriorly. The angle between the orientation of the approximated course of an isofrequency contour could deviate as much as 30 degrees from the dorso-ventral axis. The CF topography became weaker at the most dorsal extent of the ectosylvian gyrus and isofrequency contours often slanted even more posteriorly (Middlebrooks and Zook 1983, Sutter and Schreiner 1991a). Topographic data are displayed as a function of the dorso-ventral distance along the approximated orientation of the isofrequency contours. The range of CFs included for each case varied between 0.2 to 3 octaves. Since all locations included in the current data evaluation had CFs larger than 4 kHz, the actual CFs used to create the maps are only given in

one case (see Figure 31). In contrast to most previous studies, the sharpness of tuning in this study was measured as bandwidth expressed in octaves. Similar to the traditionally used Q-factor (CF/bandwidth), the bandwidth measure is essentially frequency independent and has the additional advantage that it is independent from the location of the CF within the FRA, i.e. it is not influenced by the symmetry of the FRA or tuning curve.

The spatial distribution of the integrated excitatory bandwidth for pure tones obtained in this study was consistent with that of previous reports (Schreiner and Mendelson 1990, Sutter and Schreiner 1991a). Locations with sharply tuned multiple-unit responses yielding a narrow integrated excitatory bandwidth were found in a cluster near the dorso-ventral center of the straight segment of isofrequency lines approximately 1.5 to 3 mm dorsal to the AI/AII border. Locations dorsal and ventral of this point gradually showed more broadly tuned responses.

Figure 30 illustrates multiple unit bandwidth maps obtained 10 and 40 dB above minimum response threshold for two representative individual cases. Panels A and B show the reconstructed BW40 maps. Circles connected by dotted lines show the actual values. These and other cases show a distinct bandwidth minima surrounded by areas with wider frequency tuning. Case SUTC16 (right panels) showed a larger

variability in sharpness of tuning in areas that contained wider bandwidths. The dorso-ventral progression of bandwidth changes was much smoother in case SUTC12 (left panels). To aid in demarcating the minima of bandwidth plots, a 500 micron spatially weighted smoothing algorithm was used (100% smoothing for points at the same cortical distance to no weighting for points more than 500 microns apart). The smoothed version of the BW40 maps are shown as solid lines in Figures 30 A and B, respectively. Arrows point to the location of the main minimum in each bandwidth function. The data points and the smoothed version of the BW10 map for these two cases are shown in Figure 30C and D. In both cases, the BW10 minima are located 0.5 to 1 mm dorsal to the BW40 minimum in agreement with previous findings for Q-10dB and Q-40dB (Schreiner and Mendelson, 1990). The minima of these functions (BW10 $_{min}$ and BW40 $_{min}$) served as physiological normalization points to spatially pool sharpness-of-tuning data across animals.

Single Neuron Maps

In case SUTC16 a sufficient number (27) of single unit locations were sampled to directly compare single and multiple unit topographies within the same animal (Fig. 31). The origin of the abscissa designates the location of the

combined bandwidth minimum, that is the averaged location of the BW10 and BW40 minima (BW10/40$_{min}$). For BW40 (Fig. 31A), the spatial distribution of the single neuron sharpness was quite similar to the integrative excitatory bandwidth. Neurons with the narrowest bandwidth were located at or near the multiple unit bandwidth minimum. Dorsal to the minimum, the bandwidth for single neurons increased and showed a scatter similar to that expressed in multiple-unit responses. Ventrally, the excitatory bandwidth of single neurons also increased progressively. However, sharply tuned neurons were found throughout the ventral region of AI and, overall, the integrated excitatory bandwidth appeared to be larger than the single neuron bandwidth. The distribution of BW10 values for single and multiple units (Fig. 31B) were also fairly similar. In this particular case, the minimum of the BW10 distribution was not very strongly expressed for either multiple (see Fig.30D) or single neurons. However, the apparent scatter of encountered bandwidths appeared to be the smallest near the estimated center of the bandwidth distribution. The CFs of single neurons are shown at the corresponding bandwidth values in Fig.31 C and D. The CFs covered a range of about 1 octave and did not have a strong influence on bandwidth distributions.

Pooling Data: Normalizing Location Relative to Multiple Unit Maps

The reconstruction of the spatial bandwidth distribution for case SUTC 16 was made possible by sampling a relatively large number of single (27) and multiple (28) units in the same experiment. This, however, was rare and, therefore a method for pooling data across animals was necessary to assess the topography of single neurons characteristics.

In this study, the location of single neurons within an experiment was referenced relative to the multiple unit bandwidth map. The normalization procedure is illustrated in Fig. 32 for the two cases shown in Figs. 30 and 31. To aid in visualizing this procedure, single neurons from case SUTC12 are marked by filled diamonds and single neurons from case SUTC16 are marked by crosses. The unsmoothed BW40 maps for cases SUTC12 and SUTC16 (from Figs. 30 A and D) are represented by open circles connected by lines in Fig. 32 A and B. For these two experiments, AI was approximately 6.2 and 5.3 millimeters in its dorsal-ventral extent. $BW40_{min}$ is marked by arrows. To pool data across these two experiments, the minimum in the smoothed BW40 distribution ($BW40_{min}$) was assigned the reference value of zero millimeters and all recording points were assigned values as distance in millimeters away from $BW40_{min}$. The shifted and aligned

recording locations of the two cases are shown in Fig. 32 C and D, respectively. The result of pooling locations of single neurons for both aligned maps is displayed in Fig. 32 E. No distortion of the individual recording locations is involved in this method and, accordingly, the pooled data reflect the trends discernable in individual cases. This procedure was used to pool data across all 9 cases.

BW40 Topography

Scattergrams of BW40 values for all pooled single and multiple units are shown in Figs. 33 A and B. Cortical locations were aligned relative to $BW40_{min}$ for each individual case as described above. The pooled BW40 data for multiple-unit responses show the same pattern as seen for individual cases in this and previous studies (Schreiner and Mendelson 1990, Sutter and Schreiner 1991a). In particular, a center of sharp tuning is surrounded by, on the average, gradually increasing bandwidths with increasing distance.

The pooled distribution of BW40 for single neurons (Fig. 33B) shows some similarities and some dissimilarities to the multiple-unit distribution. Dorsal to the BW40 minimum, single units show the same tendency of increasing bandwidth with dorsal distance as seen with multiple units. Partially responsible for this increase in bandwidth is the

occurrence of multi-peaked FRAs in the dorsal aspect of AI
(crosses in Fig. 33B) in accordance with a previous report of
their distribution (Sutter and Schreiner 1991a). However,
some sharply tuned single and multiple neuron responses can
be found across the entire dorsal half of AI or at least up
to 3 mm dorsal to the bandwidth minimum. In the AI sector
ventral to the bandwidth minimum, the pooled single neuron
data deviated from the trend seen in multiple unit recordings
as well as from that seen in the single neuron example shown
in Fig. 31: BW40 of almost all ventral single neurons
remained fairly sharply tuned (below 0.7 octaves), although
the multiple unit recordings showed increasing bandwidths at
greater distances from the $BW10/40_{min}$. The AI/AII border
varied from 1.65 to 3.45 millimeters from $BW40_{min}$ and no
single neurons located within AII were included. However,
even locations as close as 1 mm ventral to the BW40 minimum,
and therefore located well into AI, showed multiple unit
locations with bandwidths in excess of 1 octave whereas all
single neurons remained below that value. Figure 33C shows a
direct comparison of the single and multiple unit
scattergrams. BW40 values were binned and averaged over 500
microns. The mean BW40 values of multiple (shaded columns)
and single (solid columns) units are shown. Standard
deviations are represented by error bars. Mean and standard
deviation of BW40 increased gradually toward the dorsal end

of AI for multiple and for single units. Ventrally, mean and standard deviation of BW40 for single neurons remained constant whereas the multiple unit values increased toward and into AII.

From the location of the bandwidth minimum for multiple units, a progression to larger bandwidths or broader tuning ocurred in both the dorsal and ventral direction of the isofrequency domain. The dorsal and ventral gradients can be approximated by regression lines as shown in Figure 34A. The slope of the dorsal gradient is -0.26 octaves per millimeter. The 95% confidence interval of the slope lies between -0.14 and -0.38 octaves per millimeter. The slope of the ventral multiple unit BW40 gradient, 0.23 octaves per millimeter, is similar but slightly less than that of the dorsal slope. There is more scatter on the ventral side as the 95% confidence interval contains slopes between 0.09 and 0.36 octaves per millimeter. For both sides of the distribution, the zero slope lies outside of the 99.5% confidence intervals. Therefore, the multiple unit BW40 distribution is concave with a minimum ('V-shaped').

Contrasting the multiple unit distribution, the single unit topography (Fig. 34B) appeared to be essentially flat on the ventral side. The slope of the gradient was 0.05 oct/mm. The 95% confidence intervals comprises slopes between -0.04 and 0.13 octaves per millimeter which includes zero slope or

a flat line. Therefore, it cannot be claimed, with 95%
confidence, that the slope is greater than zero (flat). The
first confidence interval that solely contains positive
slopes is 74 percent. Dorsally the slope, -0.28 oct/mm, is
similar to the dorsal multiple unit slope. The 95% confidence
intervals of -0.13 and -0.42 contain the value of the
multiple unit slope.

Parcelling of AI: BW40 Differences

In order to test the hypothesis that the isofrequency
domain of AI may consist of more than one physiologically
distinguishable region, AI was subdivided into three regions
based on the bandwidth distribution: one millimeter to each
side of the location of minimum bandwidth was arbitrarily
defined as the 'central' two millimeters of AI; dorsal and
ventral to this area were defined correspondingly. The
minimum bandwidth measure used to pool data for this analysis
is the location of $BW40_{min}$ and $BW10_{min}$ averaged for each
particular case ($BW10/40_{min}$). This measure was used so that
the same topographical parcelling to analyze BW10 and BW40
data can be performed without biasing toward either measure.
Figure 35 shows the histograms of BW40 for dorsal, ventral
and central regions of AI for single (black bars) and
multiple (shaded bars) units. Median values for the

histograms are summarized in Fig. 35C. Deviation bars represent one half of the 75th percentile BW value minus the 25th percentile value.

Mann-Whitney non-parametric tests establish a significant difference between multiple and single units's BW40 distribution in the ventral and central parts of AI (p < 0.01) (Table 4). In dorsal AI, no significant difference was found (p > 0.05).

Analysis of variance (ANOVA) and Kruskal-Wallis non-parametric ANOVA were applied to test for differences in the values of bandwidths of the three regions. The results of these tests are shown in Table 5. Significant differences (p < 0.01) between the three regions were found for both single and multiple unit BW40 values. Post-hoc Scheffe analysis reveal that the ANOVA results were caused by central vs ventral and central vs dorsal differences for multiple units (Table 6). For single units ANOVA differences could be accounted for by dorsal vs central and dorsal vs ventral differences. Non-parametric Mann-Whitney U tests confirmed the Scheffe results.

BW10 Topography

Scattergrams of BW10 for single and multiple units are shown in Fig. 36. Locations were pooled such that $BW10_{min}$ was

assigned the reference value of zero for each case. While the
multiple unit distribution appears to be V-shaped paralleling
the multiple unit BW40 distribution, such an effect appeared
to be less pronounced, if at all present, in the distribution
of BW10 for single neurons. For both multiple and single unit
recordings, narrowly tuned FRAs were encountered throughout
the entire dorso-ventral dimension of AI. The slopes of BW10
gradients are compared in Fig. 37. Dorsal to the bandwidth
minimum, the slope is -0.10 oct/mm with 95% confidence
intervals at -0.06 and -0.15 oct/mm, for multiple units.
Ventrally, the slope is 0.11 oct/mm with 95% confidence
intervals of the slope at 0.05 and 0.18 oct/mm. For both
dorsal and ventral halves, zero slope falls outside of the
99.5% confidence interval indicating that with 99% confidence
the distribution is V-shaped and, thus, similar to the BW40
distribution.

The single unit BW10 topography did no show slopes
significantly different from zero either dorsally or
ventrally (Fig.37B). Dorsally, the slope was -0.03 oct/mm
with 95% confidence intervals for the slope at -0.08 and 0.02
oct/mm which includes zero slope. Confidence intervals which
do not include zero slope are 73% and less. Ventrally the
gradient is 0.01 oct/mm with confidence intervals for the
slope at -0.04 and 0.06 oct/mm which includes zero slope.

Parcelling of AI: BW10 Differences

For BW10, AI was parcelled the same way as for BW40 and histograms are shown for single (A, black bars) and multiple (B, black bars) units in dorsal, central and ventral AI. The summary histogram of medians is shown in Fig.38C with deviation bars similar to those shown in Fig. 35. Differences between BW10 values for single and multiple units were statistically tested (Mann-Whitney test) (Table 4). There was a significant difference between BW10 for single and multiple units in the ventral ($p < 0.01$) and dorsal ($p < 0.05$) regions of AI. Centrally, there was no significant difference of BW10 between single and multiple units ($p > 0.05$) (Table 4).

For multiple units, ANOVA and Kruskal-Wallis analyses revealed significant differences between dorsal, ventral and central regions (Table 5). Scheffe post-hoc tests revealed that the significant ANOVA was due to differences between dorsal and central and between central and ventral data. Mann-Whitney tests confirmed the Scheffe results (Table 6). For single units, ANOVA and Kruskal-Wallis showed no significant differences in BW10 between central, ventral and dorsal regions in AI (Table 5).

DISCUSSION

In this series of experiments, the bandwidth of FRAs 10 and 40 dB above minimum response threshold was used to investigate a) whether pooling of data across animals can be successfully used to study physiological topographies, and b) how single neuron response properties relate to physiological gradients obtained with multiple-unit recording techniques. The main findings of this study can be summarized as follows: 1) Multiple-unit data, pooled along the isofrequency-domain of AI, reflected the same double representation of Bandwidth as previously seen in individual cases (Schreiner and Mendelson 1990), namely, a region about 1.5 to 3 mm dorsal of the AII border contained narrow bandwidths gradually giving way to more broadly tuned responses dorsally as well as ventrally. 2) Single neuron bandwidths, pooled relative to the multiple-unit bandwidth topography, significantly differed from the multiple-unit distribution in several respects: a) in the region of AI ventral to the minimum in multiple unit bandwidth, no clear gradient in sharpness of single neuron responses was evident for either BW10 or BW40; b) in the region of AI dorsal to the minimum in multiple unit bandwidth, a spatial gradient was evident for the BW40 of single neurons similar to the one obtained for multiple units; however, c) no clear gradient was apparent in this dorsal region for BW10 of single neurons.

Methodological Considerations

Before discussing some implications of these findings, a brief look at the pooling method is in order. Single and multiple unit properties were pooled along an approximation of the isofrequency axis of AI, roughly corresponding to a line with dorso-ventral orientation. The location of the minimum in multiple-unit bandwidth either 10 or 40 dB above minimum response threshold was used as a frame of reference for the pooling of data allowing an alignment of isofrequency contours from different cortices. In order to leave the data as simple as possible, AI only was aligned at physiological centers, and not normalized or scaled for size differences. Reale and Imig (1980) gave estimates of the dorso-ventral extent of AI ranging from 4 to 7 mm. However, precise anatomical or physiological criteria for establishing the extent of that dimension are not available (see Schreiner and Mendelson 1990, Sutter and Schreiner 1991a, Schreiner and Cynader 1984). Therefore, no attempts for an extent normalization have been made. A potential consequence of differences in the absolute extent of spatial gradients may be a blurring of the topographies at the dorsal and ventral extremes of the pooled data (see below).

The pooling method did not take into account the actual CF of the units. Could CF sampling biases have strongly effected the observed spatial bandwidth distributions? It has been reported that, with increasing CF, Q-factors of cortical neurons show an overall increase, and relative bandwidth values decrease (Phillips and Irvine 1981). Previous studies (Schreiner and Mendelson 1990, Sutter and Schreiner 1991a) have shown only small CF-dependent effects on the dorso-ventral distribution pattern of tuning sharpness, at least for the CF range above 4 kHz which is the range covered in the current study. In some of the cases included in this study, CFs at locations near the ventral and dorsal end of AI tended to deviate from the projected isofrequency value toward higher frequencies (see Fig. 31C,D). These were also the regions that showed the widest integrative excitatory bandwidth. Since neurons with higher CF also tend to have narrower octave-measured bandwidths, a potential CF-influence would tend to obscure bandwidth differences between the dorso-ventral center and the dorsal and ventral margins of AI.

Finally, in interpreting this data, it is important to remember that the recordings from these experiments are limited to depths between 600 and 1000 microns below the cortical surface. The presented single neuron distributions would be expected to be limited to this primary input zone of

AI columns, roughly corresponding to deep layer III and layer IV.

Single Unit Bandwidth vs. Multiple Unit Bandwidth

The multiple unit measurements of sharpness of tuning (excitatory bandwidth 10 and 40 dB above minimum threshold) confirm the spatial pattern in the dorso-ventral dimension of AI as reported for corresponding Q-values (Schreiner and Mendelson 1990, Sutter and Schreiner 1991): all isofrequency contours contain a region of narrow integrated excitatory bandwidths with a gradual transition to more broadly tuned locations toward the ventral and dorsal end of AI. In other words, the excitatory contributions that are available at different cortical locations along the isofrequency domain appear to systematically vary. What is the source of this bandwidth gradation? Pooled single neuron data dorsal to the minimum in integrated bandwidth 40 dB above threshold showed units with progressively broader bandwidth intermingled with sharply tuned neurons. Local integration of activity from several neurons can account for the observed dorsal bandwidth gradient as reflected in similar slopes of the linear regression for multiple- and single-unit BW40 (Fig. 34). The occurrence of neurons with multi-peaked tuning curves in dorsal AI (Sutter and Schreiner 1991) contributed to the

broadening of the multiple-unit BW40. However, neurons with a broad single excitatory response area were also encountered. In the pooled data for dorsal AI, the bandwidth of the single peaked neurons occasionally exceeded the total bandwidth of multi-peaked neurons (Fig. 33). Broad single-peaked neurons did not necessarily have to reside in close proximity to recorded multi-peaked neurons, although it was possible to record any combination of single-peaked broad, single-peaked narrow, and multi-peaked broad neurons in the same penetration (personal observation).

Ventral to the minimum for integrated bandwidth, pooled BW40 values of single neurons did not reflect the same trend as seen for the integrated bandwidth. All single neurons in the ventral 3.5 mm of AI remained fairly sharply tuned that is below a bandwidth of 1 octave. By contrast, approximately 25% of the multiple units in that area had bandwidths larger than 1 octave. Accordingly, no bandwidth gradient was observed for the pooled single neuron data. Two aspects of the pooling method may have contributed to this discrepancy between multiple and single unit measurements. First, single units that were located in AII as defined by multiple unit criteria (Schreiner and Cynader 1984), were not included into the pooled data. A strict definition of the AI/AII border may have biased the single unit distribution toward lower bandwidths at the ventral end of AI; however, looking at the

multiple unit BW10 distribution indicates that this is not the case. Second, the distance between the bandwidth minimum and the border of AII could vary over more than 2 mm, even within a single case. Since the length of AI was not normalized for the pooling, a functional gradient between BW40 minimum and AII could be obscured due to the averaging. Indeed, in the most complete single unit case (see Fig. 31) a BW40 gradient was apparent in ventral AI. However, the single unit gradient appeared to be somewhat shallower than the multiple-unit gradient.

While BW40 showed a clear topographical distribution in AI, BW10 did not. BW10 has a constant median value of approximately 0.15 octaves, regardless of cortical location. This effect is is consistent with the conclusion that for single neurons Q10 shows no or few major differences between different auditory structures within the primary pathway (CN to IC to MGB to AI), while Q30 or Q50 (measures of sharpness of tuning 30 and 50 dB above threshold) show significant differences at different auditory stations (Suga and Manabe 1982; Katsuki et al. 1959a, 1959b). Measuring sharpness of tuning 10 dB above threshold probably is not a very important way of measuring differences in single unit response properties in the auditory system.

It is concluded that sharply tuned neurons can be found across the entire dorso-ventral extent of AI. The spatial

variation in integrated bandwidth in the dorsal region of AI
is paralleled by an increase in the scatter of granular and
supragranular layer single unit bandwidths, and by an
increasing occurrence of multi-peaked neurons toward the
dorsal end of AI. By contrast, the increase of integrated
bandwidth toward the AII border is not necessarily paralleled
by an increase in single unit bandwidth. In the approximate
dorsal-ventral center of AI there is a region of sharply
tuned single and multiple unit responses.

Physiological Architecture of AI

The apparent discrepancy between single and multiple
unit estimates of the excitatory bandwidth in the ventral
part of AI suggests the influence of other physiological
parameters on the bandwidth measures. Specifically, it
indicates that there are topographical differences in CF
scatter and/or in intensity threshold scatter. In the
physiological center of AI, defined by the multiple unit
bandwidth, there should be little single unit CF scatter. An
increasing scatter in CF toward dorsal, but especially,
ventral borders of AI could account for the observed increase
in multiple unit bandwidth.

As a preliminary test of the hypothesis of a varying
degree of CF scatter across AI, a post-hoc analysis of the

single neurons CF's relative to the multiple units CF was
conducted. The CF scatter was determined by either of two
methods. If a multiple unit CF was available for the same
location as that of a single neuron, the difference between
the two CF's was obtained. For single neuron locations that
did not coincide with a multiple unit measurement but were
located between two multiple unit recording locations, the
multiple unit CF at the location of the single neurons was
estimated by linear interpolation from the actual recording
locations and the difference with the single neuron CF was
obtained. Some single neurons (13) had to be excluded from
this analysis because expected CF could not be determined for
their locations. The spatial distribution of mean CF scatter,
the mean of the absolute value of the difference of the
expected CF and the actual single neuron CF in octaves,
concurred with the hypothesis (Fig. 39, N=96). Near the
bandwidth minimum, the obtained mean CF scatter was small and
below the mean BW10 values for those locations. More dorsally
but especially more ventrally, the mean CF scatter increased
dramatically. Although a proper estimate of the distribution
of single unit CF scatter in AI needs to be performed by
analyzing several single neurons at each sampled cortical
location (e.g. Hui et al. 1989), the currently applied post-
hoc analysis should provide a reasonable approximation since
multiple unit CF shows a very high degree of cochleotopocity

(Merzenich et al. 1975, Reale and Imig 1980). Combining the range of CF scatter with the range of single neuron bandwidth for each AI sector results in a close approximation of the bandwidth values obtained with multiple unit recording.

Another view to the construction of broad multiple unit responses from narrow single unit responses can be described by thinking of the multiple unit response as the total integrated response of the entire recording site. The multiple unit recording could reflect all inputs, inhibitory and excitatory, since this method can record from somas, dendrites and axons of different neurons. With this in mind the ventral difference in BW40 might be due to the recording of spikes from proximal inhibitory processes (not somas) in the vicinity of a post-synaptic neuron. Therefore broad excitatory responses might be due to the broad inhibitory input to narrowly tuned ventral neurons. Inhibitory axons might not be recorded from during single unit recording due to difficulties in holding axonal recordings. If all inhibitory and excitatory input were recorded from in multiple unit recordings, dorsally multi-peaked single neurons would be accompanied by broad single-peaked multiple unit recordings which usually is the case (personal observation).

Parcelling of AI

Dividing AI into three different regions provided a direct method of addressing questions regarding differences between single and multiple unit bandwidth measures. The selection of three areas was based on the distribution of the integrated bandwidth alone. The combined results from single and multiple units suggest that, physiologically, AI can be parceled into two functional regions: a ventral (AIv) and a dorsal (AId) region. The basis of dividing these regions are a) a reversal of the gradient of multiple unit integrated bandwidth along the dorso-ventral axis of AI, and b) a difference in the distribution of BW40 for single neurons. The observation of multi-peaked tuning curves at depths recorded in this experiment may help in defining a third area corresponding and overlapping with "the dorsal zone of AI" (Middlebrooks and Zook 1984). For purposes of this discussion, without having any dorsal border, we will include all recorded locations dorsal of $BW10/40_{min}$ within AId.

Functional Significance of Findings

A significant difference in the spectral integration properties of the granular and supragranular layers of dorsal and ventral AI implies that there should be fundamental

differences in the spectral processing in the two regions.
Functionally, AId may be particularly well-suited for an
integrative analysis of broad-band stimuli. This is reflected
in generally broader excitatory tuning of single neurons as
well as by multi-peaked neurons. Additionally a high
responsiveness to broad-band stimuli was observed in
AId.(Schreiner and Mendelson 1990, Sutter and Schreiner
1991).

Locations in AIv may be more suited for a differential
analysis of broad band stimuli since they are marked by
sharply tuned single neurons with varying degree of CF
scatter. Accordingly, the responsiveness to broad-band
stimuli is generally smaller than AId. However, the
distribution of other response parameters, in particular
minimum threshold, monotonicity rate/level functions, and
binaurality, have to be taken into account to derive a more
complete interpretation of the functional topography of AI.

The large overlap of frequency response areas of local
neurons in AId indicate that correlation based plastic groups
(e.g., as described by Edelman and Finkel 1984) might be
encountered in this region. The scatter in CF as seen in Fig.
39 does not result in a lack of FRA overlap. Units with CF's
deviating from the multiple unit response can have high
intensity thresholds (See chapter 3). The FTC of such high
threshold neurons can completely overlap with the FTC of

lower threshold single neurons and, thus, the two neurons could be strongly correlated at high intensities. AIv with CF scatter in narrowly tuned single neurons, does not have strong FTC overlap at high intensities and thus might not form cohesive groups with respect to excitatory spectral/temporal correlation. The ventral neurons are sharply tuned for the frequency and amplitude of (see Chapter 3) narrow-band stimuli. The range of CF scatter combined with the narrow-band preference of these neurons indicate that they do not fire together or synchronously for many auditory signals. An intriguing but at this time speculative possibility is that in AIv the CF/SRF acts as a hard-wired template, and that plastic correlations might occur in frequency response areas where the effects of single tones are only expressed below the spike initiating threshold. Inhibitory or two-tone facilitation frequency response areas under such a scenario might form the basis of plastic groups.

Dorsal AI, with a tendency to respond to broad band stimuli and large regions of FRA overlap, could provide a basis for processing differences within broad-band stimuli. Ventral AI with neurons that have sharp FRA's and that do not respond well to broad-band stimuli could provide a basis for processing signals with one or more narrow bands of frequency content. Because the FRA overlap of these regions is substantially different, one must assume until otherwise

shown that the expressions, representations, and/or mechanisms of plastic changes of these two regions would be different.

Relation to Previous Studies

The results of this chapter help to resolve previous discrepancies between reported CF topography and sharpness of tuning in AI. An apparent lack of CF topography, or even CF consistency within the same penetration, reported in some studies (Katsuki et al. 1959; Evans and Whitfield 1964, Goldstein et al 1968, Goldstein et al. 1970) can be due to recording from single units whose thresholds are different than the most sensitive response. Additionally there is more multiple unit CF scatter in dorsal AI than ventral (Sutter and Schreiner 1991).

The investigators who report lack of CF/BF consistency also report a wide range of tuning sharpness (50% > 0.5 octaves) and multi-peaked neurons. Other studies have claimed that almost all units in AI are sharply tuned (Phillips and Irvine 1981). Differences in sampling from dorsal and ventral AI can account for the sharpness of tuning differences. The recording of primarily sharply tuned units by Phillips and Irvine can probably be accounted for by recording primarily from the central and ventral region of AI and/or a reliance

on Q10 as the measure of sharpness. The recording of broad
and multi-peaked single neurons by the other investigators
can be accounted for from recordings which include dorsal AI,
and which are collected using higher intensity values used
(usually 50 or 60 dB SPL).

Closing Comments

A new physiological framework of AI has been reported.
This framework shows a clear topography of sharpness of
tuning in AI. Strong evidence is presented that AI should be
divided into two separate regions :dorsal AI (AId) and
ventral AI (AIv). Interpretation of physiological experiments
in AI need to account for this newly discovered physiological
architecture of AI.
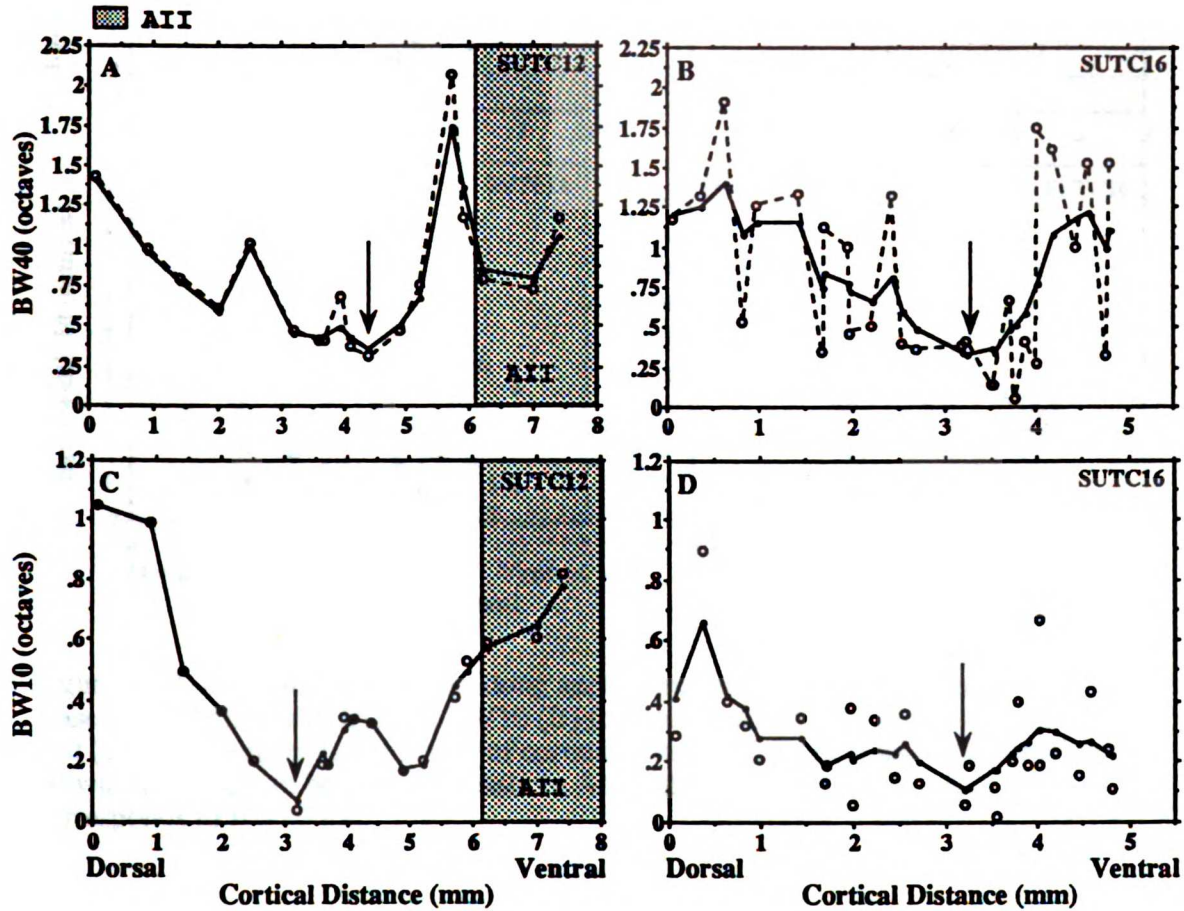
Figure 30: Distribution of multiple unit BW10 and BW40 values along the dorsal ventral axis of AI in two cortices.

A,B: BW40 values (circles) are connected by dashed lines. Solid lines represent the smoothed bandwidth distribution. A 500 micron spatially weighted algorithm was used for smoothing: 100% smoothing for points at the same location to no weighting for points 500 microns apart. Arrows mark the location with the minimum average BW40 (BW40min)

C,D: BW10 values (circles) and smoothed bandwidth distribution. Arrows mark BW10min.
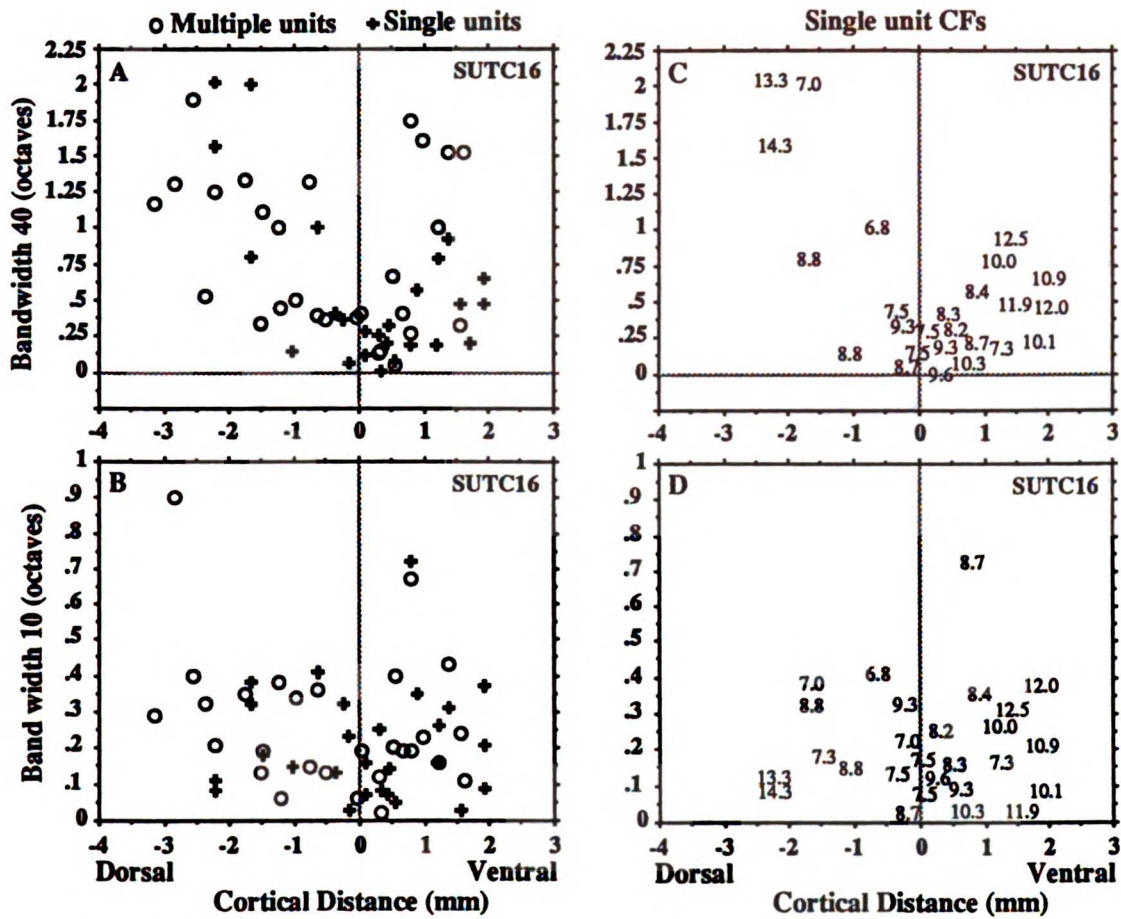
Figure 31: Bandwidth distribution along approximated isofrequency domain of AI (case SUTC16). BW40 (A) and BW10 (B) for single neuron (crosses) and multiple unit (circles) samples as a function of cortical distance. CF's of single neurons (C and D) whose points can be seen as crosses in A and B respectively.Zero millimeter corresponds to BW40min.
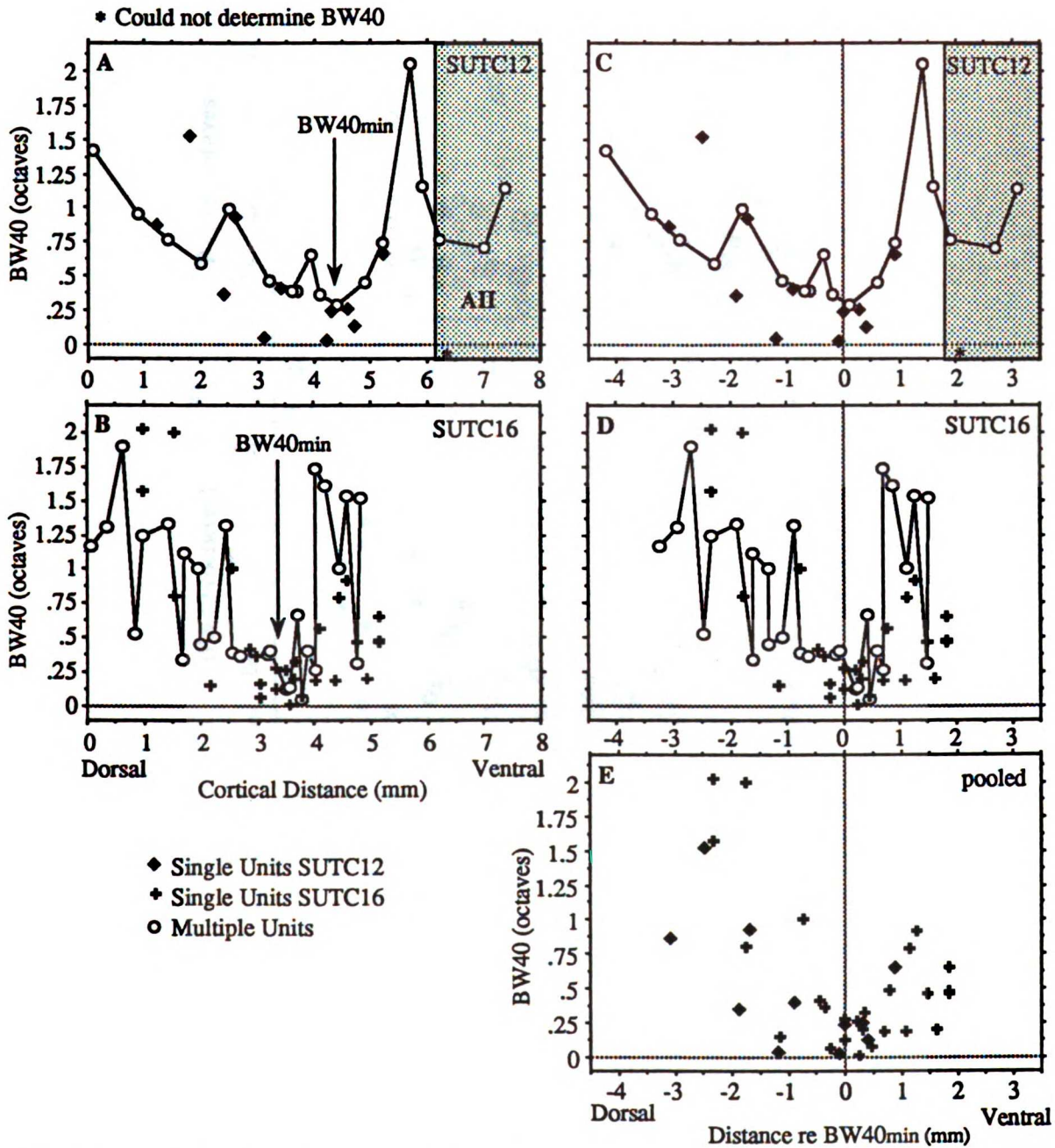
Figure 32: Demonstration of method used to pool data across animals. Top row [(A) and (C)] shows transformation for case SUTC 12. Single neurons (diamonds) are plotted on same location axis as the multiple unit BW40 map (connected circles). In (A) the most dorsal location is arbitrarily assigned the location of 0 mm. In (C) BW40min is assigned a value of 0, and all other locations are referenced as millimeters dorsal (negative) or ventral (positive) from this BW40min. For case SUTC 16 (B) and (D) is the same (A) and (C) for SUTC12 except for case SUTC 16 single neuron BW40's are depicted by crosses. BW40min for the two case is aligned [(C) and (D)] and then the single neurons are superimposed on the same coordinate frame (E) to yield the pooled result.

Figure 33: Pooled BW40 data . Reference for pooling is the most sharply tuned location 40 dB above threshold, BW40min.

(A) Distribution of all multiple unit recordings.

(B) Distribution of all single neuron recordings.

(C) Mean value of BW40 over 0.5 mm bins for multiple (light shaded bars) and single (black bars) units. Standard deviations (NOT standard error of the mean) are represented by error bars.

Figure34: Linear regression fits to estimate the slopes of BW40 gradients in cat AI. The BW40 of each unit is plotted as a function of cortical location. Alignment is as previously described where the most sharply tuned area (BWmin) is used as a reference for pooling data. Correlation coefficients (r) indicate the scatter around the slope, while confidence intervals reveal the reliability of the estimated mean slope.

(A) Multiple unit gradients. For the dorsal half of AI the mean slope (middle regression line) is -0.26 octaves per millimeter. Ninety five percent confidence intervals (two outer regression lines) of the slope span from -0.14 to -0.38 octaves per millimeter. For the ventral half of AI the mean slope is 0.23 octaves per millimeter. Ninety five percent confidence intervals of the slope span from 0.09 to 0.36 octaves per millimeter. For both dorsal and ventral halves the slopes significanlty excludes zero slope.

(B) Single unit gradients. For the dorsal half of AI the mean slope is -0.28 octaves per millimeter. Ninety five percent confidence intervals of the slope span from -0.13 to -0.42 octaves per millimeter. For the ventral half of AI the mean slope is 0.05 octaves per millimeter. Ninety five percent confidence intervals of the slope span from -0.04 to 0.13 octaves per millimeter, which includes zero slope.

Figure 35: Comparison of three regions within AI. Central region includes the area 1 millimeter to both sides of BWmin for a total of two millimeters. A Dorsal region is more than 1 millimeter dorsal to BW10/40min; a ventral region was more than 1 millimeter ventral to BW10/40min.
(A) Histogram of BW40 values for single (top, black bars) and multiple (bottom, shaded bars) unit recordings.
(B) Mean values (bars) of BW40 histograms shown in (A). Error bars represent one half of the difference between 75th and 25th precentile values.
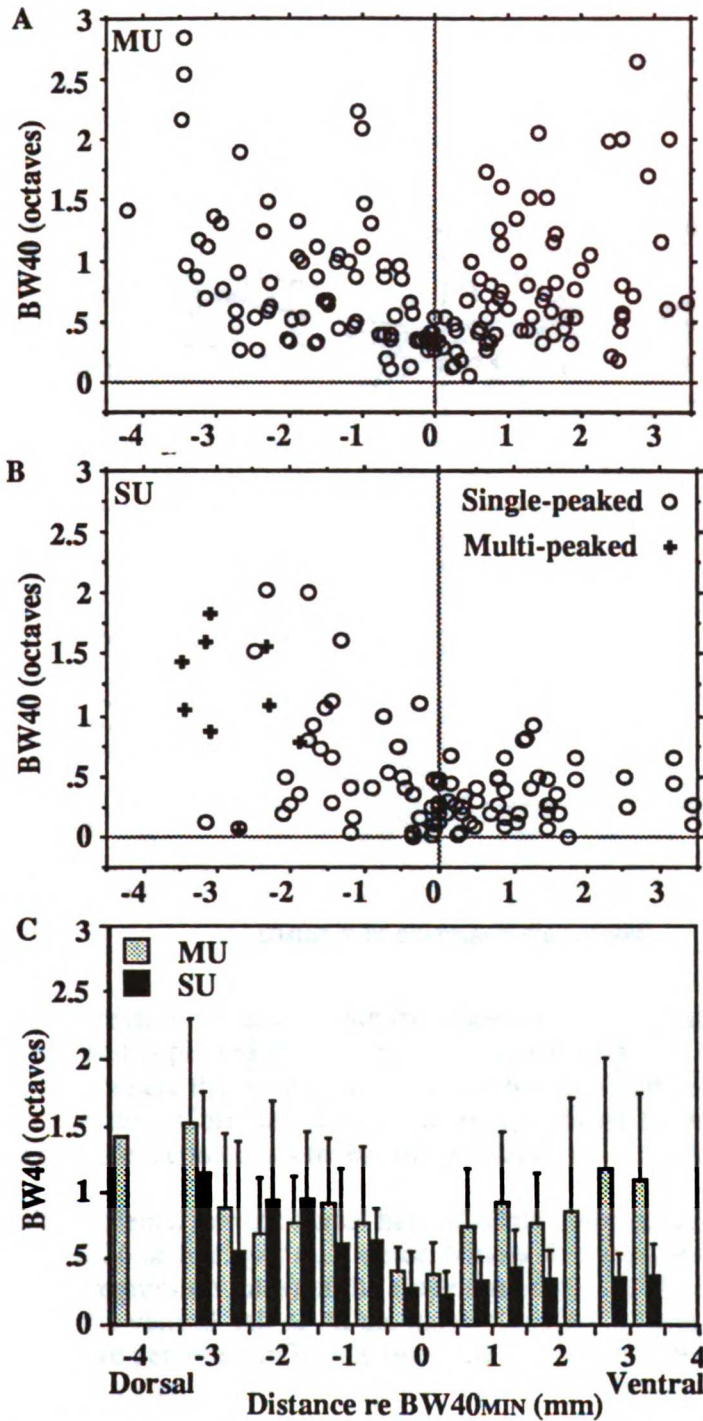
Figure 36: Pooled BW10 data . Reference for pooling is the most sharply tuned location 10 dB above threshold, BW10min.
(A) Distribution of all multiple unit recordings.
(B) Distribution of all single unit recordings.
(C) Mean value of BW10 over 0.5 mm bins for multiple (light shaded bars) and single (black bars) units. Standard deviation are represented by error bars.
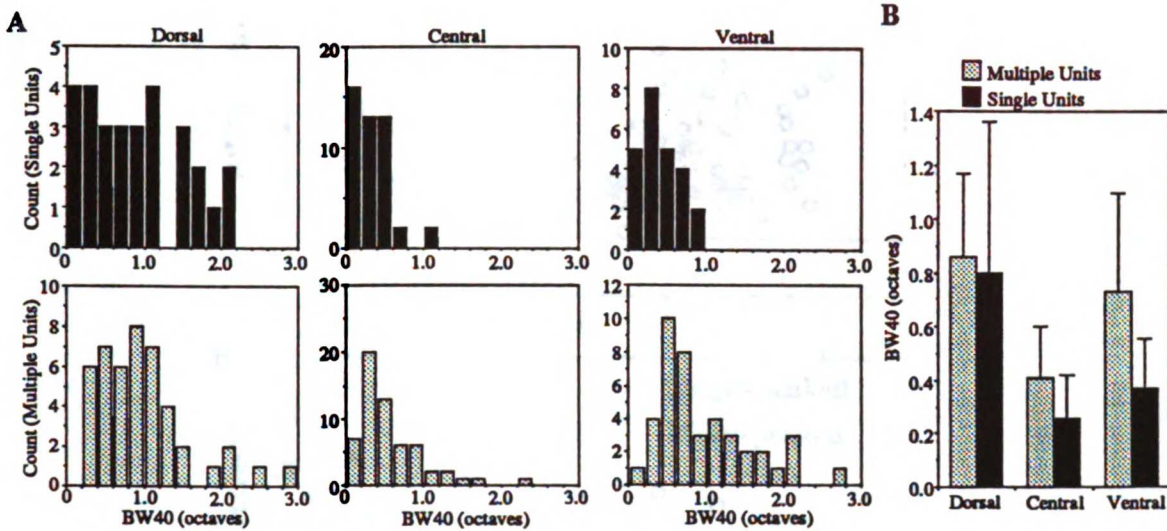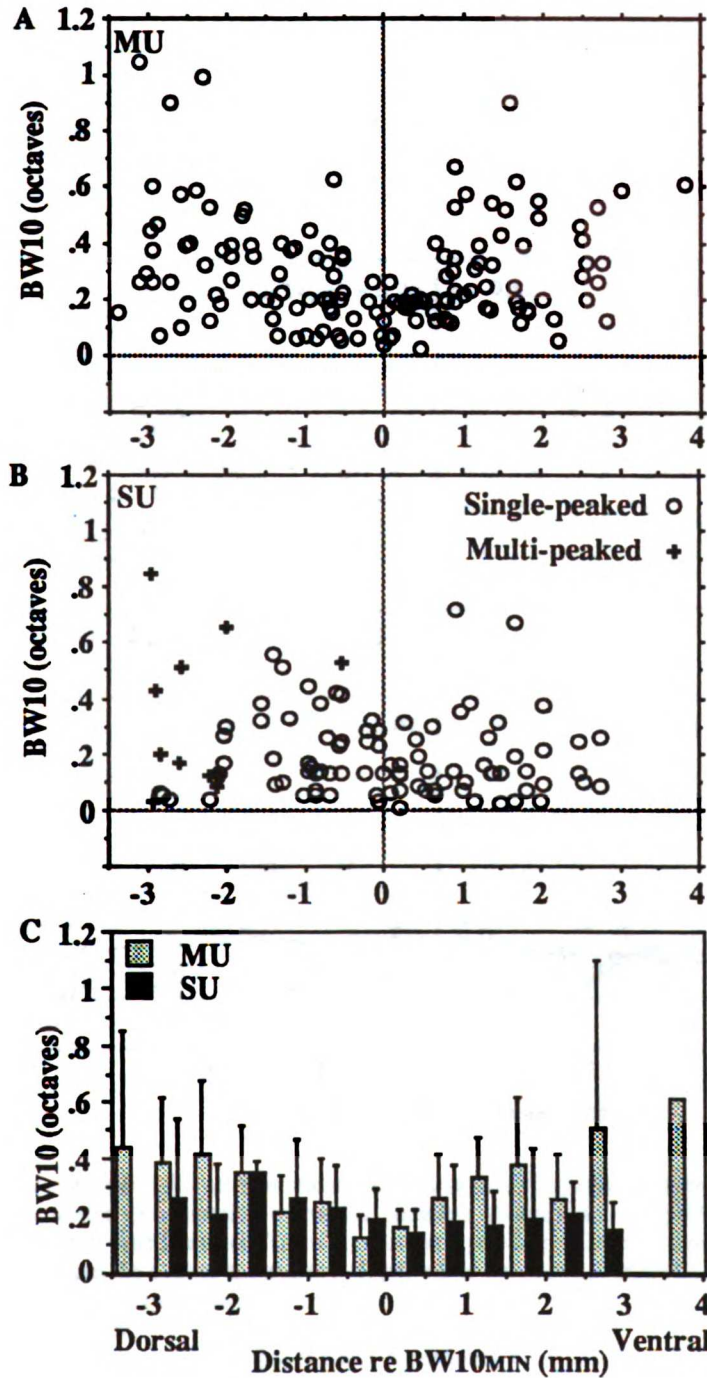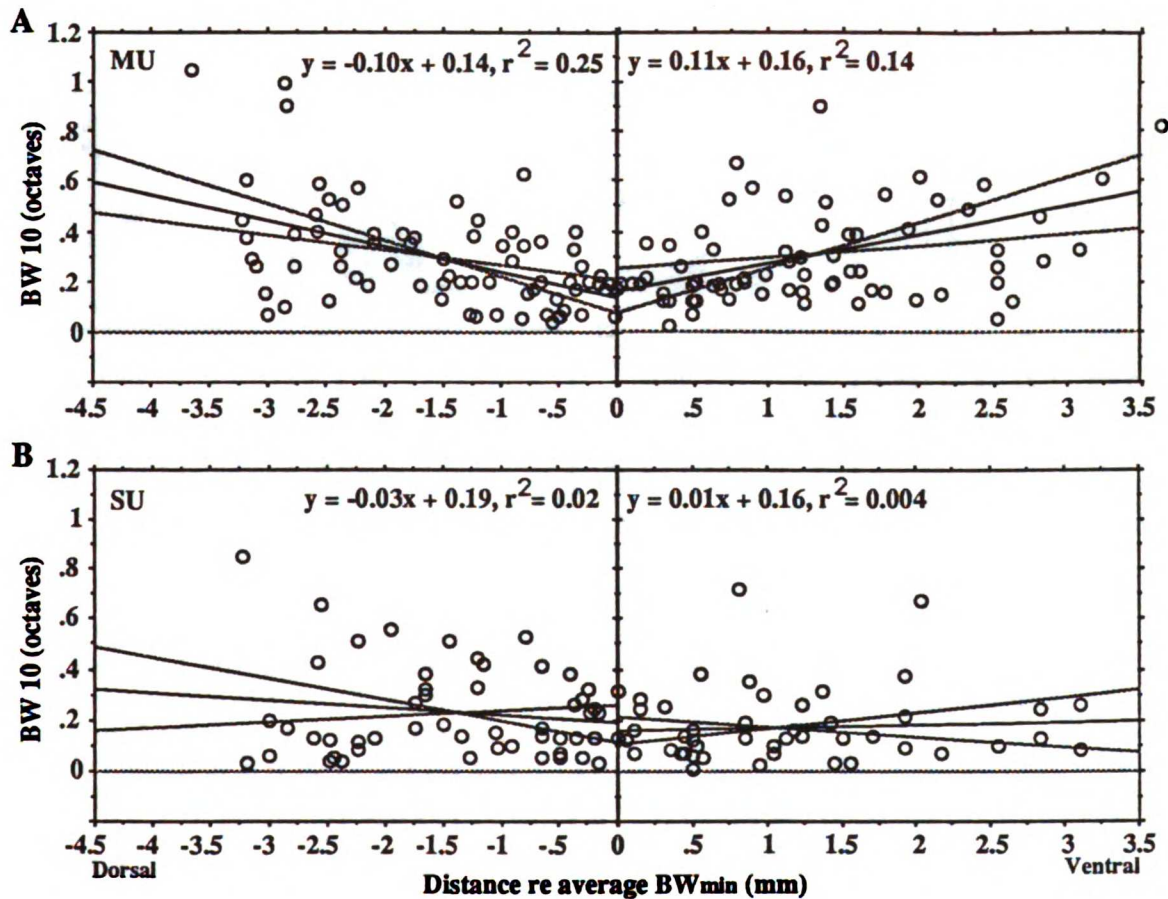
Figure 37: Linear regression fits to estimate the slopes of BW10 gradients in cat AI. The BW10 of each neuron is plotted as a function of cortical location. Alignment is as previously described where the most sharply tuned area (BWmin) is used as a pooling reference. Correlation coefficients (r) indicate the scatter around the slope, while confidence intervals reveal the reliability of the estimated mean slope.

(A) Multiple unit gradients. For the dorsal half of AI the mean slope (middle regressio line) is -0.10 octaves per millimeter. Ninety five percent confidence intervals (two surrounding regression lines) of the slope span from -0.06 to -0.15 octaves per millimeter. For the ventral half of AI the mean slope is 0.11 octaves per millimeter. Ninety five percent confidence intervals of the slope span from 0.05 to 0.18 octaves per millimeter. For both dorsal and ventral halves the slopes are significantly different from zero.

(B) Single unit gradients. For the dorsal half of AI the mean slope is -0.03 octaves per millimeter. Ninety five percent confidence intervals of the slope span from -0.08 to 0.02 octaves per millimeter. For the ventral half of AI the mean slope is 0.01 octaves per millimeter. Ninety five percent confidence intervals of the slope span from -0.04 to 0.06 octaves per millimeter.
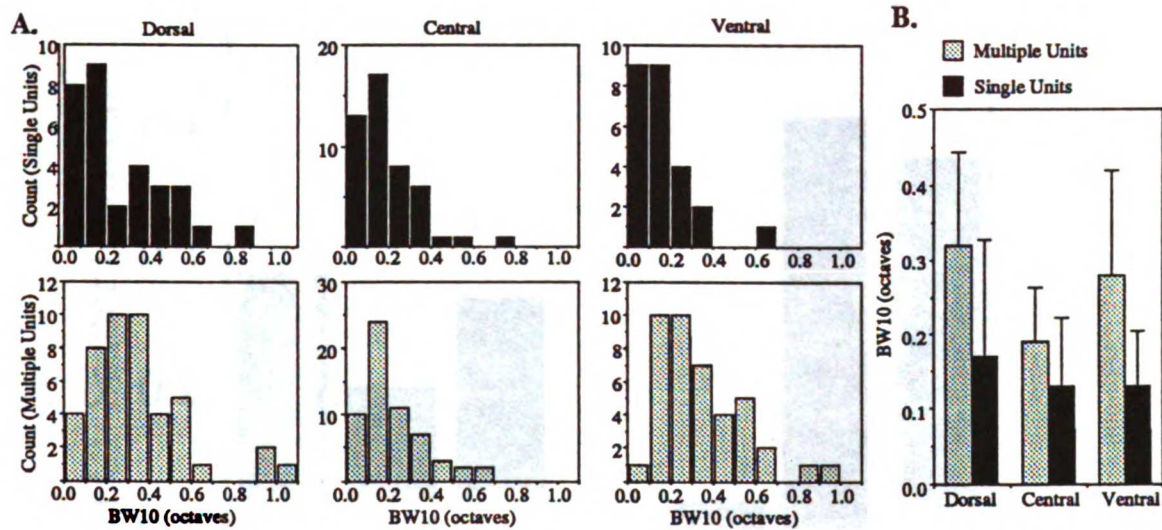
Figure 38: Comparison of BW10 values in three regions within AI. Central region includes area 1 millimeter to both sides of BWmin for a total of two millimeters. Dorsal region is more than 1 millimeter dorsal to BWmin, and ventral region was more than 1 millimeter ventral to BWmin.

(A) Histogram of BW10 values for single (top, black bars) and multiple (bottom, shaded bars) unit recordings.

(B) Mean values (bars) of BW10 histograms shown in (A). Error bars represent one half of the difference between 25th and 75th percentile values.
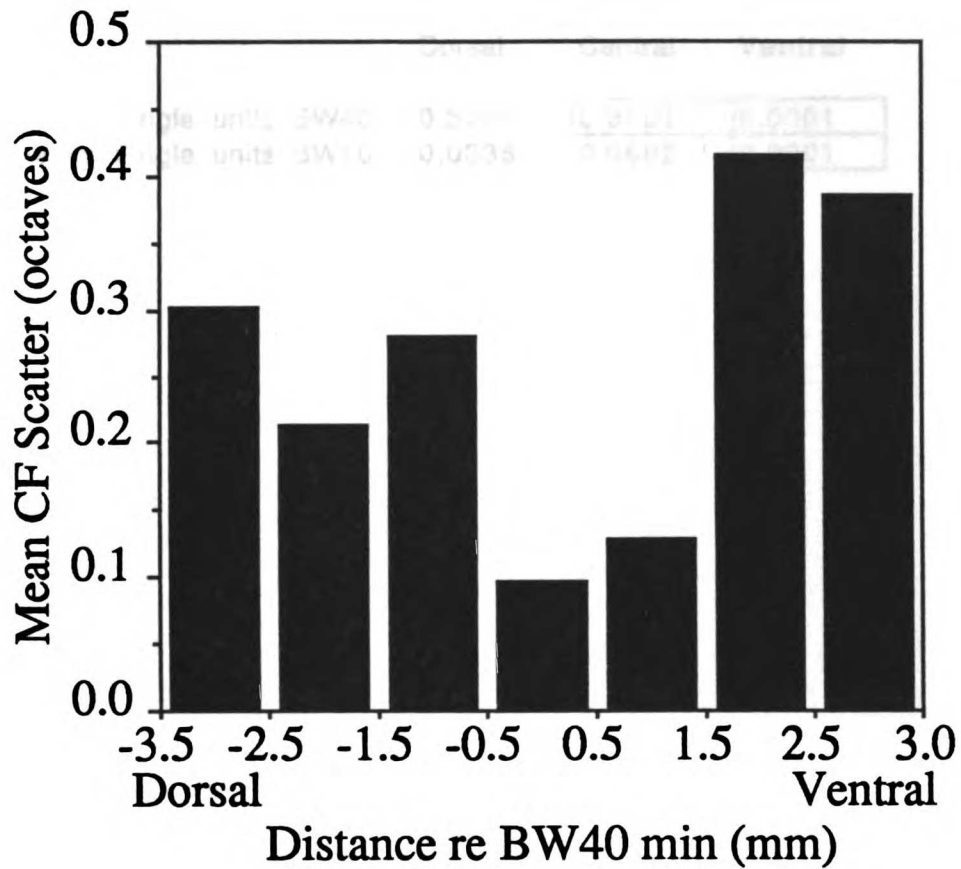
Figure 39: Estimated scatter of CF as a function of cortical location. Expected CF for single neurons was interpolated by 3 point triangulation from multiple unit CF topography when possible (For 96 single units). CF scatter = single neuron CF - expected CF. Values are then averaged over 1 mm bins to derive a mean CF scatter value.

TABLE 4:

Difference Between Single and Multiple Units

| | Mann Whitney U test | | p values |
	Dorsal	Central	Ventral
Multiple vs Single units BW40	0.5064	0.0001	0.0001
Multiple vs Single units BW10	0.0336	0.0992	0.0001

TABLE 5:

3 Group Comparison (Dorsal, Ventral & Central)

	F test p=	Kruskal-Wallis p=
Multiple Unit BW40	0.0001	0.0001
Single Unit BW40	0.0001	0.0001
Multiple Unit BW10	0.0017	0.0004
Single Unit BW10	0.0798	0.221

TABLE 6

Pair Comparison Between Zones

	BW40 Multiple Unit		BW10 Multiple Unit		BW40 Single Unit		BW10 Single Unit	
	Scheffe	Mann-Whitney	Scheffe	M-W	Scheffe	M-W	Scheffe	M-W
		p=		p=		p=		p=
Dorsal vs. Central	**	0.0001	*	0.0005	**	0.0001		0.2018
Central vs. Ventral	**	0.0001	**	0.0012		0.1294		0.5000
Dorsal vs. Ventral		0.6373		0.9593	**	0.0029		0.1024

* = 95% Significance   ** 99% Significance   Boxed = Significant at p < 0.01

CHAPTER 3

Functional Topography of Cat Primary Auditory Cortex:
Sharpness of Intensity Tuning (Monotonicity) for Single
Neurons

SUMMARY AND CONCLUSIONS

(1) The topography of the sharpness of amplitude tuning (monotonicity) of single neurons was studied within the isofrequency domain of primary auditory cortex (AI). To pool data across animals, a multiple unit monotonicity map was used as a frame of reference. Amplitude selectivity of multiple units is known to vary systematically along isofrequency contours which run roughly in the dorsal ventral direction, with the most sharply tuned unit clusters near the center of the contour. A second non-monotonic area can be found several millimeters dorsal to the center (Schreiner et al. 1988, Schreiner et al. 1991). The locations of these two non-monotonic areas were used as reference points to normalize data across animals. Additionally, to compare this study to Chapter 2 results, measures from multiple unit bandwidth maps were used as references to pool data.

(2) Monotonicity ratios were assigned to every single neuron and multiple unit recording. The "monotonicity ratio" is simply the spike count at the highest tested intensity divided by the largest spike count evoked at any intensity. Units with monotonicity ratios less than 0.5 were considered to be strongly non-monotonic. Monotonicity

ratios between 0.5 and 0.8 were classified as intermediately non-monotonic, and ratios greater than 0.8 were classified as monotonic. The choice of 0.8 as the cut off for monotonicity was overly strict so as to insure that neurons were not falsely identified as monotonic.

(3)   The multiple unit topographies recorded in previous studies were confirmed. Pooled multiple unit maps closely approximated the previously reported individual case maps (Schreiner wt al 1988) when the multiple unit monotonicity or BW40 map were used as the pooling reference. When the BW10 map was used as part of the measure, the pooled spatial distribution of multiple units was sharply degraded.

(4)   There was a higher percentage of non-monotonic single neurons than there were for multiple units. While common in single neuron recordings (28%), strongly non-monotonic recordings were uncommon (8%) in multiple unit recordings. Intermediately non-monotonic neurons occurred with nearly equal probability in single neuron (28%) and multiple unit (26%) recordings

(5)   In ventral AI, the spatial distribution of single-neuron monotonicity ratios paralleled the shape of multiple

unit monotonicity ratios. In dorsal AI, pooled single
neurons did not display any clear topography related to the
multiple unit topography.

(6)   Threshold scatter for single neurons displayed two
minima that lined up with the two non-monotonic areas.
Combining the threshold scatter with the relative spike
rate contribution of monotonic and non-monotonic neurons,
differences between multiple unit and single unit
monotonicity topography in dorsal AI could be explained.

(7)   Pooling data relative to the BW40 map slightly
degraded the above-described effects, while pooling
relative to Bw10/40 caused severe degradation.

(8)   Implications of these data for a functional parcelling
of AI are discussed. Of BW10/40, BW40, and monotonicity
ratio, BW40 seems to be a versatile compromise for
consistently defining the dorsal ventral extent of AI.
While parcelling AI into dorsal (AId) and ventral (AIv)
regions still seems justified, consideration of the area
near the dorsal boundary needs to be considered in more
detail.

The existence of an "intensity fovea" for near-
threshold stimuli along the AIv/AId border is revealed in

these experiments. This region is sharply tuned for BW40 and amplitude, has low intensity thresholds with a small scatter, and selectively fires only for narrow-band stimuli within 40 dB of the cortical intensity threshold. These neurons have been shown to shift their spike count vs. level functions linearly in response to a continuous noise masker (Phillips et al 1985). The non-monotonic regions, thus, might serve as fine spectral filters for narrow-band stimuli that are less than 40 dB above the pure-tone threshold in the presence of background noise.

INTRODUCTION

Understanding the fundamental patterns of representation of stimulus frequency and amplitude are requisite for understanding sound analysis in the auditory system. In mammals, the topographic representation of characteristic frequency (CF) has been well established in primary auditory cortex (AI) (Merzenich et al. 1975, Reale and Imig 1980). Roughly orthogonal to the rostro-caudal tonotopic gradient in the cat, sharpness of frequency tuning is topographically represented (Schreiner and Mendelson 1990). Multiple unit clusters are sharply tuned approximately at the center of dorso-ventrally oriented isofrequency contours, multiple unit clusters are sharply tuned. Tuning of neuron clusters becomes progressively broader in the dorsal and ventral portions of AI.

Neurons in cat auditory cortex that respond weakly to high intensity stimuli have been described since the earliest microelectrode studies of AI (Erulker et al. 1956, Evans and Whitfield 1964). The firing rate of such neurons increases above threshold over approximately a 10 to 40 dB range, then decreases with further elevation of stimulus intensity (Brugge et al. 1969, Phillips and Irvine 1981, Phillips et al. 1985, Phillips and Hall 1987). The term "non-monotonic" has been used to characterize these

neuronal responses because the shapes of their stimulus intensity versus firing rate plots are non-monotonic (Greenwood and Murayama 1965). Phillips and colleagues (1985) have reported that the response of most non-monotonic neurons is almost completely eliminated at high intensities, and thus, their frequency tuning curves can be described as being circumscribed (e.g., see Fig. 2)

While earlier studies provided preliminary evidence of spatially systematic representation of non-monotonicity in AI (Reale et al. 1979, Phillips et al. 1985), a detailed description of such a topography has only recently been described (Schreiner et al. 1991). Multiple unit mapping experiments by those investigators have demonstrated spatial distributions of best-level, threshold, and monotonicity (the sharpness of amplitude tuning) in cat AI (Schreiner et. al 1988, Schreiner et. al 1991). Near and overlapping the area that was sharply tuned for frequency in AI, there is a strongly non-monotonic region. A second non-monotonic area is located in the dorsal third of AI (Fig. 40). The degree and location of the dorsal non-monotonic region varies substantially across animals. Some of these monotonicity results have recently been confirmed by other investigators (J.C Clarey Personal Communication).

To date, the intensity and frequency maps described by Schreiner and colleagues have been obtained using multiple

unit techniques. Deriving single neuron topographies is substantially more difficult. Single neuron experiments yield fewer recorded units because of difficulties encountering and holding single neurons, resulting in a less dense sampling of the mapped area. Attempts to pool single neuron topographical data based on anatomical landmarks in the past have not yielded results that strongly corroborated multiple-unit mapping results. For example, the well-established tonotopic organization of AI was substantially degraded when such a pooling technique is applied (Goldstein et al. 1970). Recent evidence indicates that pooling data based on physiological landmarks more useful and appropriate (Sutter and Schreiner 1991). Comparing single neuron and multiple-unit topography would be useful to help understand how basic neuronal elements contribute to the recorded, integrated multiple-unit map.

In an earlier paper (Chapter 2), single-neuron and multiple-unit sharpness-of-frequency tuning maps were compared for AI of the cat. In dorsal AI (AId) multiple unit and single unit topography of BW40 (Q40) were quite similar. However, in ventral AI (AIv), almost all single units were sharply tuned at 40 dB above threshold, even though progressively more ventrally located multiple units showed a progression towards broader tuning. A

topographical distribution of CF scatter could be used to describe the single unit/multiple unit differences in AIv.

In this chapter, single and multiple unit topographies for the representations of in sharpness of amplitude tuning or monotonicity are compared in AI of the cat. The multiple unit maps of sharpness of frequency tuning and monotonicity were used to pool single neuron data across several animals. As in the bandwidth paper, topographical differences in integrative mechanisms across the isofrequency axis of AI have been discovered.

RESULTS

Results are based on recordings of 108 topographically localized single neurons from 9 cats. Seven neurons were excluded from the database because recordings did not cover at least 50 dB of dynamic range above the neurons threshold. Single neuron population results were compared to the 147 multiple units that were recorded in the initial mapping procedure in the same set of experiments.

A wide range of single neuron monotonicity ratios (see methods) were encountered in these experiments (Fig. 42). Throughout AI, single neuron recordings yielded a higher percentage of non-monotonic responses than did multiple unit recordings. Single neurons, particularly those in ventral AI, tended to display a steeper reduction of activity at high intensity levels (i.e. smaller monotonicity ratios) than was observed for multiple unit responses. While the multiple unit topography showed two clear non-monotonic regions, the dorsal non-monotonic area was difficult to reconstruct from single unit data. Furthermore, single neuron topography of non-monotonicity functions was noisier than multiple unit topography using the same measures.

Differences between single and multiple unit topographies can be accounted for by two separate results.

(1) a greater scatter in intensity thresholds in monotonic areas. The non-monotonic areas, with lower threshold scatter, contain non-monotonic neurons with similar best amplitude. (2) Non-monotonic neurons contribute more spikes in topographically non-monotonic areas than in topographically monotonic areas.

Within-Experiment Monotonicity Topography

As reported in an earlier paper (Schreiner et al. 1988, Schreiner et al 1991), at least two multiple-unit non-monotonic areas were found for each case (Figure 43). In some cases, a third non-monotonic region was found in the ventral extreme of AI near the AI/AII border (e.g. Figure 45C, Fig. 46).

Within each experiment, single neuron topography tended roughly to correspond to multiple unit topography. Single neurons tended to be more non-monotonic, i.e. they had lower monotonicity ratios than did multiple units (Figure 44). This difference tended to be more pronounced in the ventral non-monotonic area. While within these two cases the single neuron topography roughly corroborated the multiple-unit topography, there is a large degree of scatter in the measured monotonicity values. Throughout the entire dorso-ventral extent of AI monotonic single neurons

were found. The large scatter found in the individual cases indicated that a large number of topographically identified neurons are needed to pull the map out of the scatter. Even though pooling data across animals is often difficult, the small number of single neurons which can be recorded within any one experiment make pooling a necessity for single unit mapping to reconstruct topographies in an area as large as AI.

Normalizing Multiple-unit Maps to Permit Pooling of Data

To use the monotonicity map as a reference for pooling single unit data, the two consistent non-monotonic regions identified in each case. Illustrative examples are provided to aid in the explanation of the identification and normalization procedure (Fig. 43). The monotonicity ratio of all recorded multiple unit clusters for case SUTC16 is shown in Figure 43A. For initial purposes, in Figure 43A and 43B the most dorsal recording site was arbitrarily assigned a value of 0. Approximately 1.00 mm and 3.75 mm from the most dorsal recording site two non-monotonic areas were encountered. The data were then re-plotted using a weighted 0.50 millimeter smoothing algorithm (Fig. 43B, see legend). (The convention of placing dashed lines at the two minima of the monotonicity ratio used in Figure 43B is also

used in other figures). From the resulting smoothed curve,
the minima in monotonicity ratio were extrapolated (e.g.,
Fig 43B and Fig 45C).

The ventral and dorsal non-monotonic regions do not
have a spatially exact relationship across animals. The
distance between the two minima ranged between 2.9 and 3.4
millimeters with a mean of 3.1 (Median 3.05) in the 5
animals in which recordings were performed more than 3
millimeters dorsal to the ventral non-monotonic area. In
order to align the non-monotonic regions across animals,
normalization of this distance was required. For pooling
data, the distance between these minima was normalized to
"3.0" millimeters (transformation from Fig. 43B to 43C),
which approximates the median difference. For the case
depicted in Fig. 43, normalization distorted distance by
about 7%. This distortion can be seen by directly comparing
Fig. 43B, which is less than 5.0 millimeters with Fig. 43C,
which is slightly more than 5 normalized millimeters. After
normalization, the two monotonicity ratio minima were
assigned locations of 0.0 and 3.0 millimeters.

The method of pooling data across animals is
demonstrated in Fig. 45. The un-normalized spatial
distributions of single neurons superimposed with the
smoothed multiple unit maps (open circles) for 2 cats (A =
cat SUTC16, C = cat SUTC12) shows the variation of dorsal-

ventral extent in AI. The multiple unit maps are normalized as described above, and the location of single neurons are assigned locations from the normalized coordinate system (Fig 45B = SUTC16 and Fig. 45D = SUTC12). For case SUTC16 (Fig. 45A and C) single neurons are represented by crosses and for case SUTC12 (Fig. 45B and D) single neurons are depicted by diamonds. After normalization, single neurons for both cases have been assigned values relative to the monotonicity map and are directly comparable (compare crosses and diamonds in Fig. 45E to those of 45D and 45B). The same pooling process, as demonstrated in Fig. 45 for cats SUTC12 and SUTC16, was repeated for all other cases. (Fig. 46)

Pooled Monotonicity Data

For multiple unit recordings, pooling did not degrade the topographical distribution of monotonicity. The pooled multiple unit data had a shape similar to that described for individual cases. A weak non-monotonic area near the dorsal non-monotonic reference and a stronger non-monotonic area about 3 mm more ventral were observed (Fig. 46). A scatter plot of the topography of all recorded multiple unit monotonicity ratios is shown in Fig. 46A. The dashed line connecting filled rectangles displays the mean

monotonicity ratios averaged over 0.5 or 1.0 millimeter bins; rectangles are located at the center of the bins. One half millimeter bins were used if at least ten neurons were located within the bin, otherwise 1.0 millimeter bins were used. The number of recordings in each bin are displayed at the top of the panels in Fig 47. A similar curve for single neurons is shown in Fig. 46B. Notice that non-monotonic neurons (crosses with low monotonicity ratio) occur throughout AI, and that the dorsal non-monotonic area is barely detectable.

By expanding the mean monotonicity ratio axis (Fig. 46C), some trends can be seen for multiple unit (dashed lines connecting filled rectangles) and single neuron (solid lines connecting open circles) topographies. Single neurons on average were more strongly non-monotonic throughout the dorsal-ventral extent of AI. A large number of strongly non-monotonic single neurons were located near the ventral non-monotonic area at 3.0 mm. While the shape of the monotonicity ratio vs location curve was similar for multiple and single units in ventral AI, the single neuron distribution was relatively flat dorsal to 2.5 millimeters. The dorsal non-monotonic area at 0.0 mm could be seen for the multiple unit topography, but was only weakly evident in the single neuron topography. Also, notice that a second non-monotonic area can be seen at the ventral extreme of AI

(from 5-6 mm) for both multiple and single unit
topographies. This region may already be a part of cortical
field AII.

The topographic distribution of mean monotonicity
ratio can be better understood by classifying neurons as
monotonic (monotonicity ratio > 0.8 Fig. 42 E,F), strongly
non-monotonic (monotonicity ratio <0.5 Fig. 42 A,B), or
intermediately non-monotonic (monotonicity ratio between
0.5 and 0.8 Fig 42 C,D). A criterion of 0.8 as the
monotonic/non-monotonic cutoff is somewhat arbitrary, and
was chosen to be conservative in classifying a unit as
"monotonic". There were few strongly non-monotonic multiple
units. No topographical bin contained more than 25% of
strongly non-monotonic neurons (black bars in Fig. 47A).
While this small percentage of strongly non-monotonic
multiple unit responses roughly inversely followed the
monotonicity ratio distribution, the distribution of the
percentage of intermediately non-monotonic clusters
(stippled bars) show a more pronounced effect. The
percentages of all non-monotonic units (all clusters with
monotonicity ratio < 0.8) can best explain the spatial
distribution seen in the multiple-unit maps.

A similar explanation does not apply to single
neurons. The percentage of strongly non-monotonic single
neurons follows the topographical distribution for

monotonicity ratio in the ventral, but not the dorsal, non-monotonic areas (Fig. 47B).

Although there is a small percentage of strongly non-monotonic neurons in dorsal AI, there is a large percentage of intermediately non-monotonic neurons (0.8 > monotonicity ratio > 0.5, represented by stippled bars in Fig. 47). Differences in the percentages of all non-monotonic neurons (strongly non-monotonic plus intermediately non-monotonic) were small in the dorsal AI and more pronounced in ventral AI. It, therefore, appears that the ventral non-monotonic area contains strongly non-monotonic neurons, whereas the dorsal non-monotonic region is composed mainly of intermediately non-monotonic neurons.

Contribution of Firing Rate

There are a two possible explanations of how a multiple-unit monotonicity topography can be created in dorsal AI, while a similar topography is not evident in the monotonicity of single neurons. One is that non-monotonic neurons contribute more spikes to clusters in non-monotonic regions than do monotonic neurons. The other is that in some non-monotonic regions, thresholds of non-monotonic neurons show a very small scatter ("line up") to create narrow best-level tuning.

For every neuron, the firing rate at the best amplitude, "FRmax" was calculated. Within each 0.5 or 1.0 mm bin, this firing rate was added for all non-monotonic single neurons ($FRmax_{non-mono}$). FRmax was also added for all monotonic neurons in each bin to arrive at $FRmax_{mono}$. $FRmax_{mono}$ was then divided by $FRmax_{non-mono}$ to arrive at the spike ratio for any given location (Fig. 48). Ratios greater than 1 indicate that non-monotonic neurons contributed more spikes, at best intensity, than monotonic neurons. The spatial distribution of spike ratios that of monotonicity ratios in the dorsal non-monotonic area. Differential contribution of spikes between monotonic and non-monotonic neurons, therefore, at least partially helps to explain the formation of a multiple unit topographic representation of monotonicity from a relatively non-topographic single neuron distribution in dorsal AI.

Contribution of Threshold

Changes in threshold scatter could also contribute to the creation of "monotonic regions" from underlying non-monotonic neurons. Single neuron thresholds (relative to the minimum multiple-unit threshold encountered in the isofrequency contour) were less scattered in the multiple-unit non-monotonic regions than they were in the multiple

unit monotonic areas. This was apparent in individual cases
(Fig. 49) as well as in the pooled data (Fig 50). Notice
that the non-monotonic area near the AI/AII border does not
show less scatter.This probably reflects a pooling artifact
because the cases in which this area was not mapped (such
as SUTC16, Figs. 49 and 43) contributed scatter. Thresholds
in the non-monotonic areas were relatively similar across
animals (Fig 50B), and the non-monotonic areas might
correspond to low threshold regions as reported by
Schreiner et al. (1991).

Relation of Monotonicity Topography to Sharpness of Tuning
(BW) Topography

The monotonicity topography has a weak relationship to
the sharpness of tuning topography. For pooling data
relative to the most sharply tuned "center" of AI (see
Chapters 1 and 2 for pooling method), the measure of the
point of alignment chosen is critical. When pooled relative
to the area of sharpest frequency tuning as determined by
BW40; i.e., the bandwidth of pure-tones to which the neuron
responds 40 dB above the neuron's minimum threshold, there
is a good correspondence. However, when the data were
pooled relative to a measure that incorporates the BW10
distribution the pooled topography was degraded.

Relative to the minima in the BW40 map, the dorsal-ventral properties of monotonicity ratio remain similar (Fig. 51A and Figs. 52A,B). The ventral minima is located from 0.0 to 0.5 mm ventral of the sharply tuned BW40 region and the dorsal non-monotonic area is 2 to 3 mm dorsal to it. As with the monotonicity normalization, the shape of the mean monotonicity ratio vs. location plot are similar in ventral AI, but quite different in dorsal AI (Fig. 51A). However, when the data is pooled by a measure that includes BW10,i.e., the bandwidth of pure tones to which the neuron responds 10 dB above threshold, the dorsal-ventral delineation for amplitude properties degrades (Fig 51B). That is consistent with the interpretation that non-monotonicity topography is more dependent on high intensity rather than near threshold properties of sampled neurons.

Discussion

A series of experiments were performed to investigate
the topographical distribution of the intensity selectivity
of single neurons in cat AI. As reported in an earlier
study two multiple-unit non-monotonic areas in AI spaced
about 3 millimeters apart were usually identified. The
ventral non-monotonic area was consistently within a
millimeter of BW40min. Strongly non-monotonic neurons were
concentrated in this ventral non-monotonic area. In dorsal
AI, many neurons whose firing rates were reduced at high
intensities were encountered. The magnitude of this
reduction on the average was smaller than those in the
ventral non-monotonic area,

While the ventral non-monotonic area could be clearly
identified after topographically pooling the mean
monotonicity ratios for sampled single units, the dorsal
non-monotonic area could not be detected in single unit
response data. Differences between single unit and multiple
unit representational topographies in dorsal AI could be
accounted for by topographical differences in the threshold
scatters of contributing neurons, and by the spike
contributions (response strength) of non-monotonic single
neurons.

The topographical distributions for multiple unit maps was still apparent in the maps which were pooled using the multiple unit monotonicity map for landmarks. While these multiple unit maps were sufficiently preserved using BW40min as a pooling landmark, they were substantially degraded when other landmarks are included, e.g., BW10/40min.

Methodological Implications:

The method of determining the degree of monotonicity in this paper is substantially different than that of others (e.g. Phillips et al 1985; Phillips 1985). Collecting data for FRA's with a pseudo-random order of 675 different frequency/level combinations substantially reduced habituation effects (Fig. 53) compared to recording peristimulus time histograms (PSTH's) of 50 repetitions at different intensity levels of CF tones. Changes in absolute spike count/presentation does not effect monotonicity ratio so long as the shape of the spike count vs. level function remains proportional at different intensities. Reduced habituation is traded off with problems introduced by adding responses to tones within a 1/4 octave of CF.

This investigation differs from a previous report (Phillips et al. 1985) in reporting a substantial number of

non-monotonic neurons that are not completely unresponsive
at high intensities. The high proportion of intermediate
non-monotonic neurons encountered in this study might be at
least partly accounted for by methodological differences.
Neurons that do not respond to high intensity CF tones
might still respond to tones whose frequencies are within a
quarter octave of CF. The neuron whose FRA is depicted in
Fig. 41 and whose spike vs level functions are displayed in
Fig. 53 exemplifies such an off-CF effect. The FRA's firing
rate falls off rapidly at the CF; however, at intensities
to which the neuron did not respond to CF tones, there were
still responses at slightly lower frequencies. The low-
frequency response causes the FRA determined spike vs.
level profile to fall off less steeply than the PSTH
determined spike vs. level profile (Fig. 53). Non-monotonic
neurons which respond to off-CF tones at high intensities
which do not elicit CF responses have been previously shown
(Fig. 3 of Phillips et al. 1985). Small frequency response
shifts as a function of intensity were often observed in
these data. Many of the intermediate non-monotonic neurons
identified in this study are of this type. The employed
technique showed no evidence that the intermediate non-
monotonic neurons had spike vs. level functions that
asymptote at intermediate response rates. Instead, almost
all intermediate non-monotonic neurons showed a downward

slope of their spike vs. level functions at the highest
tested intensities (e.g. Fig 42).

Percentage of Non-monotonic Neurons

Recording from similar cortical depths, previous
studies in the cat found that 44% of single neurons (N=61)
are strongly non-monotonic, 13% intermediately non-
monotonic and 43% monotonic (Phillips et al. 1985).
Comparison of percentages must account for previously
reported potential topographical sampling biases of
Phillips (and Irvine 1981) towards central and ventral AI
(see Chapter 2 discussion), and a later non-monotonicity
study's bias towards the rostral bank of the posterior
ectosylvian sulcus (Phillips 1985, Phillips and Cynader
1985). In a preliminary report Barone and colleagues (1990)
have reported that 40% (data base of 333 neurons) of
recorded AI neurons were strongly non-monotonic

With the above mentioned caveat in mind, the
percentage of non-monotonic neurons recorded in this
experiment is summarized. In the two millimeters centered
around BW10/40min, 33% of neurons are strongly non-
monotonic, 28% are intermediately non-monotonic, and 39%
monotonic. Dorsal to this region 10% are strongly non-
monotonic and 38% are intermediately non-monotonic.Ventral

to this region, 35% are strongly non-monotonic and 19% are intermediately non-monotonic. These results are consistent with previous findings that roughly 40-60% of neurons are non-monotonic (see also Figs. 47 and 52).

Mustached Bat Studies

Aside from the recent cat studies by Schreiner and colleagues, only one other species has shown functional maps of amplitude related parameters in AI. In the mustached bat there is a map of best amplitude that runs roughly orthogonal to the frequency map (Suga 1977; Suga and Manabe 1982). These authors state that "a majority" of AI neurons in the bat are non-monotonic and imply that 96% of sampled neurons are amplitude selective. Without explicitly stating the percentage of non-monotonic neurons Suga and Manabe (1982, pg 233) say:

"Of 540 neurons studied, 19 showed monotonic impulse count functions and responded better to stronger tonal stimuli (f). But a majority of neurons showed a non-monotonic impulse count function with peaks at particular amplitudes (a-e)."

They go on to say that 25 of 153 neurons studied were completely inhibited at high intensities. This lack of clarity, makes it difficult to directly compare the percentages of non-monotonic neurons in mustached bats and

cats, although the implications is that there may be a higher percentage of non-monotonic neurons in the bat.

For echolocation, the amplitude of the returned pulse conveys information about object size. The findings of topography of monotonicity and best level in the cat (Schreiner et al 1991) combined with the single neuron results presented herein indicate that topographical representation of intensity parameters might be a general mammalian auditory cortical property. For both species, the amplitude of the stimulus also appears to be encoded orthogonal to the tonotopic axis in AI. While Suga and Manabe did not study the sharpness of amplitude tuning, there is some indication that suggests an orderly organization of monotonicity (see Fig. 10 from Suga and Manabe 1982).

Relation to sound localization studies

Recent evidence has shown that neurons with circumscribed spatial receptive fields are predominantly non-monotonic. The spatial distribution of minimum thresholds (Fig 50) strongly indicates that the multiple unit non-monotonic area with its restricted intensity response and threshold range cannot encode intensity independent location. The more monotonic multiple unit

regions might serve such a function, as there are still
many non-monotonic single neurons comprising the monotonic
multiple unit response. Stacking non-monotonic neurons with
varying best intensities might be an element in the
encoding of auditory space in AI.

*Possible Purpose of Non-monotonic Multiple Unit Areas: An
Intensity Fovea?*

If the non-monotonic multiple unit areas in AI are not
encoding intensity-independent location information, what
are they encoding? It is possible that the strongly non-
monotonic neurons are encoding spectral information just
above the background noise. The ventral non-monotonic area,
which closely overlaps BW40min, could serve this purpose
well.

The hypothesis of an area specialized for signal
analysis just above noise is supported by (1) the low
thresholds of these neurons (Fig 50), and (2) the low
scatter in threshold values, (3) the sharp frequency
tuning, and (4) the effect of an increase of background
noise on the responses of these neurons (Phillips 1985,
Phillips and Cynader 1985). Neurons in the ventral non-
monotonic region consistently had the lowest thresholds
within the isofrequency domain and have the smallest range

of threshold values (Fig 50). This implies that the intensity sensitivity is restricted to a small range of low levels. When tones are presented in the presence of continuous (ongoing) background noise the spike vs. intensity function of non-monotonic neurons shifts the adjusted threshold is a linear function of the intensity of the noise masker (Phillips 1985, Phillips and Cynader 1985). The same non-monotonic neurons were completely inhibited by noise bursts.

In addition to being able to shift their spike count vs. level functions relative to background noise, neurons in this ventral AI non-monotonic area respond to a narrow range of frequencies, and respond weakly if at all to broad-band stimuli (Schreiner et al. 1991, Phillips et al. 1985). Accordingly, the spectral analysis of signals close to the background signal benefits from a narrow band analysis in order to determine coherent fluctuations of the noise from a narrow-band transient stimulus. The ventral non-monotonic area approximately lines up with BW10min, BW40min, and the lowest threshold region. Topographically, the region near the "physiological center" of AI looks like an intensity fovea that is highly selective for detecting the frequency and amplitude of narrow-band stimuli just above the background noise. The narrow-band frequency response of this area and the spatial selectivity of non-

monotonic neurons (Imig et al. 1990) combined with their low thresholds indicate that the two non-monotonic areas may play an important role in spectral-spatial processing for stimuli whose intensities are within about 40 dB of the detection threshold of background noise. Note that natural stimuli to which this region would respond must be contain at least one narrow-band because non-monotonic units do not respond well to broad-band stimuli (Phillips et al. 1985, Schreiner and Mendelson 1990).

Parcelling of AI

The results of this study raise some questions about the division of AI. While the previous chapter strongly suggested that there are at least two physiologically distinct regions in AI, the implied dividing line was the BW10/40min (Q-max) as derived from multiple unit mapping of BW40 and BW10. In this current study, BW10/40min was not as strong a topographical pooling landmark as was BW40 or the monotonicity map. The topographical analysis for monotonicity was critically dependent on using high intensity properties of neurons.

With this in mind, the question must be raised as to whether there is a dividing line between dorsal and ventral AI. The answer appears to be that there is no sharp

boundary or one unambiguous line that can be drawn to determine functionally distinctive AI regions. The AIv, AId classification from Chapter 2 was adequate for studying bandwidth properties. For studying the spatial distribution of a given property, the multiple unit topography of that property serves for the best topographical pooling landmarks. The BW40 map probably is the most useful predictor of the location of other response properties studied up to this time. A low-threshold region, with neurons sharply tuned for frequency and amplitude (the intensity fovea), comprises about plus or minus 1 millimeter from BW40min. Ventral to BW40min almost all single neurons are sharply tuned, and the topography of non-monotonicity for single and multiple neurons display a similar shape. Dorsal to BW40min, pooled single neurons become progressively more monotonic and broadly tuned for frequency. The frequency tuning closely follows the multiple-unit map, while amplitude tuning does not. The construction of the dorsal non-monotonic area, which is present in multiple unit monotonicity map, but not in pooled single neuron maps, can be accounted for by a combination of threshold scatter and the differential spike contribution of single neurons.
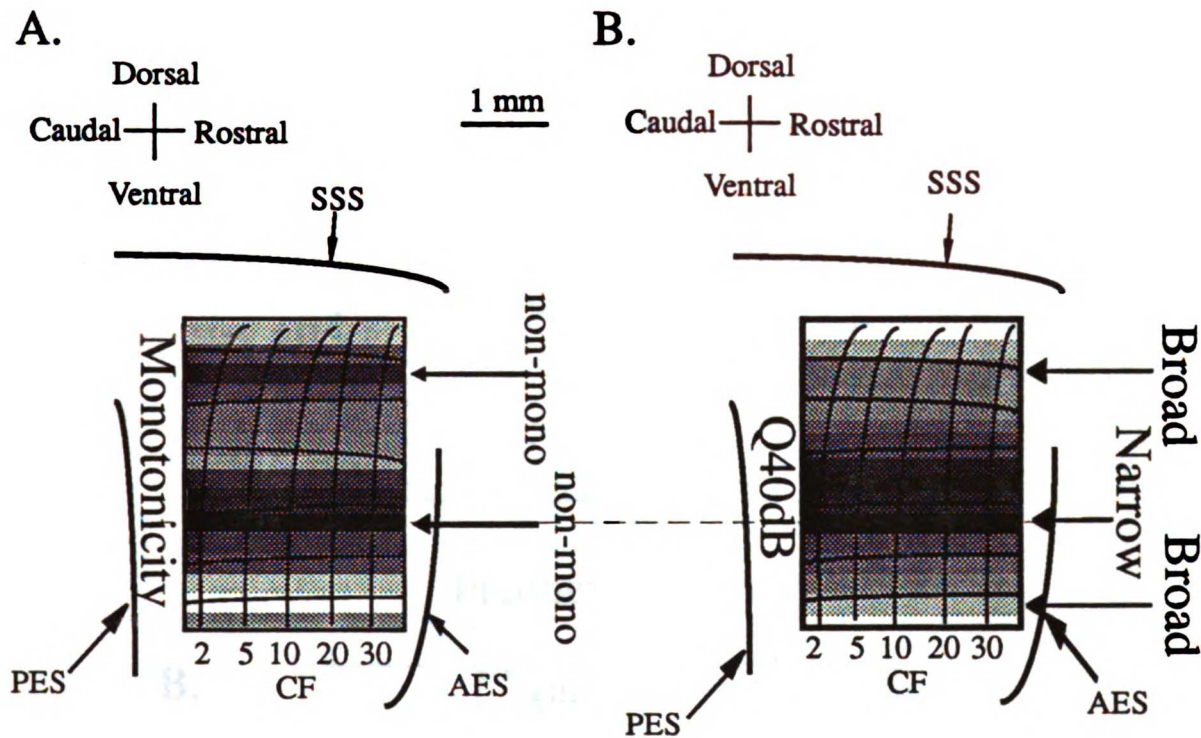
Figure 40: Cartoon of multiple unit sharpness of amplitude (A) and frequency (B) tuning maps of previous studies (Schreiner et al. 1988, Schreiner and Mendelson 1990, Schreiner et al. 1991). Monotonicity map (A) shows two non-monotonic (dark) areas sandwiched between monotonic (light) areas. The sharpness of frequency tuning (Q40db) map shows a sharply tuned region (dark) which gradually gives way to broader frequency tuning (light). The ventral non-monotonic areas roughly lines up with the sharply tuned area (dashed line). Both maps are roughly aligned to the isofrequency domain. SSS: suprasylvian sulcus; PES: posterior ectosylvian sulcus; AES: anterior ectosylvian sulcus.
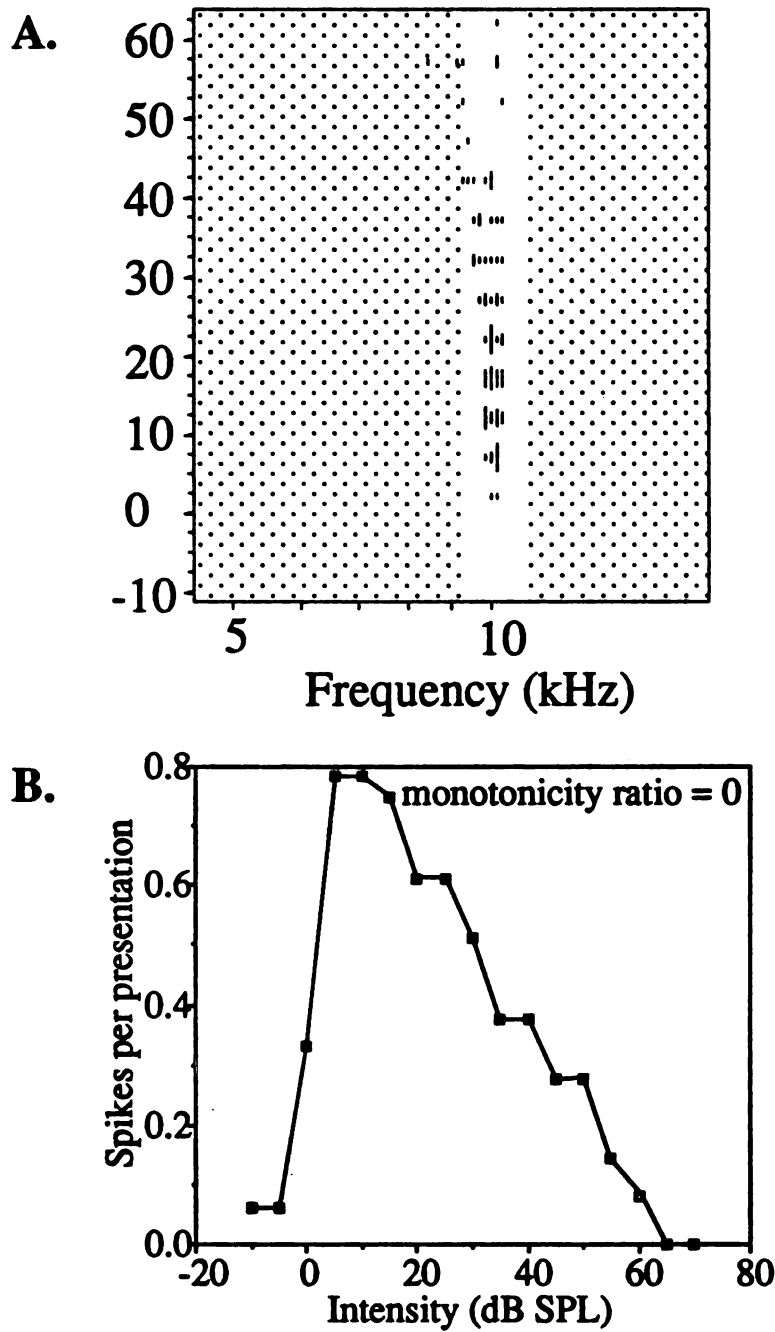
A.

B.

Figure 41: FRA (A) and corresponding spike count vs. level function (B) for a non-monotonic neuron. Gap in dotted background in (A) represents 1/4 octave band over which spikes were counted. Two spikes on the low frequency side were outside of the 1/4 octave band and thus were not counted for the spike count vs. level plot. The spike count vs. level plot incorporates data from another FRA (not shown) which covered from 0 to 70 dB SPL.
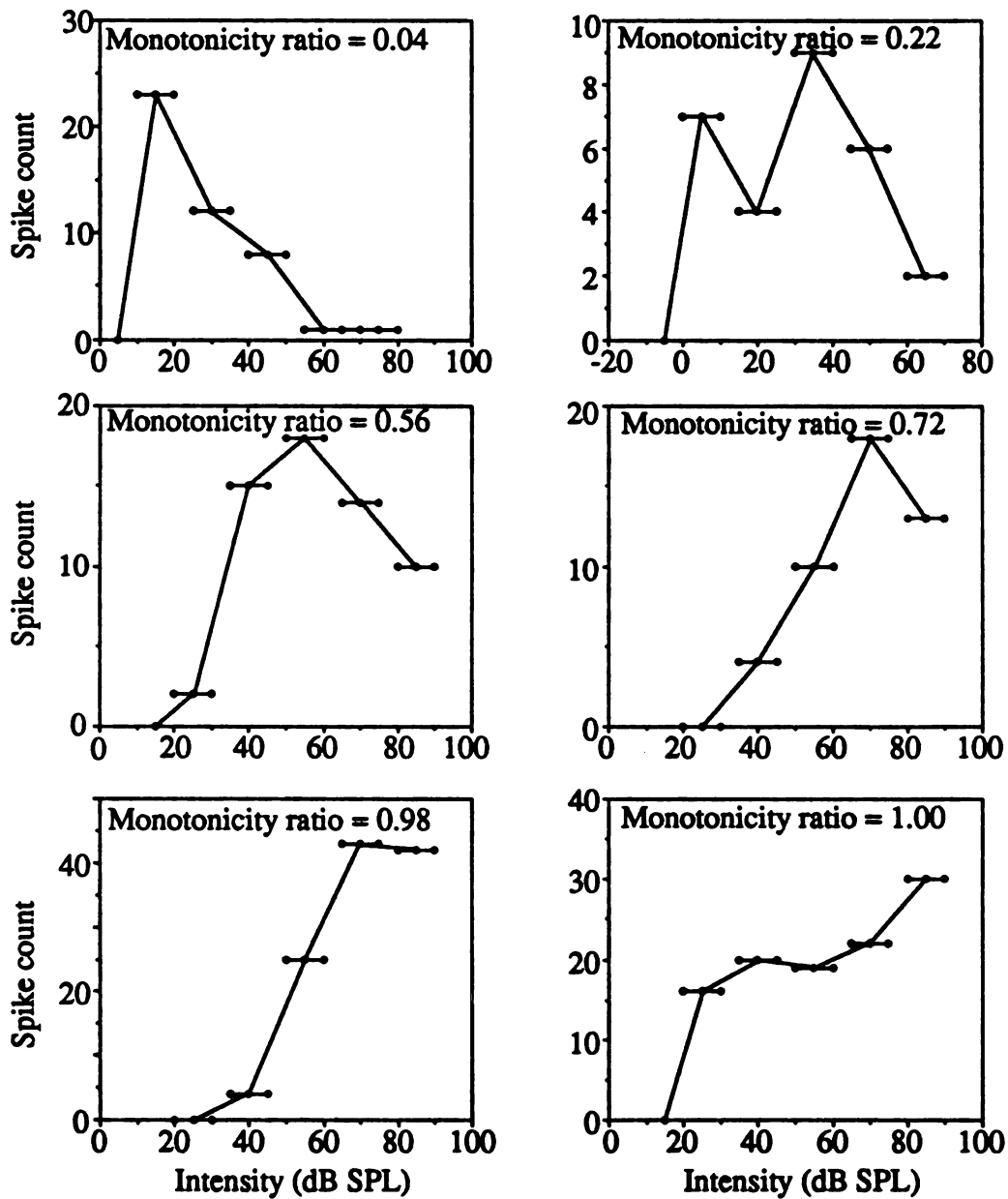
Figure 42: Spike count vs. level functions for six neurons. All spikes from an FRA are counted over 15 dB (3 levels) and 1/4 octave (5 frequencies). Some are based on more than 1 repetition of the FRA procedure, and/or responded to less than a 1/4 octave frequency range (see text for further discussion).

A. Multiple Units

B. Multiple Units with Spatial Smoothing

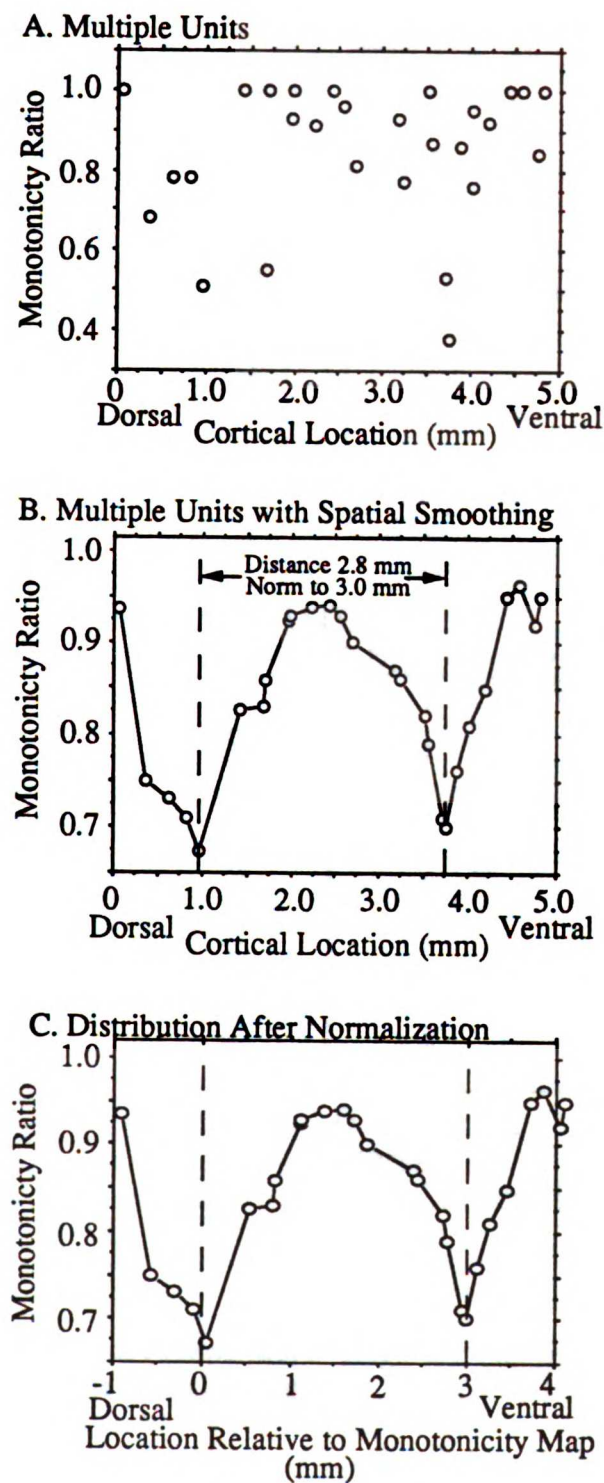## C. Distribution After Normalization

Figure 43: Spatial distribution of monotonicity ratio within isofrequency domain.
(A) Multiple unit data points. (B) Spatially smoothed topography. Clusters within the same dorsal-ventral location were assigned weights of 1.0. Recording sites within 0.10 millimeters of each other were assigned weights of 0.75. Multiple units between 0.11 and 0.25 millimeters were assigned weights of 0.5, and neighbors between 0.26 and 0.50 millimeters were assigned weights of 0.25. Then a weighted average was performed based on the sum of the weights. The two minima in the function were identified (dotted lines). (C) The distance between the minima then was normalized to "3 millimeters" which in this case expanded the real distances by 7%. Notice that in (B) the map was less than 5 millimeters but in (C) it was more than 5. For all graphs the ventral non-monotonic area is assigned the value "3" and the dorsal non-monotonic area is assigned the value "0".

Figure 44: Comparison of single and multiple unit topography collected within the same animal for cat SUTC12 (A) and SUTC16 (B). Open circles are multiple units, crosses are single units. Dashed lines correspond to minima in monotonicity ratio and normalization to 3 millimeters was NOT performed.
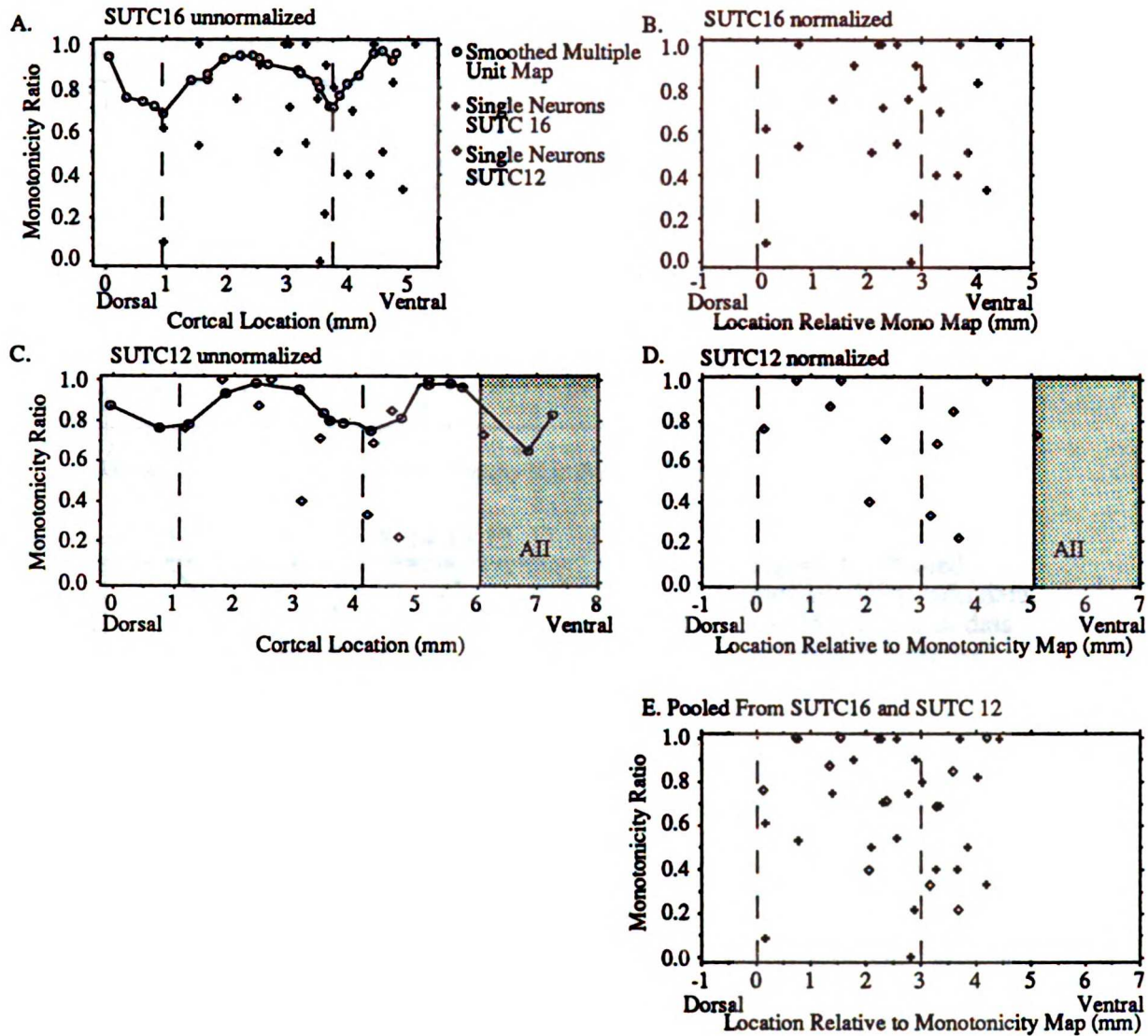
Figure 45: Illustrative example of pooling method using the two cases shown in Fig 44.
A,C: Multiple unit map (connected open circles) with single unit points (crosses for cat
SUTC12 and open diamonds for case SUTC16).
B,D: Single unit points (same symbols as in A and C) displayed after normalization of
locations to "3 millimeters" from the multiple unit map as in Fig. 43.
E: Single units from the 2 cats superimposed with their common normalized coordinate
system.
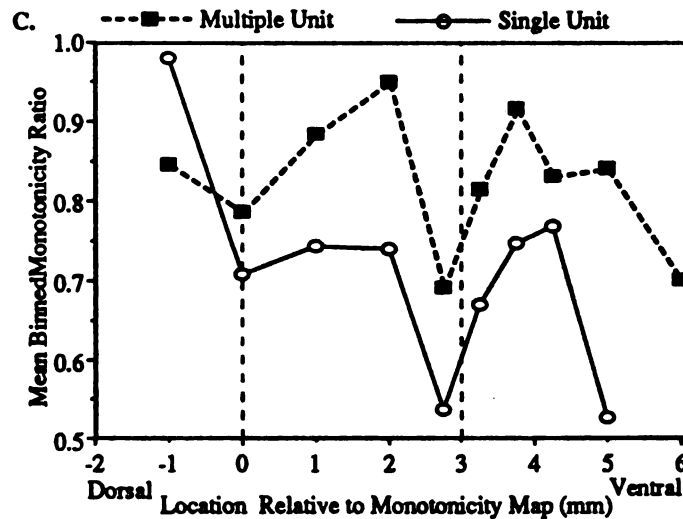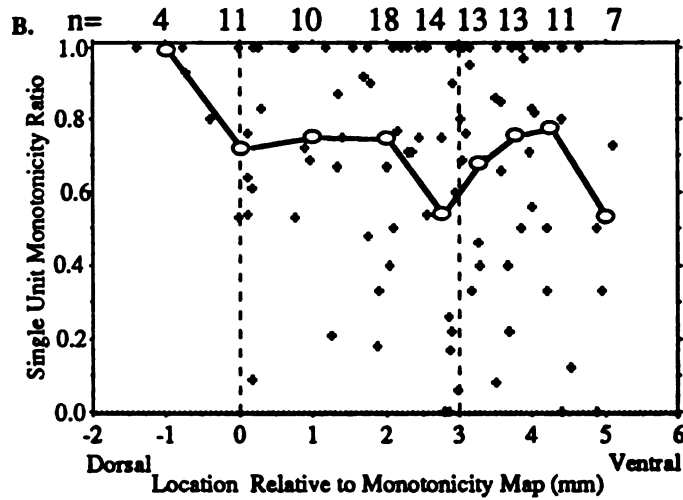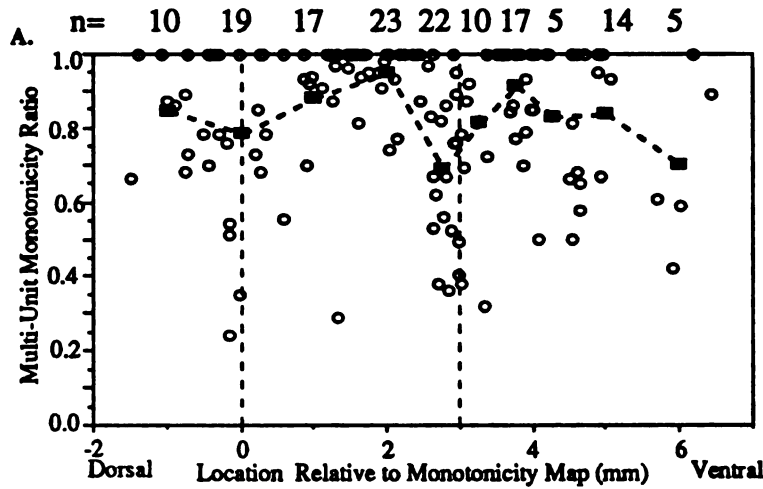Notice that point in AII (C and D) is not included in final pooled data

Figure 46: Pooled monotonicity ratio data.
(A) Multiple unit data points (open circles) and mean binned data (filled rectangles connected by dotted lines).
(B) Single unit data points (crosses) and mean binned data (open circles connected by heavy lines).
(c) Mean binned data for single and multiple units with magnified monotonicity ratio scale.
Binning was performed so as to include at least ten neurons per bin when possible (see text for details). N values for each bin can be found in Fig. 47.

■ Strongly Non-monotonic (% Reduction < 50)

▨ Intermediately Non-monotonic (% Reduction Between 51 and 80)
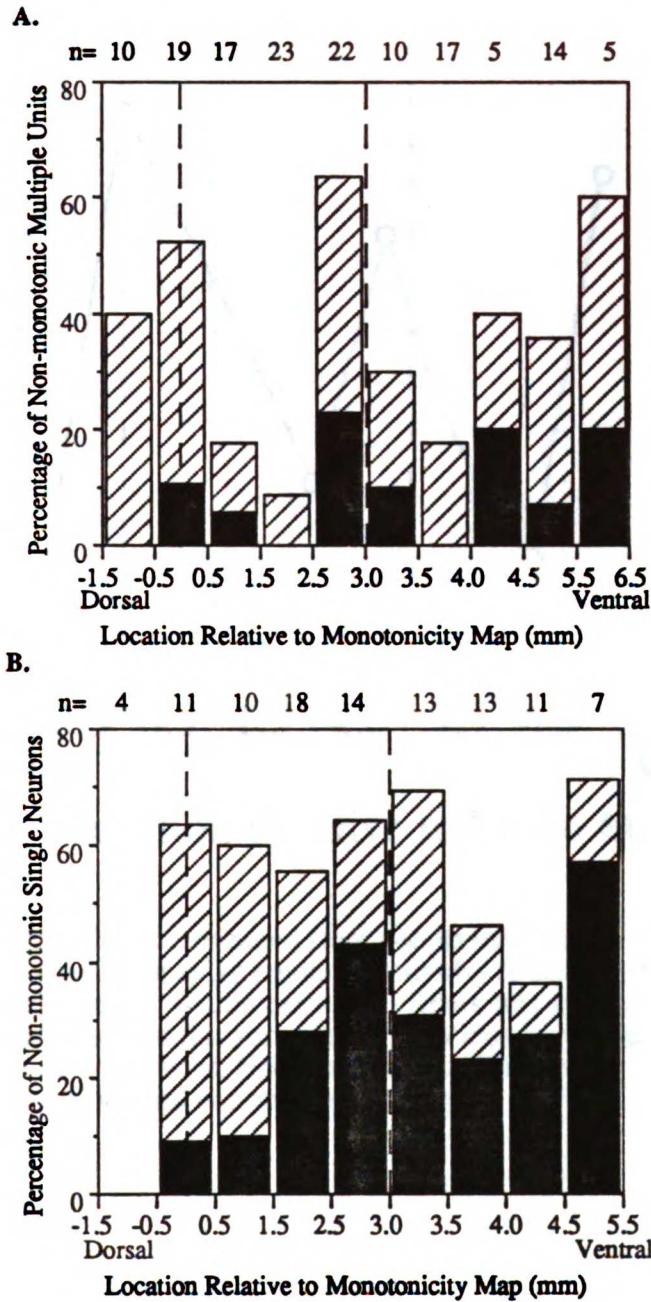
A.

B.

Figure 47: Percentage of strongly (black filled) and intermediately (hatched) non-monotonic neurons for topographically pooled multiple (A) and single (B) units. Number of units pooled for each bin is shown by n value on top of each plot.

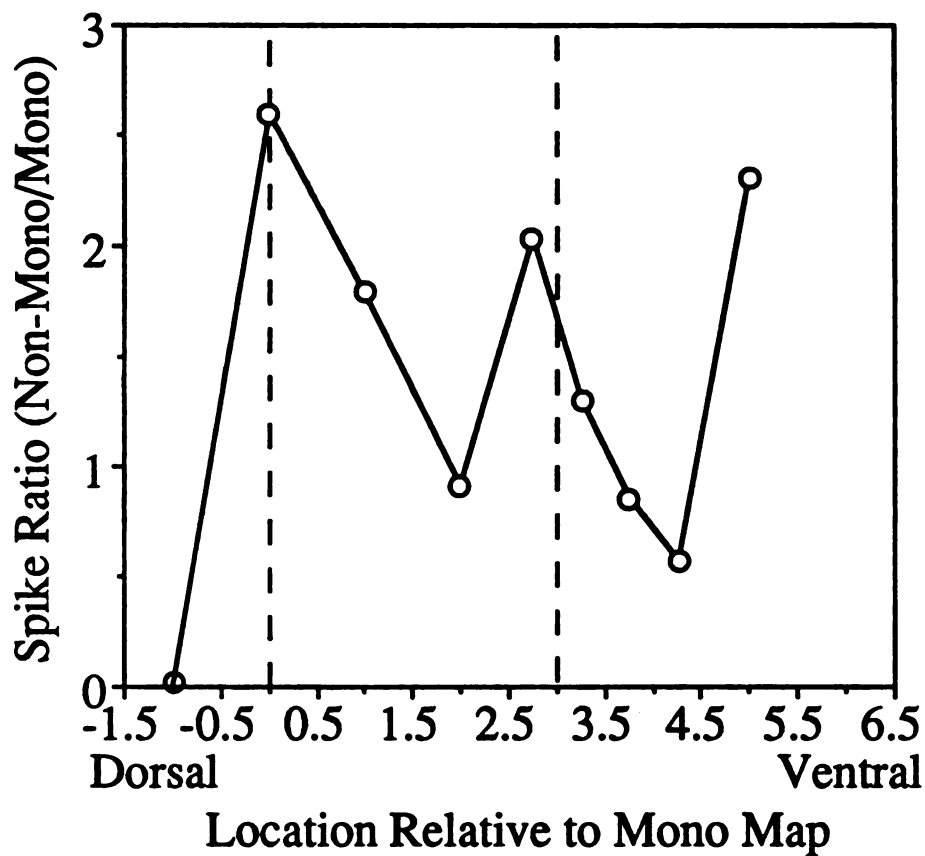Figure 48: Ratio of spikes contributed from non-monotonic units and monotonic units. Maximum spike count per stimulus to tones (FRmax) were calculated for each neuron. Within each bin, FRmax was added for all non-monotonic neurons and this sum was then divided by the equivalent measure for monotonic neurons. Notice that a maximum in the ratio occurs both in the dorsal and ventral non-monotonic areas.
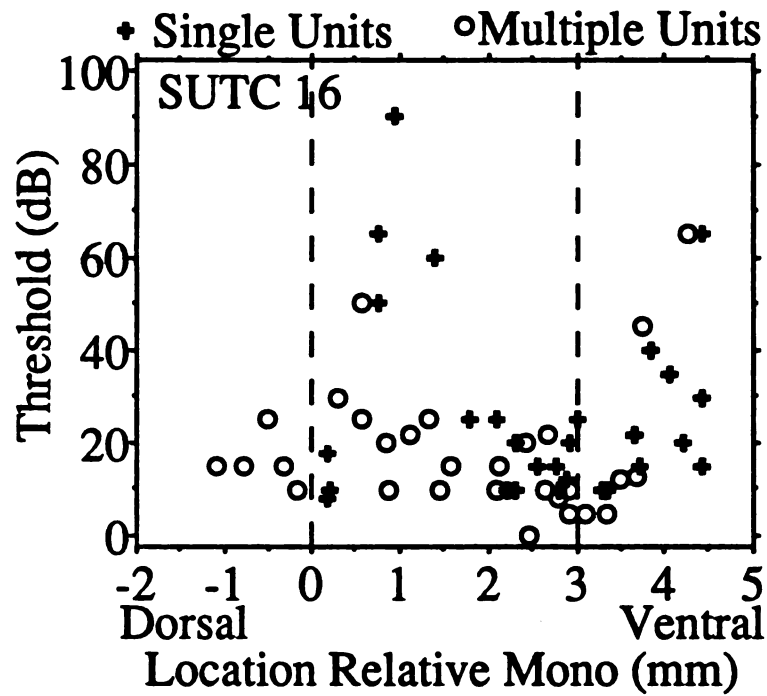
Figure 49: Spatial distribution of single (crosses) and multiple (open circles) unit threshold for case SUTC16. Minima in the scatter of single unit threshold occur at the two non-monotonic areas.
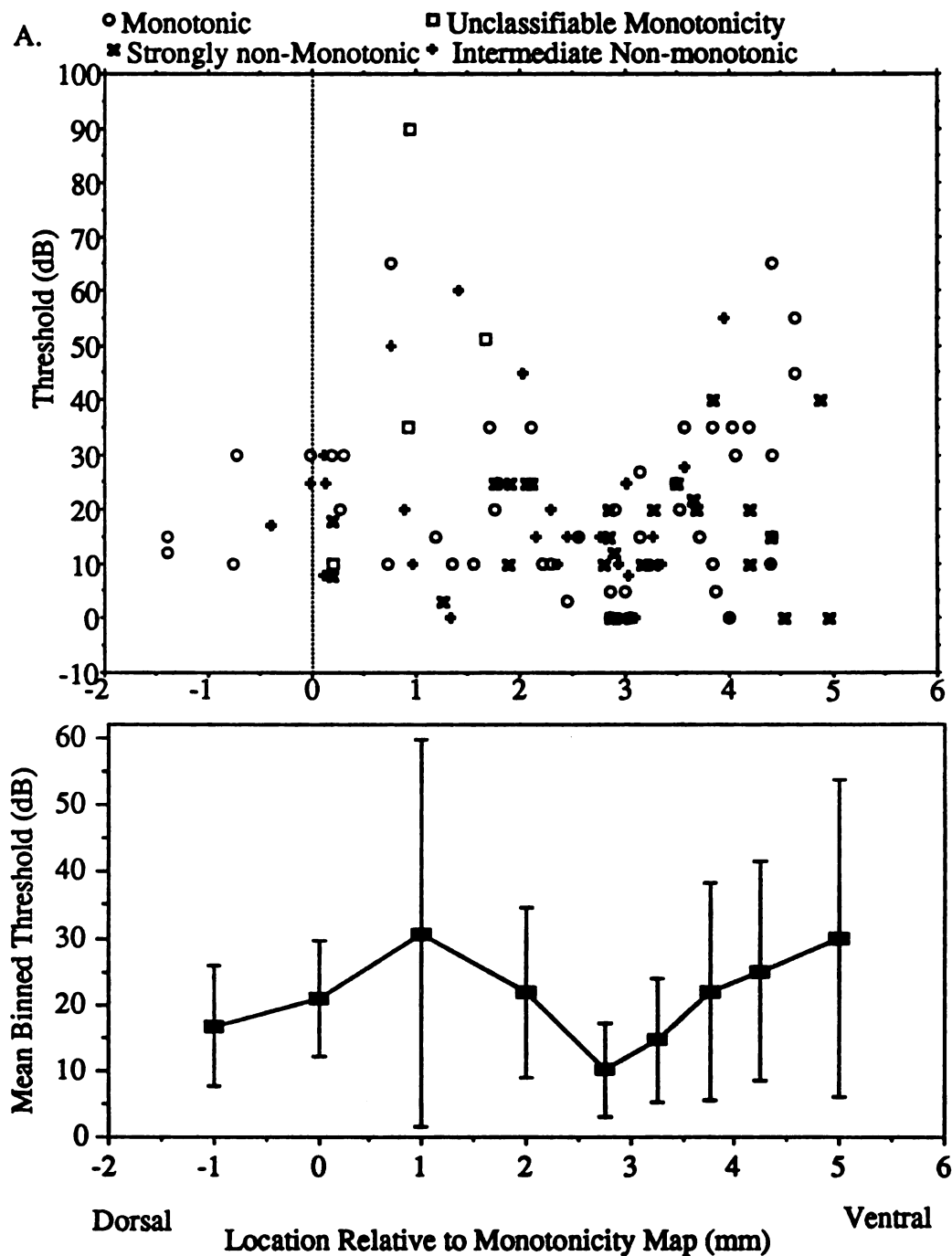
Figure 50: Threshold data pooled across animals. Zero and three millimeters correspond to two non-monotonic areas. Threshold was referenced such that for each animal 0 dB corresponded to the lowest multiple unit threshold encountered. Notice the minima in threshold scatter at the two non-monotonic areas and the threshold minimum at the ventral non-monotonic area.

(A) Scatter plot of all neurons. Symbol legend in Figure.

(B) Mean binned threshold with standard deviation (error bars) to represent threshold scatter.

A

B

Figure 51: Mean binned monotonicty ratio pooled relative to BW40min and BW10/40 min as described in Chapter 2.

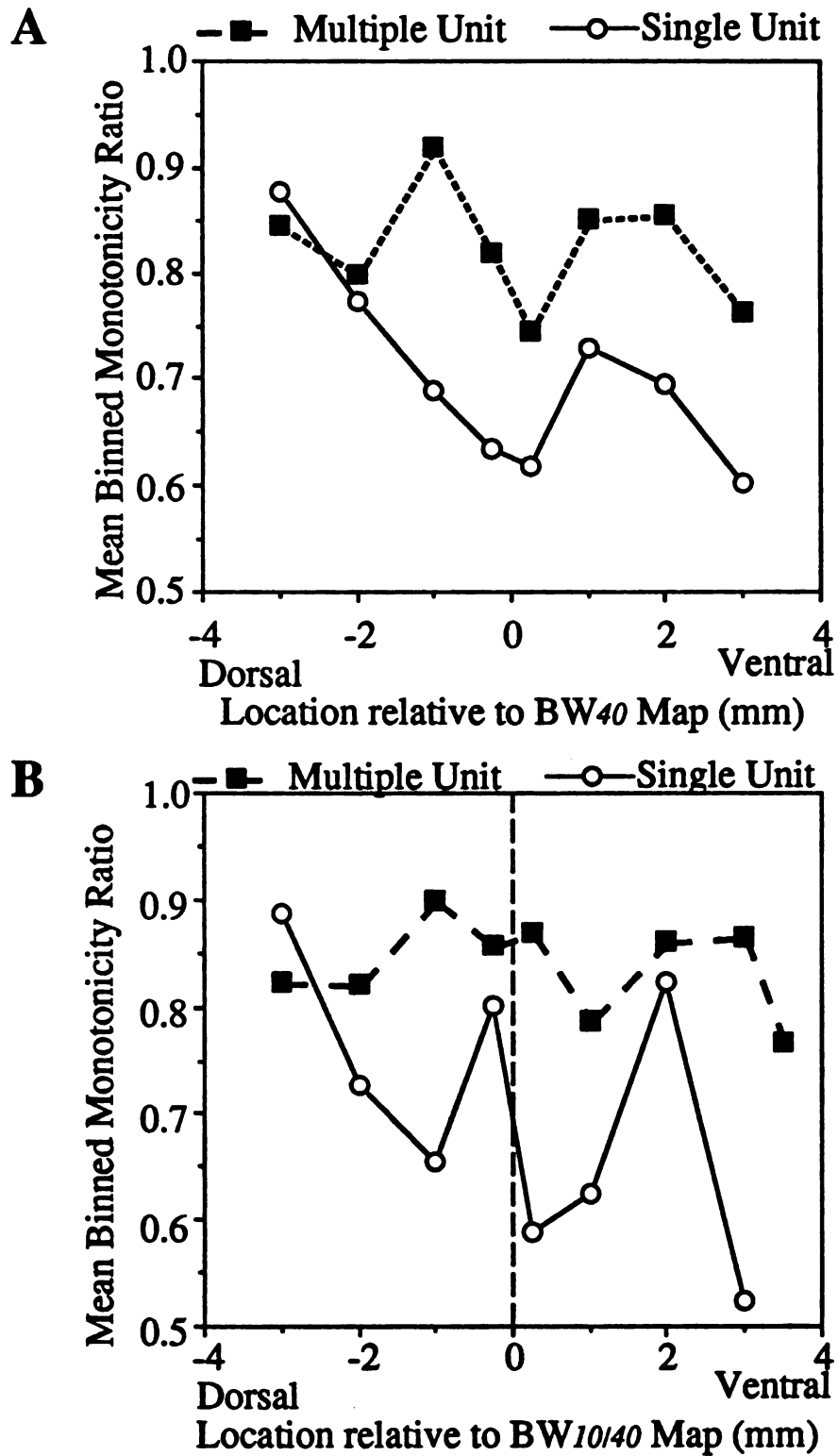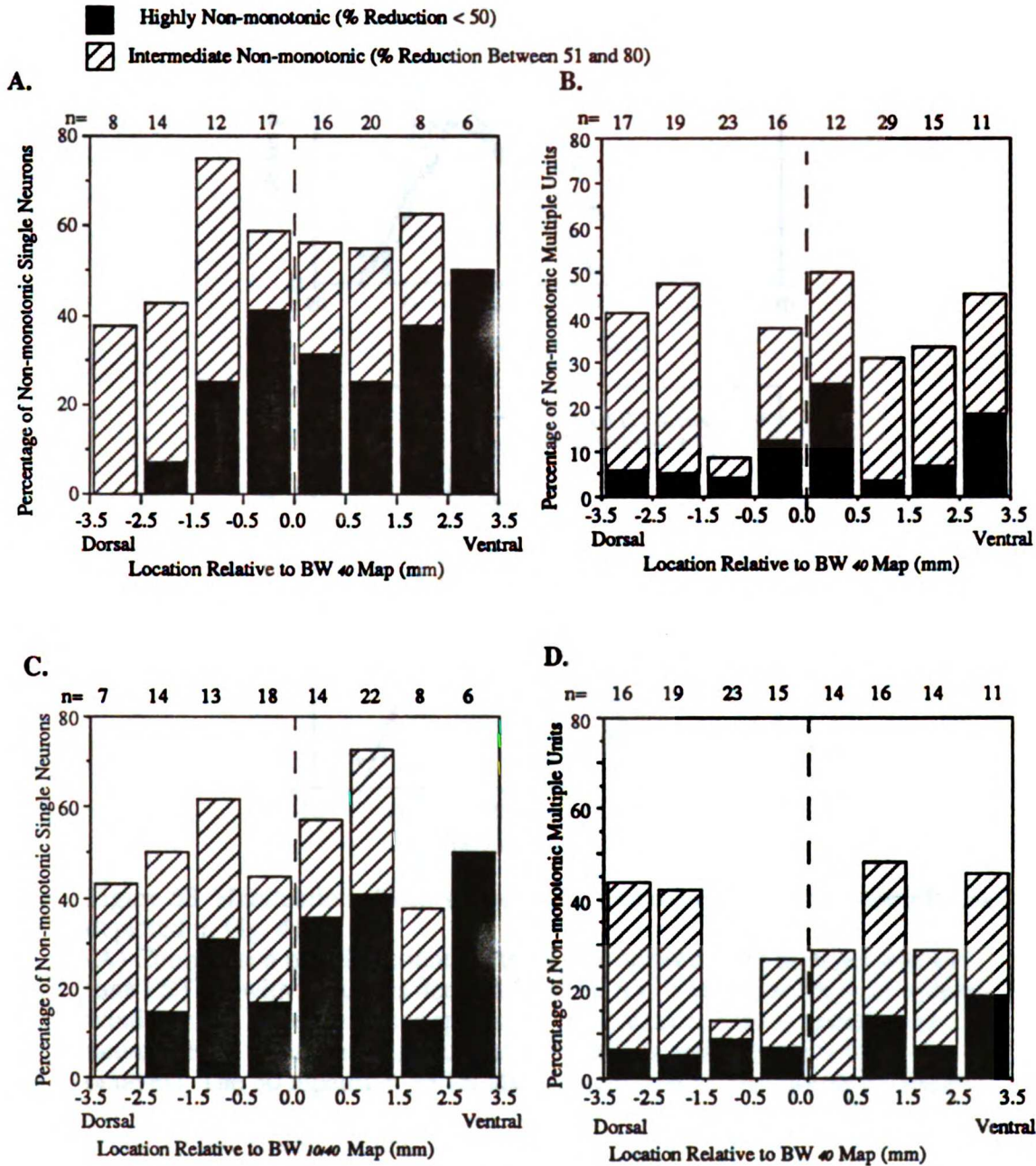Figure 52: Percentage of strongly (black) and intermediately (stippled) non-monotonic single (A,C) and Multiple (B,D) units. Topographical pooling performed relative to BW40min and BW10/40min.
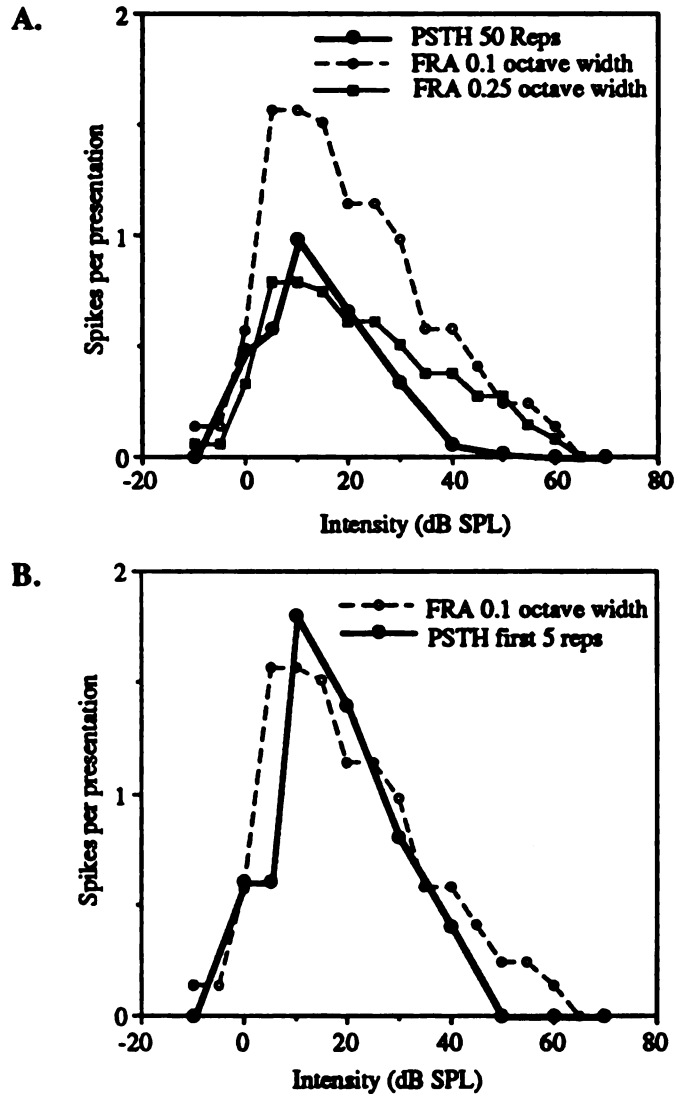
Figure 53: Habituation effects of the PSTH method for neuron whose FRA is depicted in Fig. 41.

(A) Comparison of spike count vs. level plot derived from 50 repetition CF tone PSTH's with measures derived from FRA's. Notice that the 0.25 octave window used underestimates spikes per presentation, This is because the neurons FTC is less than 1/4 octave wide (BW is approximately 0.15 octaves). The 50 repetition PSTH also underestimates the number of spikes per presentation as compared to the random order FRA method. This is probably due to habituation.

(B) When only the first 5 repetitions of each PSTH are counted, the habituation effect disappears. The 0.1 octave FRA method and the PSTH method now yield comparable results.

Notice, though, that the descending branch (intensities greater than 20 dB) is less sharply sloped for the FRA method as compared to PSTH's. This is because at high intensities, at which the CF response is substantially reduced, off-CF responses are still present (see Fig 41).

Conclusions and Closing Discussion

CONCLUSIONS

This dissertation provides the first detailed analyses of the spatial distributions of monaural response properties of single neurons within the isofrequency domain of AI in the cat. Previously, several investigators had reported a spatial clustering of binaural response properties into "bands" with their main axis oriented orthogonal to the CF gradient (Imig and Adrian 1977; Middlebrooks et al. 1980; Reale and Kettner 1986). However, using binaural properties to define the dorsal-ventral extent of AI is unreliable because the number of and specific identities of binaural bands within AI are not consistent across animals, and because no reliable relationship can be found between binaural properties and the AI/AII border (Schreiner and Cynader 1984). More recently, some attempts at single unit mapping of AI have been made for monotonicity (Phillips et al. 1985) and spatial location (Rajan et al. 1990), but neither study mapped more than a 2 millimeter isofrequency strip, and thus did not reconstruct spatial representations across the entire isofrequency dimension of AI. Even a conservative estimate of AI's extent (Reale and Imig 1980) would almost always comprise more than 4 millimeters; our experiments

indicate that AI usually covers from 5 to 7.5 millimeters in its dorsal-ventral extent.

Within the past two years, multiple unit maps of spectral and intensity parameters have been found to physiologically characterize the extent of AI with a great degree of consistency across animals (Schreiner and Mendelson 1990, Schreiner et al 1991, Mendelson et al. 1991). Results of this dissertation add to the understanding of the composition of such maps, through single neuron mapping. In general, it was found that single unit maps of the primary auditory cortex systematically relate to their multiple unit counterparts.

One important conclusion of this dissertation is that AI is not a physiological monolith into which one can randomly record from neurons and conclude that "AI neurons do this or that". Rather AI has a complex physiological topography in both its dorsal-ventral and rostro-caudal dimension. Any future investigations of specific response features must take this spatial diversity and order into account.

Prior work in AI has been marred by a lack of clear definition of the dorsal-ventral borders of the field. Without positioned references, it is not surprising that some single neuron studies report a precisely tonotopic AI, having almost exclusively narrowly tuned, low threshold

neurons (Phillips and Irvine 1981), while others have reported an AI with weak CF topography and a diverse range of bandwidths and thresholds (Goldstein et al. 1970; Evans and Whitfield 1964).

Methodological Considerations: Combined Single/Multiple Unit Studies

The presented dissertation results have important ramifications on the methodology of mapping studies. Many authors have applied combined multiple and single unit mapping techniques (e.g., Merzenich et al 1975; Reale and Imig 1980; Middlebrooks and Zook 1983; Phillips et al. 1985; Imig et al. 1990) in auditory cortex. While this method proved useful for mapping CF (Merzenich et al. 1975; Reale and Imig 1980), our data indicate that mixing results for single and multiple unit recordings will add noise to bandwidth and monotonicity maps. In AIv, for example, including single neurons in the database would add more sharply tuned responses to the broadly tuned multiple unit area, and thus, obscure the clear topography of the frequency integration as revealed by multiple unit mapping. Similarly, wherever single units were used in a monotonicity map, the mean monotonicity ratio would be reduced simply due to specific differences between single

and multiple unit properties. By comparing single and multiple unit maps, one can gain insight into the properties of the local cortical circuitry that are difficult to achieve with single unit recordings alone.

Comparison to Primary Visual Cortex: Transplanted Ferret Experiments

In primary visual cortex (area 17), a full representation of the retina has been established (Talbot and Marshall 1941; Daniel and Whitteredge 1961). Because the visual receptive organ, the retina, is inherently two dimensional, both dimensions of area 17 are occupied by the retinotopic map. Aside from retinotopy, there are also full representations of ocular dominance, and angular orientation of bars in area 17 (Hubel and Wiesel 1962; 1968; 1974a). These parameters are topographically arranged by a fine internal structure (columns) within the retinotopic map. For every point in space, Hubel and Wiesel (1974) posit that a "hypercolumn" exists that contains the machinery to fully analyze binocular and orientation properties. Each ocular dominance and orientation column is roughly 1 millimeter wide; there is no overlap between receptive fields within area 17 for sites separated by about 2 mm..

The frequency representation in AI takes up only one field dimension, leaving the orthogonal spatial dimension open for the representation of some other basic parameters. In ferrets a series of experiments have been performed in which optic nerve input was re-directed to the auditory thalamus after ablating the nerve's usual visual targets -- the lateral geniculate nucleus and the superior colliculus (Sur et al. 1988; Pallas et al. 1990; Roe et al. 1990). These experiments permit a comparison between AI and area 17 processing.

When investigators recorded from AI in these ferrets, there was a complete retinotopic map with azimuth replacing frequency information and elevation replacing the sharpness of tuning gradient (Roe et al. 1990). Orientation selectivity was reported for about 20% of single neurones in manipulated AI (Sur et al. 1988), but a topographical distribution of orientation has yet to be examined in detail.

In normal hearing ferrets, there may be a sharpness of tuning gradient in AI similar to that reported in the cat (Flemming personal communication), but systematic variations in the sharpness of elevation tuning in manipulated ferrets has yet to be studied. We do not know whether the map of integrated excitation (Schreiner and Mendelson 1990) is a general property of AI. The initial

experiments of Sur and colleagues opens the door for a plethora of theoretically intriguing experiments regarding fundamental similarities and differences between the topographical organization of auditory and visual cortex.

Comparison to Primary Visual Cortex: Receptive Field Size (Sharpness of Tuning) verses Cortical Magnification

In normal area 17, foveal receptive fields are much smaller than eccentric receptive fields. This organization with small receptive fields in the center of area 17 and larger receptive fields in the representation of the periphery is similar to that described for the frequency receptive field organization in AI. There is, however, one very important difference.

In area 17 small (sharply tuned) receptive fields are restricted to regions with a large cortical representation. For example, the foveal region of the retina occupies a large part of area 17, and each visual receptive field within this region is small (e.g. Hubel and Wiesel 1974). The peripheral visual field occupies a small part of area 17 and the corresponding receptive fields are quite large. A simplistic interpretation is that to obtain high spatial resolution you need many small receptive fields. A similar relationship between receptive field size and magnification

has been found in the somatosensory cortex (Sur et al.

1980).

The relationship between receptive field (RF) size and

cortical representation was studied quantitatively by Albus

(1975). He posited an anatomical construct called the

spatial subunit calculated from single neurons as follows

$$\text{spatial subunit} = ((\text{total RF scatter})^2 + (\text{average RF size})^2)^{1/2}/\text{magnification factor}$$

The numerator terms roughly correspond to multiple unit

receptive field size (degrees) and the denominator

corresponds to the size of cortex devoted to a given

spatial location (degrees visual field per mm of cortex).

The spatial subunit was of a constant size (approximately

2.7 mm) in area 17, i.e. independent of location in the

retinotopic map. The result can be simplified as saying the

size of a multiple unit receptive field is inversely

proportional to the size of cortex devoted to that part of

visual space (see also inverse rule of Edelman and Finkel

1984). Hubel and Wiesel (1974) expressed this idea more

intuitively by stating that for every 2 millimeters

(slightly smaller than Albus) an electrode is moved in

cortex, there would be no overlap between recorded

receptive fields (including scatter). A similar property

might hold for frequency representation in the rostro-

caudal axis of AI in the bat, where the highly magnified
58-61 kHz representation is composed of very sharply tuned
single neurons (e.g., Suga 1984). It should be noted that
in bat AI, like area 17, part of the magnification effect
can be attributed to effects at the periphery, including
the receptor organ (Hanson 1973; Suga et al. 1975; Suga and
Jen 1977; Review in Suga 1978)

A constant spatial subunit for frequency
representation cannot hold true for the entire isofrequency
domain of AI in the cat. While receptive field size
(sharpness of frequency tuning) varies systematically with
dorsal-ventral position (Schreiner at al. 1988; Schreiner
and Mendelson 1990; Chapter 2), the extent of frequency
representation (magnification factor) for a given frequency
does not (e.g. Tunturi 1952; Merzenich et al. 1975).
Therefore in dorsal and ventral AI the spatial subunit
would be larger than in the physiological center of AI.

With the knowledge of systematic representations of
bandwidth and amplitude within the isofrequency domain,
many experiments can be performed to test for similarities
and differences in basic organizational principles between
visual and auditory cortex. The generality of such concepts
as the cortical spatial subunit need to be further studied
within the isobandwidth domain, particularly along the
"intensity fovea".

Future Directions

The data presented in this dissertation help to resolve previous differences in the definition of AI by characterizing a slab of AI from 600-1000 microns in depth below the cortical surface. Future studies need to investigate how physiologically defined AI properties vary with depth. Maps of responses to pure-tone stimuli as described in this dissertation provide a basic outline of the structures of AI. Within the defined physiological frame of reference, future studies with more complex stimuli, are now possible, which can be used to better understand how complex information is processed in AI.

BIBLIOGRAPHY

Abeles, M., and Goldstein, M.H. Jr. Functional architecture in cat primary auditory cortex: columnar organization according to depth. *J. Neurophysiol*. 33:172-187, 1970.

Abeles, M., and Goldstein, M.H. Jr. Responses of single units in the primary auditory cortex of the cat to tones and tone pairs. *Brain Research* 42:337-352, 1972.

Ades, H., Mettler, F.A., and Culler, E.A. Effect of lesions in the medial geniculate bodies upon hearing in the cat. Am. J. Physiol 125: 15-23, 1939.

Ades, H.W. Connections of the medial geniculate body in the cat. *Arch. Neurol. Psychiatr*. 45:138-144, 1941.

Ades, H.W. A secondary acoustic area in the cerebral cortex of the cat. *J. Neurophysiol*. 6:59-63, 1943.

Albus, K. A quantitative study of the projection area of the central and paracentral visual field in area 17 of the cat. I. The precision of the topography. Exp. Brain Res. 24: 159-179, 1975.

Anderson, J.W. The production of ultrasonic sounds by laboratory rats and other mammals. *Science* 119: 808-809, 1954.

Barone, P., Irons, W.A., Clarey, J.C., and Imig, T.J. A comparison of the directional properties of nonmonotonic neurons in the auditory thalamus and primary auditory cortex (AI) of cat. Soc. Neurosci. Abstr. 16: 719, 1990.

Beck, Adolph. [Translated Dissertation] The determination of localizations in the brain and spinal cord with the aid of electric phenomena. Eng. ed. Warszawa: Polish Scientific Publishers, 1973. Acta neurobiologiae experimentalis. Supp: 3, 1891.

Blasdel ,G.G., and Pettigrew, J.D. Degree of interocular synchrony required for maintenance of binocularity in kittens visual cortex. *J. Neurophysiol*. 42:1692-1710, 1979.

Brandner, S., and Redies, H. The projection from medial geniculate to field AI in cat: organization in the isofrequency dimension. *J. Neuroscience* 10(1):50-61, 1990.

Brazier, Mary A.B. (1987). A history of Neurophysiology in the 19th century. Raven Press, N.Y.

Bremer, F. and Dow, R.S. The cerebral acoustic area of the cat. A combined oscillographic and cytoarchitectonic study. J. Neurophysiol. 2: 308-319, 1939.

Broca, Pierre P. (1861a) Perte de la parole, ramollissememt
    chronique et destruction partielle du lobe anterieur
    gauche du cerveau. (Loss of speech, chronic softening
    and partial destruction of the left anterior lobe of
    the brain). Bulletins de la societe d'anthropologie
    2:235-238. Translated in Wilkens 1965.

Broca, Pierre P. (1861b) "Remarques sur la siege de la
    faculte du langage articule; suivies d'une observation
    d'aphemie." ("Remarks on the seat of the faculty of
    articulate language, followed by an observation of
    aphemia."). Bull. Soc. Anat., Paris 6:330-357.
    Translated in von Bonin 1960.

Brown, K.A., Buchwald, J.S., Johnson, J.R., and Mikolich,
    D.J. *Vocalization in the cat and kitten.* Dev.
    Psychobiol. 11(6):559-570, 1978.

Bouillaud, J.B. (1825). "Recherches cliniques propres a
    demontrer que la perte de la parole correspond a la
    lesion des lobules anterieurs du cerveau, et a
    confirmer l'opinion de M. GALL, sur le siege de
    l'orange du langage articule." Archives Gen de Med,
    1st series, 8:25-45.

Brugge, J.F., Dubrovsky, N.A., Aitken, L.M. and Anderson, D.J. Sensitivity of single neurons in auditory cortex of cat to binaural tonal stimulation; effects of varying interaural time and intensity. J. Neurophysiol. 32: 1005-1024, 1969.

Caird, D. and Klinke, R. Processing of interaural time and intensity differences in the cat inferior colliculus. *Exp. Brain Res.* 68: 379-392, 1987.

Campbell, A.W. Histological studies on localization of cerebral function. University Press: Cambridge, 1905

Caton, R. On the electric relations of muscle and nerve. Liverpool Med Chir. J, 1875a.

Caton, R. The electrical currents of the brain. Brit. Med. J. 2:278, 1875b.

Caton, R. Interim report on investigation of the electric currents of the brain. Brit. Med. J. Suppl, L:62-65, 1877.

Clark, S.A., Allard, T.A., Jenkins, W.M., and Merzenich, M.M. Receptive fields in the body-surface map in adult cortex defined by temporally correlated inputs. *Nature* 332:444-445, 1988.

Clarke, Edwin and Jacyna, L.S. Nineteenth-Century Origins of Neuroscientific Concepts. University of California Press: Berkeley California, pp 212-308, 1987.

Daniel, P.M. and Whitteridge, D. The representation of the visual field on the cerebral cortex in monkeys. *J. Physiol.* 159: 203-221, 1961.

Danilevsky, V. Y. Electrical phenomena of the brain (in Russian). Fitziologischeskit Sbornik (Physiological Collection) 2: 77-88, 1891.

deRibaupierre, F., Goldstein, M.H. Jr., and Yeni-Komshian, G. Intracellular study of the cat's primary auditory cortex. *Brain Res.* 48:185-204, 1972.

Ehret, G. Development of sound communication in mammals. *Advances in the Study of Behavior* 11: 179-225, 1980

Ehret, G. and Bernecker, C. Low frequency sound communications by mouse pups (*Mus musculus*): wriggling calls release maternal behavior. *Anim. Behav.* 34:821-830, 1986.

Erulker, S.D., Rose, J.E., and Davies, P.W. Single unit activity in the auditory cortex of the cat. Johns Hopkins Hospital Bulletin 39: 55-86, 1956.

Evans, E.F. Normal and abnormal functioning of the cochlear nerve. In *Sound Reception in Mammals*. Ed. R.J. Bench, A. Pye, and J.R. Rye. London: Academic Press. pp. 133-165, 1975.

Evans, E.F. Single unit studies of mammalian cochlear
    nerve. In Auditory investigation: the scientific and
    technical basis. Ed. H.A. Beagley. Oxford: Clarendon
    Press. pp. 324-367, 1979.

Evans, E.F. and Whitfield, I.C. Classification of unit
    responses in the auditory cortex of the unanesthetized
    and unrestrained cat. *J. Physiol. (London)* 171: 476-
    493, 1964.

Ferrier, D. Experiments on the brain of monkeys with
    especial reference to the localisation of sensory
    centres in the convolusions. Brit. Med. J. 2:277,
    1875.

Ferrier, D. Functions of the Brain. Dawsons of Pall Mall:
    London, 1876.

Fischer, B. Overlap of receptive field centers and
    representation of the visual field in the cats optic
    tract. *Vision Res.* 13: 2113-2120, 1973.

Fritsch, Gustav T., and Hitzig, Eduard. (1870). "Uber die
    elektrische Erregbarkeit des Grosshirns. (The
    Electrical Excitability of the Cerebrum). Arch f Anat,
    Phsiol und wissen schaftl Mediz leipzeg 37:300-332.
    Translated in von Bonin 1960 pp 73-96, and Wilkens
    1965, pp 15-27.

Funkenstein, H.H., and Winter, P. Responses to acoustic
    stimuli of units in the auditory cortex of awake
    squirrel monkeys. *Exp. Brain Res*. 18:464-488, 1973.

Gall (1835). On the functions of the brain of each of its
    parts: with observations on the possibility of
    determining the instincts, propensities, and talents,
    or the moral and intellectual dispositions of men and
    animals, by the configuration of the brain and head.
    Translated by Winslow Lewis Jr. Marsh, Capen and Lyon:
    Boston.

Gerard, R.W., Marshall, W.H., and Saul, L.J. Electrical
    activity of the cat's brain. Archives of Neurology and
    Psychiatry 36: 675-738, 1936.

Glass, I., and Wollberg, Z. Responses of cells in the
    auditory cortex of awake squirrel monkeys to normal
    and reversed vocalizations. *Hearing Res*. 9:27-33,
    1983.

Goldstein, M.H., Abeles, M., Daly, R.L. Functional
    architecture in cat primary auditory cortex: tonotopic
    organization. *J. Neurophysiol*. 33: 188-197, 1970.

Goldstein, M.H. Jr.and Abeles, M. Single unit studies of
    the auditory cortex. In *Handbook of Sensory
    Physiology*. Ed. W.D. Keilda, and W.D. Neff, Berlin:
    Springer. pp 199-218, 1975.

Goldstein, M.H Jr., Hall, J.L. II, and Butterfield, B.O. Single-unit activity in the primary auditory cortex of unanesthetized cats. *J. Acoust. Soc. Amer.* 43:444-455, 1968.

Greenwood, D.D. and Maruyama, N. Excitatory and inhibitory response areas of auditory neurons in the cochlear nucleus. *J. Neurophysiol.* 28: 863-892, 1965.

Haack, B., Markl, H., and Ehret, G. Sound communication between parents and offspring. In *Psychobiology of the Mouse*. Ed. J.F. Willot. Springfield: Charles C. Thomas. pp 57-97, 1983.

Haertel, R. Zur Struktur und Funktion akustischer Signale im Pflegesystem der Hauskatze. *Biol. Zentralbl.* 94:187-204, 1975.

Haskins, R. A causal analysis of kitten vocalization: an observational and experimental study. Anim. Behav. 27:726-736, 1979

Head, Henry Sir. Aphasia and Kindred disorders of speech. MacMillan: New York, 1926.

Hellweg, F.C., Koch, R. and Vollrath, M. Representation of the cochlea in the neocortex of the guinea pig. Exp. Brain Res. 29: 467-474, 1977.

Henson, M.M. Unusual nerve-fiber distribution in the cochlea of the bat *Pteronotus p. parnellii* (Gray). *J. Acoust. Soc. Am.* 53: 1739-1740, 1973.

Hind, J.E. An electrophysiological determination of
    tonotopic organization in auditory cortex of cat. J.
    Neurophysiol 16: 475-489, 1953.

Hind, J.E. Jr., Benjamin, R.M. and Woolsey, C.N. Auditory
    cortex of squirrel monkey (*saimiri sciuteus*). *Fed.*
    Proc. Fed. of Amer. Soc. Exp. Biol. 17:71, 1958.

Hubel, D.H. and Wiesel, T.N. Receptive fields, binocular
    interaction and functional architecture in the cat's
    visual cortex. *J. Physiol.* 160: 106-154, 1962.

Hubel, D.H. and Wiesel, T.N. Receptive fields and
    functional architecture of monkey striate cortex. J.
    Physiol. 195: 215-243, 1968.

Hubel, D.H. and Wiesel, T.N. Sequence regularity and
    geometry of orientation columns in the monkey striate
    cortex, *J. Comp. Neurol.* 158: 267-295, 1974a.

Hubel, D.H. and Wiesel, T.N. Uniformity of monkey striate
    cortex: a parallel relationship between field size,
    scatter and magnification factor. *J. Comp. Neurol.*
    158: 295-306, 1974b.

Hui, G.K., Cassady, J.M., and Weinberger, N.M. Response
    properties of single neurons within clusters in
    inferior colliculus and auditory cortex. *Soc.*
    Neuroscience Abstr. 15: 746, 1989.

Imig, T.J., and Adrian, H.O. Binaural columns in the
    primary field (AI) of cat auditory cortex. *Brain Res*.
    138:241-257, 1977.

Imig, T.J. and Brugge, J.F. Sources and terminations of
    callosal axons related to binaural and frequency maps
    in primary auditory cortex of the cat. *J. Comp.*
    Neurol. 182: 637-660, 1978.

Imig, T.J. and Reale, R.A. Ipsilateral corticocortical
    projections related to binaural columns in cat primary
    auditory cortex. *J. Comp. Neurol*. 203: 1-14, 1981.

Imig, T.J., Ruggero, M.A., Kitzes, L.1M., Javel, E. and
    Brugge, J. Organization of auditory cortex in the owl
    monkey *(Aotus trivargatus) J. Comp. Neurol*. 171: 111-
    128, 1977.

Imig, T.J., Irons, W.A. and Samson, F.R. Single-unit
    selectivity to azimuthal direction and sound pressure
    level of noise bursts in cat high frequency primary
    auditory cortex. *J. Neurophysiol*. 63: 1448-1466, 1990.

Katsuki, Y., Wantanabe, T. and Maruyama, N. Activity of
    auditory neurons in upper levels of brain of cat. *J.*
    Neurophysiol. 22: 343-359, 1959a.

Katsuki, Y., Wantanabe, T. and Suga, N. Interaction of
    auditory neurons in response to two sound stimuli in
    cat. *J. Neurophysiol*. 22: 603-623, 1959.

Kawamura, K. Variations of the central sulci in the cat. *Acta Anat.* 80: 204-221, 1971.

Kelly, J.B., Judge, P.W. and Phillips, D.P. Representation of the cochlea in primary auditory cortex of the ferret (*mustela putorius*). *Hearing Res.* 24: 111-115, 1986.

Kelly, J.P. and Gilbert, C.D. The projections of different morphological types of ganglion cells in the cat retina. *J. Comp. Neurol.* 163: 65-80, 1975.

Kornmuller, A.E. Bioelektrische Erscheinungen architectonischer Felder. Eine Methode der Lokalisation auf der Grosshirnrinde. *Dtsch. Z. Nervenheilk.* 130: 44-60, 1933.

Larionev, V.E. (1897) On the cortical centers of hearing in dogs (In Russian). Oboxr. Psychiatr. Nevrol. St. Petersburg. 2:419-424.

Larionev, V.E. (1899) Uber die musikalischen Centren des Gehirns. Pfluger's Arch. f. d. ges. Physiol. 76:608-625.

Licklider, J.C.R. and Kryter, K.D. Frequency localization in the auditory cortex of the monkey. Fed. Proc. 1: 51, 1942.

Lombroso, C.T. and Merlis, J.K. Suprasylvian auditory responses in the cat. *EEG Clin. Neurophysiol.* 9: 301-308, 1957.

Marler, P.R. The structure of animal communication sounds.
In *Recognition of Complex Acoustic Signals*. Ed. T.H.
Bullock. Berlin: Dahlem Konferenzen. pp. 17-35, 1976.

McMullen, N.T. and Glaser, E.M. Tonotopic organization of
rabbit auditory cortex. Experimental Neurology 75:
208-220, 1982.

Mendelson , J.R., Schreiner, C.E., Grasse, K., and Sutter,
M.L. Spatial distribution of response to FM sweeps in
cat primary auditory cortex. in preparation, 1991.

Merzenich, M.M. and Brugge, J.F. Representation of the
cochlear partition on the superior temporal plane of
the macaque monkey. Brain Research 50: 275-296, 1973.

Merzenich, M.M., Jenkins, W.M. and Middlebrooks, J.C.
Observations and hypothesis on special organizational
features of the central auditory nervous system. In:
Dynamic Aspects of Neocortical function. Ed. G.M.
Edelman, W.E. Gall and W.M. Cowan. New York: John
Wiley and Sons, pp. 397-424, 1984.

Merzenich, M.M., Kaas, J.H. and Roth, G.L. Auditory cortex
in the grey squirrel: tonotopic organization and
architectonic fields. J. Comp. Neurol 166: 387-402,
1976.

Merzenich, M.M., Knight, G.L., and Roth, G.L.
Representation of cochlea within primary auditory
cortex in the cat. *J. Neurophysiol*. 38:231-249, 1975.

Merzenich, M.M., Schreiner, C.E., Recanzone, G.H., Beitel, R.E. and Sutter, M.L. Topographic organization of cortical field AI in the owl monkey (Aotus trivargatus). ARO Abstracts, 1991.

Middlebrooks, J.C., Dykes, R.W., and Merzenich, M.M. Binaural response-specific bands in primary auditory cortex in the cat. *Brain Res.* 181:31-48, 1980.

Middlebrooks, J.C., and Zook, J.M. Intrinsic organization of the cat's medial geniculate body identified by projections to binaural response-specific bands in the primary auditory cortex. *J. Neuroscience* 3(1):203-224, 1983.

Moiseff ,A., and Konishi, M. Neuronal and behavioral sensitivity to binaural time differences in the owl. *J. Neuroscience* 1(1):40-48, 1981.

Moiseff, A., and Konishi, M. Binaural characteristics of units in the owl's brainstem auditory pathway: precursors of restricted spatial receptive fields. *J. Neuroscience* 3(12):2553-2562, 1983.

Musicant, A.D., Chan, J.C.K., and Hind, J.E. Direction-dependent spectral properties of cat external ear -- new data and cross-species comparisons. *J. Acoust. Soc. Am.* 43:456-461, 1990.

Myerson, J., Manis, P.B., Miezin, F.M., and Allman, J.M.
Magnification in striate cortex and retinal ganglion
cell layer of owl monkey: a quantitative comparison.
Science 198: 855-857, 1977.

Newman, J.D., and Wollberg, Z. Multiple coding of species-
specific vocalizations in the auditory cortex of
squirrel monkeys. *Brain Research* 54:287-304, 1973.

Nitschke, W. *Acoustic Behavior in the Rat.* New York:
Praeger, 1982.

Oonishi, S., and Katsuki, Y. Functional organization and
integrative mechanism on the auditory cortex of the
cat. *Jap. J. Physiol.* 15:342-365, 1965.

Pallas, S.L., Roe, A.W., and Sur, M. Visual projections
induced into the auditory pathway of ferrets. I. Novel
inputs to primary auditory cortex (AI) from the
LP/pulvinar complex and the topography of the MGN-AI
projection. *J. Comp. Neurol.* 298: 50-68, 1990.

Pelleg-Toiba, R., and Wollberg, Z. Tuning properties of
auditory cortex cells in the awake squirrel monkey.
Exp. Brain Res. 74:353-364, 1989.

Phillips, D.P. Temporal response features of cat auditory
cortex neurons contributing to sensitivity to tones
delivered in the presence of continuous noise. *Hearing
Research* 19:253-268, 1985.

Phillips, D.P. and Cynader, M.S. Some neural mechanism in
the cat's auditory cortex underlying sensitivity to
combined tone and wide-spectrum noise stimuli. *Hearing
Research* 18: 87-102, 1985.

Phillips, D.P. and Hall, S.E. Responses of single neurons
in cat auditory cortex to time-varying stimuli: linear
amplitude modulations. Exp. Brain Res. 67: 479-492,
1987.

Phillips, D., and Irvine, D.R.F. Responses of single units
in physiologically defined primary auditory cortex
(AI) of the cat: frequency tuning and response to
intensity. *J. Neurophysiol..* 45(1):48-58, 1981.

Phillips, D.P., Orman, S.S., Musicant, A.D. and Wilson,
G.F. Neurons in the cat's primary auditory cortex
distinguished by their response to tones and wide-
spectrum noise. Hearing Research 18:73-86, 1985.

Pribraum, K.H., Rosner, B.S., and Rosenblith, W.A.
Electrical responses to acoustic clicks in monkey.
Extent of neocortex activated. J. Neurophysiol 17:336-
344, 1954.

Rajan, R., Aitken, L.M., Irvine, D.R.F and McKay, J..
Azimuthal sensitivity of neurons in primary auditory
cortex of cats. I. Types of sensitivity and the
effects of variations in stimulus parameters. J.
Neurophysiol. 64: 872-901, 1990a.

Rajan, R., Aitken, L.M. and Irvine, D.R.F. Azimuthal sensitivity of neurons in primary auditory cortex of cats. II. Organization along frequency-band strips. J. Neurophysiol. 64: 888-902, 1990b.

Reale, R.A., and Imig, T.J. Tonotopic organization in auditory cortex of the cat. *J. Comp. Neurol.* 192:265-291, 1980.

Reale, R.A. and Kettner, R.E. Topography of binaural organization in primary auditory cortex of the cat: effects of changing interaural intensity. J. Neurophysiol. 56: 663-682, 1986.

Reale, R.A., Imig, T.J. and Sinex, D.G. Rate intensity functions of single neurons located with binaural suppression columns of cat primary auditory cortex. Soc. Neurosci. Abstr. 5:29, 1979.

Rhode, W.S. Some observations of two-tone interactions measured with the mossbauer technique. In Psychophysics and Physiology of Hearing. Ed. E.R. Evans and S.P. Wilson. Academic: London, pp 27-38, 1977.

Roe, A.W., Pallas, S.L., Hahm, J., and Sur, M. A map of visual space induced in primary auditory cortex. Science 250: 818-820, 1990.

Romand, R. and Ehret G. Development of sound production in normal, isolated and deafened kittens during the first post-natal months of development. Dev. Psychobiol. 17(6): 629-649, 1984

Rose, J.E. The cellular structure of the auditory region of the cat. *J. Comp. Neurol.* 91: 409-440, 1949.

Rose, J.E. and Woolsey, C.N. The relations of thalamic connections, cellular structure and evocable electrical activity in the auditory region of the cat. *J. Comp. Neurol.* 91: 441-466, 1949.

Schreiner, C.E., and Cynader, M.S. Basic functional organization of secondary auditory cortical field (AII) of the cat. *J. Neurophysiol.* 51(6):1284-1305, 1984.

Schreiner, C.E. and Langner, G. Periodicity coding in the inferior colliculus of the cat. II. Topographical organization. J. Neurophysiol. 60(6): 1823-1840, 1988.

Schreiner, C.E., Mendelson, J.R., Grasse, K., and Sutter, M.L. Spatial distribution of basic response properties in cat primary auditory cortex. *Assoc. Otolaryngol. Abstr.* 11:36, 1988.

Schreiner, C.E. and Mendelson, J.R. Functional topography of cat primary auditory cortex: distribution of integrated excitation. *J. Neurophysiol.* 64: 1442-1460, 1990.

Schreiner, C.E., Mendelson, J.R., and Sutter, M.L.
Functional topography of cat primary auditory cortex:
representation of tone intensity *Exp. Brain Res.*
submitted, 1991

Shamma, S.A. and Fleshman, J.W. Spectral orientation
columns in the primary auditory cortex. ARO abstracts
13: 222, 1990.

Shipley, C., Buchwald, J.S., and Carterette, E.C. The role
of auditory feedback in the vocalizations of cats.
Exp. Brain Res. 69:431-438, 1988.

Stryker, M.P., and Strickland, S.L. Physiological
segregation of ocular dominance columns depends on the
pattern of afferent electrical activity. *ARVO*
Abstracts 125(3):278, 1984.

Suga, N. Amplitude-spectrum representation in the doppler-
shifted-CF processing area of the auditory cortex of
the mustache bat. Science 196: 64-67, 1977.

Suga, N. Specialization of the auditory system for
reception and processing of species-specific sounds.
Fed Proc. 37: 2342-2354, 1978.

Suga, N. The extent to which biosonar information is
represented in the bat auditory cortex. In: *Dynamic*
Aspects of Neocortical function. Ed. G.M. Edelman,
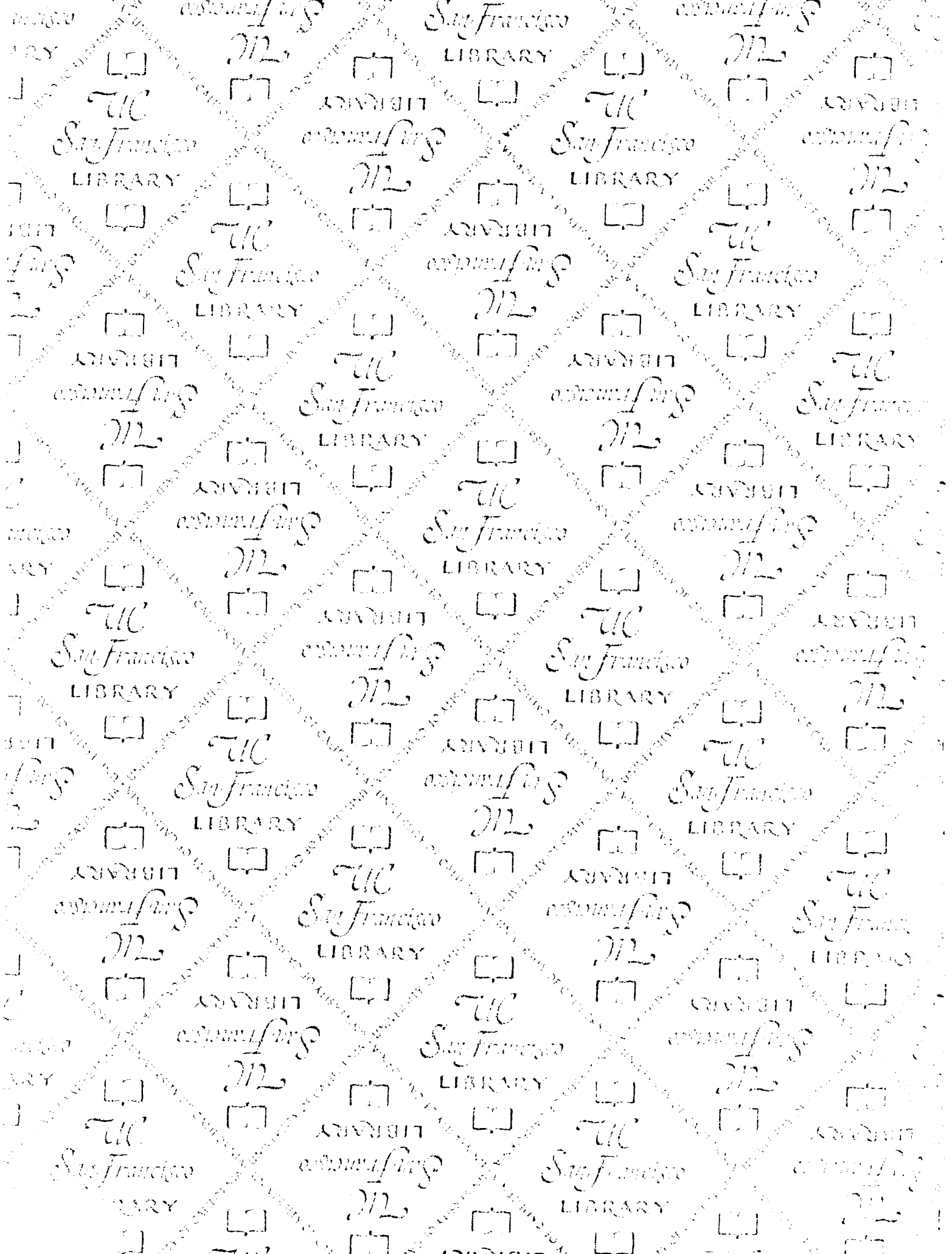W.E. Gall and W.M. Cowan. New York: John Wiley and
Sons, pp. 315-373, 1984.

Suga, N. Auditory neuroethology and speech processing:
complex-sound processing by combination sensitive
neurons. In: *Auditory Function: Neurobiological Bases
of Hearing*. Ed. G.W. Edelman, W.E. Gall and W.M.
Cowan. New York: John Wiley and Sons, pp 679-720,
1989.

Suga, N. and Manabe, T. Neural basis of amplitude-spectrum
representation in auditory cortex of the mustached
bat. J. Neurophysiol. 47: 225-255, 1982.

Suga, N. and Jen, P. H-S. Further studies on the peripheral
auditory system of the CF-FM bats specialized for the
fine frequency analysis of Doppler-shifted echoes. *J.
Exp. Biol.* 69:207-232, 1977.

Suga, N., O'Neill, W.E., and Manabe, T. Harmonic-sensitive
neurons in the auditory cortex of the mustache bat.
Science 203:270-273, 1979.

Suga, N., O'Neill, W.E., Kujirai, K., and Manabe, T.
Specialization of "combination-sensitive" neurons for
processing of complex biosonar signals in the auditory
cortex of the mustached bat. J. Neurophysiol. 49:1573-
1626, 1983.

Suga, N., Simmons, J.A., and Jen, P. H.-S. Peripheral
specialization for fine analysis of Doppler-shifted
echoes in "CF-FM" bat *Pteronotus parnellii*. J. Exp.
Biol. 63:161-192, 1975.

Suga, N., and Tsuzuki, K. Inhibition and level-tolerant tuning in the auditory cortex of the mustached bat. *J. Neurophysiol.* 53(4):1109-1145, 1985.

Sutter, M.L., and Schreiner, C.E. Topography and physiology of multipeaked units in cat primary auditory cortex. *Soc. Neurosc. Abstr.* :1116, 1989.

Sur, M., Garraghty, P.E., and Row, A.W. Experimentally induced visual projections into auditory thalamus and cortex. Science 242: 1437-1441, 1988.

Sur, M., Merzenich, M.M., and Kaas, J. Magnification, Receptive-Field area, and hypercolumn size in areas 3b and 1 of somatosensory cortex in owl monkeys. *J. Neurophysiol.* 44:295, 1980.

Takahashi, T., Moiseff, A., and Konishi, M. Time and intensity cues are processed independently in the auditory system of the owl. *J. Neuroscience* 4(7):1781-1786, 1984.

Talbot, S.A. and Marshall, W.H. Physiological studies on neural mechanisms of visual localization and discrimination. *Amer. J. Opthal.* 24: 1255-1264, 1941.

Thomas, L.B. Spontaneous and evoked patterns of activity of single cortical cells in auditory and visual cortex. *Electroencephalog. & Clin. Neurophysiol.* 4: 376, 1952.

Tunturi, A.R. Physiological determination of the boundary
    of the acoustic area in the cerebral cortex of the
    dog. *Am. J. Physiol.* 160: 395-401, 1950.

Tunturi, A.R. Physiological determination of the
    arrangement of the afferent connections to the middle
    ectosylvian auditory area in the dog. *Am. J. Physiol.*
    162: 489-502, 1952.

Vogt, O. Sur la myelinisation de l'hemisphere cerebral du
    chat. C.R. Soc. Biol., Paris 10: 54-56, 1898.

von Bonin, Gerhardt. Some papers on the cerebral cortex.
    Translations from French and German. Thomas:
    Springfield, Ill, 1960.

Walker, A.E. The projection of the medial geniculate body
    to the cerebral cortex in the macaque monkey. J. Anat.
    71: 319-331, 1937.

Walzl, E.M. and Woolsey, C.N. Cortical auditory area of the
    monkey as determined by electrical excitation of nerve
    fibers in the osseous spiral lamina and by click
    stimulation. Fed. Proc. Fed. of Amer. Soc. Exp. Biol.
    2: 52, 1943.

Wantanabe, T. and Katsuki, Y. Response patterns of single
    auditory neurons of the cat to species-specific
    vocalization. *Jap. J. Physiol.* 24:135-155, 1974.

Wilkens, R.H. Neurosurgical Classics. Johnson Reprint
    Corporation: New York, 1965.

Wilson, J.R. and Sherman, M.S. Receptive field characteristics of neurons in cat striate cortex: changes with visual field eccentricity. *J. Neurophysiol.* 39: 512-533, 1976.

Winer, J.A. Anatomy of layer IV in cat primary auditory cortex (AI). *J. Comp. Neurol.* 224:535-567, 1984.

Winter, P., and Funkenstein, H.H. The effect of species-specific vocalization on the discharge of auditory cortical cells in the awake squirrel monkey (Saimiri sciureus). *Exp. Brain Res.* 18:489-504, 1973.

Wollberg, Z., and Newman, J.D. Auditory cortex of squirrel monkey: response patterns of single cells to species-specific vocalizations. *Science* 175:212-214, 1972.

Woolard, H.H. and Harpman, A. The cortical projection of the medial geniculate body. J. Neurol. Psychiat., London 2: 35-44, 1939.

Woolsey, C.N. and Walzl, E.M. Topical projection of nerve fibers from local regions of the cochlea to the cerebral cortex of the cat. Am. J. Physiol. 133: P498-P499, 1941.

Woolsey, C.N. and Walzl, E.M. Topical projection of nerve fibers from local regions of the cochlea to the cerebral cortex of the cat. John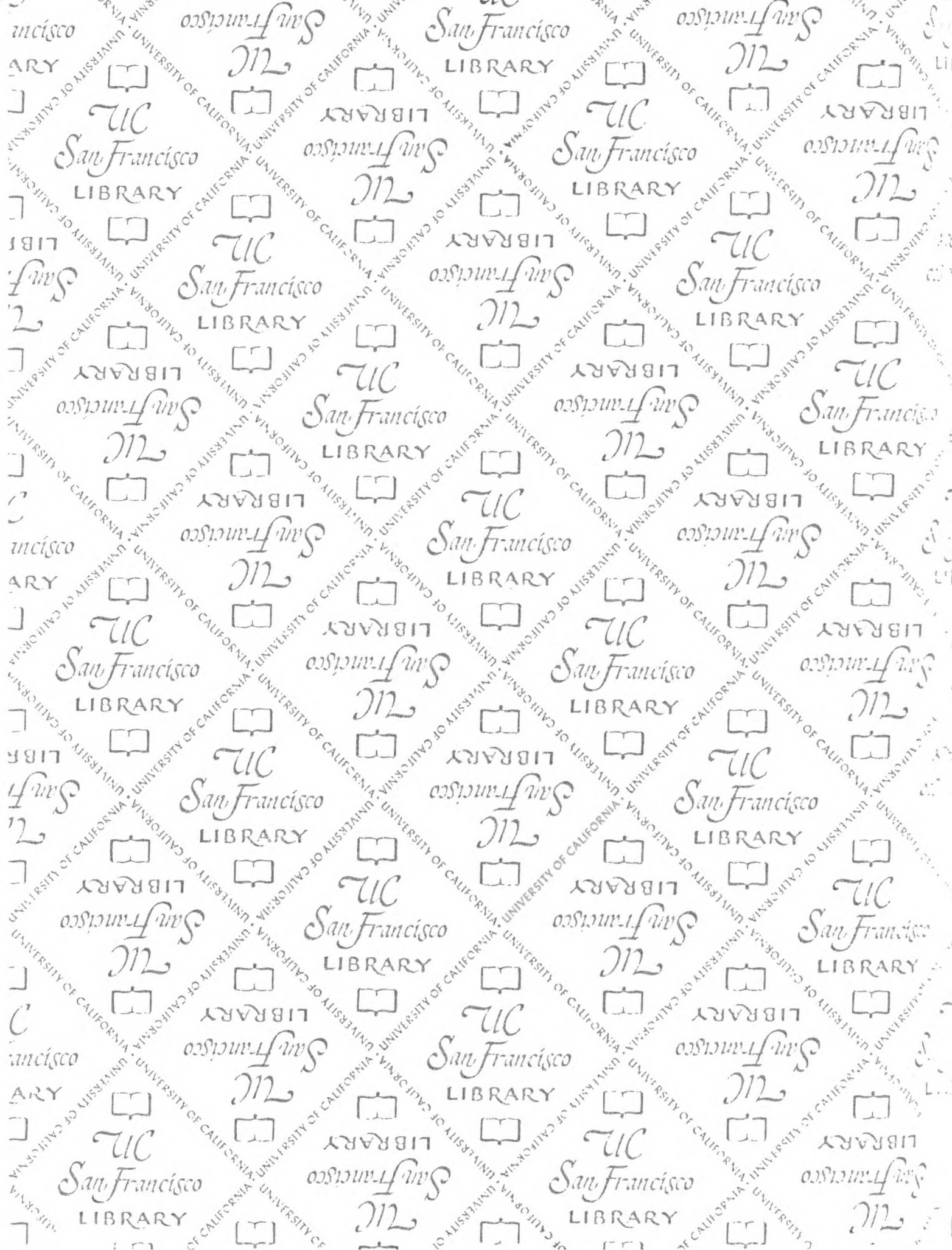s Hopkins Hospital Bulletin 71: 315-344, 1943.